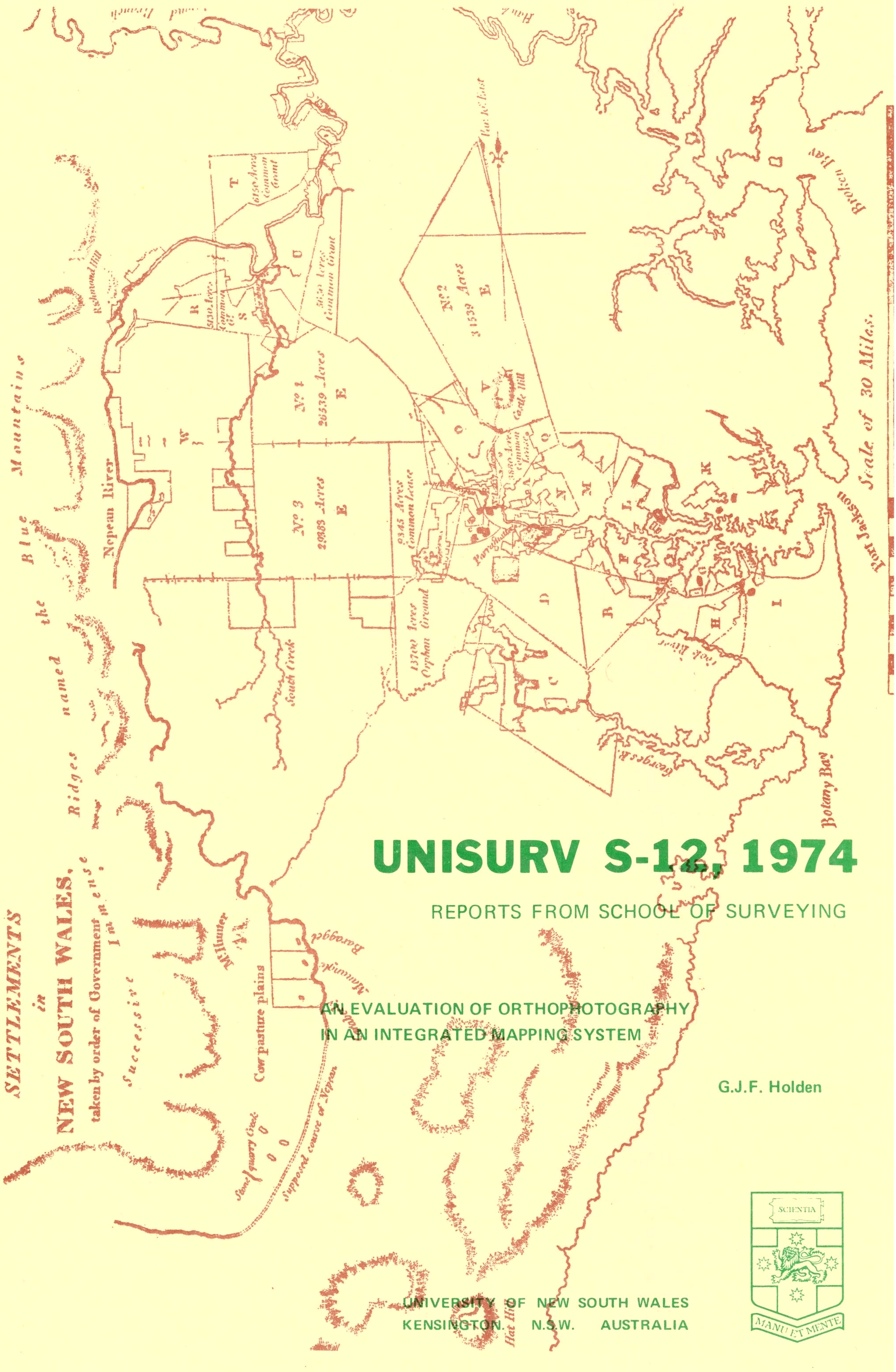

UNISURV S-12, 1974

REPORTS FROM SCHOOL OF SURVEYING

AN EVALUATION OF ORTHOPHOTOGRAPHY IN AN INTEGRATED MAPPING SYSTEM

G.J.F. Holden

UNIVERSITY OF NEW SOUTH WALES
KENSINGTON, N.S.W. AUSTRALIA

Reference to Districts.

A Northern Boundaries

B Liberty Plains

C Banks Town

D Parramatta

EEEE Ground reserved
for Govt. purposes

F Concord

G Petersham

H Bulanaming

I Sydney

K Hunters Hills

L Eastern Farms

M Field of Mars

N Ponds

O Toongabbey

P Prospect

Q

R Richmond Hill

S Green Hills

T Phillip

U Nelson

V Castle Hill

W Evan

The cover map is a reproduction in part of a map noted as follows:

London: Published by John Booth, Duke Street, Portland Place, July 20th, 1810

Reproduced here by courtesy of The Mitchell Library, Sydney

UNISURV REPORT NO. S12, 1974

An Evaluation of Orthophotography in an Integrated Mapping System

G.J.F. Holden

Received March 1974

School of Surveying,
The University of New South Wales,
P.O. Box 1,
Kensington, N.S.W. 2033. Australia

National Library of Australia
Card No. and SBN
0 85839 014 0

ABSTRACT

Since the modern revival of interest in Orthophotography, and in particular since early 1960 when production instruments for the technique became available, a number of practical tests have been carried out in order to determine the mapping accuracies which can be achieved in practice. Several mapping projects have incorporated orthophotographic processes, and a few have been conceived as orthophotomap projects. An analysis is made of current projects and previous tests, and the analysis shows that to a large extent both the projects and the tests have been rather biased by conventional mapping criteria, and that many of the tests have been concerned solely with the problems of very large scale mapping. It is contended that this is rather paradoxical, because this technique is one which should be most advantageously used in quite a different context, namely that of medium scale mapping for underdeveloped terrain; a sphere of surveying in which world mapping capability is quite unable to cater with the demand.

From this viewpoint a series of tests was carried out, in which planning, fieldwork, and production phases were integrated from the initial stages of ground control intensification, through the aerial triangulation phase, culminating in the production of orthophotographs. Additionally the concept of

producing contours from drop line profile charts was investigated under rather more realistic terrain conditions than has been attempted previously, in order to obtain data on production times for the cartographic treatment. It proved necessary to devise a technique, namely that of drainage interpretation, in order to be able to deal with the problem of profile interpretation in broken terrain; and it is thought that this technique may have general application to other pictorial profile methods. During the progress of the work, other problems were identified, and in particular investigations were made into calibration methods for perspective centres in Independent Model Triangulation. Also a series of computer programs were developed for photogrammetric work with small programmable desk calculators, including a program for strip formation.

It was shown by the results of the tests that the planimetric accuracy of orthophotography is consistently rather high, and contributes only small errors to the final product of the integrated mapping project. It was shown that the intrinsic accuracy of profiling is high, but that a rather marked degradation occurs in the contouring phase, suggesting that somewhat reduced criteria should be adopted for elevation specifications in orthophotomap medium scale mapping projects when based on the drop line technique.

CONTENTS

1. ORTHOPHOTOGRAPHY: PRINCIPLES, DEVELOPMENT OF INSTRUMENTS, AND MAPPING APPLICATIONS.

1.1 Introduction

An orthophotograph is in principle a photograph in which individual images are at a uniform scale, located in correct relative position to one another; as if the corresponding object points had been projected by parallel orthogonal projection into the image plane. A camera registers images by central projection through the camera lens, producing a photographic image which is a central perspective of the corresponding object points. In the general case, the central perspective images are neither of uniform scale, nor are the shapes of areas delineated by groups of point images conformal with an orthogonal projection of the object shapes.

Photographs produced in an aerial camera are characterised by image displacements in relative position, and by scale variations; quantitatively influenced both by the extent of elevation differences in the terrain and by the extent to which the camera axis is tilted out of the vertical. Terrain objects which are on relatively higher elevated ground are registered as larger scale images apparently displaced in position away from the camera nadir. In the exceptional case of flat terrain devoid of elevation differences, the small unavoidable tilts of the camera axis transform area shapes through central projection into shapes which are not conformal with an orthogonal projection in a horizontal datum such as a map. It follows that the individual images are not of uniform scale.

1.2 The relationship between Rectification and Orthophotography.

Aerial photographs of flat or uniformly sloping terrain can be transformed by a reversal of central projection into orthogonal projection. The transformation may be numerical or analytical, given image coordinates of points (x, y) and the corresponding orthogonal projection coordinates of object points (X, Y); and can be represented by the well known projective transformation *(Helava, 1968, 10)*:

$$X = \frac{a_1 x + b_1 y + c_1}{a_o x + b_o y + 1} \qquad (1.i)$$

$$Y = \frac{a_2 x + b_2 y + c_2}{a_o x + b_o y + 1} \qquad (1.ii)$$

The coefficients of x, y are functions of the elements of inner and outer orientation of the aerial camera.

More usually the transformation is either graphical, or optical-mechanical by the process of photographic rectification; through which images of flat or constant gradient terrain may be transformed to restitute the displacements and scale variations. The process, in order to be rigorous, is a plane area transformation. When there is relief present in the object terrain, plane area transformation is not possible from a theoretical point of view; but an approximate transformation can be achieved by partitioning the whole photograph into smaller zones of nearly equivalent elevations, and rectifying separately for each part, which can be called differential rectification, or rectification by facets. The originator of the idea, which is the fundamental principle of orthophotography, was SCHEIMPFLUG, who in 1898 patented a method of rectification in zones for the preparation of photo maps *(Brunnthaler, 1972, 93)*. Such a process with single photographs is clearly very time-consuming, and requires either extensive ground control or alternatively map information in order to determine the parts of nearly equivalent elevations.

Double-point model restitution, the ordinary system of analogue plotting machines, gives continuous information on position coordinates (X, Y, Z); provided that the plotting cameras are oriented in correct relative and exterior orientation with respect to a datum plane. Such instruments are therefore capable of controlling the differential rectification of one of the two photographs in the plotting cameras, and of producing a new photograph which is an orthogonal projection of model points at a specific model scale.

The image transfer of points from the rectifying photograph of the pair may be represented by equations of the collinearity type; which specify the condition that image coordinates, (x, y, -f) of the plotting camera, coordinates of the perspective centre (X_c Y_c Z_c), and the coordinates in the model (X, Y, Z) are collinear. The equations reduce to the form:

$$X = \frac{Z(a_1x + b_1y + c_1)}{a_ox + b_oy + 1} \qquad (1.iii)$$

$$Y = \frac{Z(a_1x + b_1y + c_1)}{a_ox + b_oy + 1} \qquad (1.iv)$$

In principle the transformation could be a physical transfer of images on a point by point basis from camera image to projected image; but in practice the requirement to expose on film a new photographic image in a reasonable period of time imposes limitations. The image transfer is usually made through the medium of very small area elements which have both finite width and length. This exposure element is commonly a slit the length of which is rather small compared to the width, and can be considered effective as a short line element.

1.3 Development of Instruments for Orthophotography

Instruments capable of differential rectification have developed since the 1920 decade, but the major advances occurred in the 1950 decade. FERBER made a patent application in Germany in 1927 and described the principles of the Gallus apparatus for photo-reconstruction in 1928 *(Ferber, 1928)*. The Gallus-Ferber Photorestituteur is described by HASSETT as a type of orthophotograph instrument *(Hassett, 1966, 867)*. In 1929 LACMANN designed a rectifier for uneven terrain which utilised the projection system of the then current Zeiss Stereoplanigraph plotting camera. Vertical (Z) control was achieved pneumatically with the aid of wooden profile templates, and a direct connection was also possible between the separate components of rectifier and plotting machine *(Lacmann, 1931, 10)*.

BEAN in the U.S.A. carried out experimental work from 1936, and the revival of interest post World War II in orthophotography as a production mapping process is due to his efforts more than any other individual. His approach utilised direct double-projection instruments operating on the anaglyphic projection system, in order to expose in the model space a blue sensitive film to the projected images from the blue-filtered projection camera *(Bean, 1968, 38)*. An acceptable image quality of the projected images is possible on account of the depth of focus due to the small aperture of the projection lens. BEAN produced an engineered prototype in 1956, and a production model U-60 utilising either ER-55 (Balplex) or Kelsh projectors, as plotting cameras. Models T-61 and T-64 followed in 1961 and 1967.

A characteristic of the BEAN instruments is that the projected images are exposed in the model space, with the necessity to provide for the film platform and exposure slit transport mechanisms; so that the instruments can only be used in an orthophotographic function. There is also a limitation on the maximum enlargement possible between photograph and orthophotograph of about X3 on account of the optimum focus zone of the projectors.

GIGAS in 1960 developed the ideas of LACMANN and in conjunction with the Zeiss company devised the Gigas-Zeiss 1 orthoprojector, introduced at the International Congress of Photogrammetry in Lisbon in 1964 *(Meier, 1968, 57)*. Essentially the orthoprojector is one plotting camera component of a Zeiss

Stereoplanigraph, complete with the Zeiss Bauersfeld telephoto focussing system for critical focus at all projection distances. The G-Zl may be coupled directly to a stereo plotter, not necessarily of the optical projection type; so that the projected images move across a film easel in exact correspondence with the movements of the model points in the plotter, but the possibility exists to change the model scale to a different rectification scale. Alternatively the G-Zl may function completely off-line to the plotting machine under control of data stored during a model scanning operation. All of the previously described instruments function on the principle of direct optical projection for the image transfer operation, but the G-Zl may of course be used under storage control in conjunction with a mechanical type plotter.

The manufacturers of mechanical type plotting machines have been slower to develope orthoprojection systems since the direct projection restitution system is not a feature of such instruments. The optical viewing systems of mechanical projection instruments are essentially complex stereoscopes, by which the mechanical image points are marked. Normally the optical axis of the observation system is orthogonal to the photograph dispositive, and in order to project an image forming ray it is necessary to incorporate an auxiliary image transfer system. Orthoprojector instruments incorporating such a system may be classified as "non-direct optical image transfer systems" in contrast to "direct projection image transfer systems" as previously described *(Blachut, 1972, 82-85)*.

C. Zeiss VEB Jena were the first instrument company to incorporate a differential rectification device by an auxiliary image transfer system, in a mechanical analogue projection system. The device was first utilised in the universal plotter Stereotrigomat in which a pencil of rays in the left plotting camera photograph was separated from the visual observation train, and brought to a projection plane by means of an electromechanical inversor *(Cimerman, Tomasegović, 1970, 195)*. A version of the image transfer device is now available with the topographic plotter Topocart B, and is designated Orthophot B.

In the period 1968-1970 the Wild Company of Switzerland developed an orthophoto attachment PPO-8 for the precision plotter A8 Autograph *(Höhle, Schneider, 1973, 77)*. The image transfer is from the left photograph in on-line operation. A small image segment is optically rectified for tip and tilt of the plotting camera, and projected orthogonally onto a light-proof film drum at the rear of the plotting machine *(Bormann, 1970)*.

In 1967 the Italian company Ottico Meccanicca Italiana introduced an orthoprinter now marketed as the O.M.I. Nistri orthoprinter; which is a separate unit to the analytical plotter AP-C which monitores the optical image transfer from a duplicate photograph. In the image transfer system, corrections are introduced for scale variations and rotation of the image due to tip and tilt of the photograph and variations in terrain height *(Parenti, 1968, 21-28)*.

An entirely different system of image transfer utilises cathode ray tubes or electronic image transfer. These systems operate with automatic image correlation in the plotting and orthophotographic mode of operation, and permit much faster scanning than is possible with human manual operation.

Consequently it is possible to use very much smaller line or area elements for the exposure, so that accuracy is in principle hardly dependent on topography as it is ordinarily. At present however, automatic systems cannot discriminate between ground features and the upper surface of buildings and tree-cover, so that the automatic and very fast scanning possibilities are restricted usually to the production of relatively small-scale orthophotos *(Blachut, 1972, 90)*.

Instruments utilising automatic image correlation and electronic orthophoto image transfer are *(Brunnthaler, 1972, 93)*:

Integrated Mapping System	1961
Digital Automatic Map Compilation.. ..	1962
Automatic Stereo Mapping System	1963
Stereomat Wild B8	1964
Stereomat A2000 Wild-Raytheon	1968
Gestalt Orthomapper Hobrough	1970

Detailed descriptions will not be given of the instruments mentioned, since there are extensive explanations in literature in the references quoted; except that a description of the image transfer system will be detailed in the case of the Orthophot B, used in the system tests described in this work.

1.4 Mapping Applications of Orthophotography

Practical applications of orthophotography are, even at this time, still in an evolutionary stage of development. The major application is in the Orthophotomap, which can be defined as an orthophotographic base combined with conventional cartographic line or area overprinted data. At the very least the additional data will comprise a locational guide and a point reference system. At a further stage of utility the orthophotograph may be combined with a contour overlay, which may have been produced in the source instrument concurrently with the image transfer; or alternatively may have been produced off-line in a conventional plotting mode. Additional possibilities are overprints containing names, highway classifications, cadastral boundaries and parcel numbers, land-utilisation classifications, and administrative boundaries. The orthophotomap may be available as a simple continuous tone bromide print, a screened dyeline print, a single colour lithographic print, or a multi-coloured lithographic print.

Opinion on the status of orthophotography in mapping programmes has been epitomised by extreme viewpoints. On the one hand there is the conservative cartographically-biased conclusion that orthophotomaps are no more than map substitutes of a temporary or second-rate nature compared to high-quality conventional line rays. At the other extreme are enthusiasts who regard the orthophotomap as a superior product on account of the wealth of detail and completeness of information content; particularly in view of the faster rate of production with consequential cost-effectiveness. BLACHUT has put the matter in its proper perspective *(Blachut, 1968, 207)*, by pointing out that the orthophoto technique may offer a new approach to conventional mapping in a variety of applications; and that there is not much value in approaching this complex question by accepting as valid, criteria applicable to conventional maps. It is instructive to examine some of the projects which have been commenced by various authorities in recent years, as listed in Table 1.I.

Table 1.I is not a complete listing of orthophoto projects in recent years, but with the exception of Item 2, only projects involving large numbers of map sheets of the order of several hundred, have been included. Item 2 is not a production project, but rather a concept of mapping for developing countries, due to JERIE.

Of the 10 production projects listed, only Items 3, 5, 7, 9, 10 and 11 can be claimed to have been conceived as orthophotomaps from the initial planning stage, whereas the others are projects in which the orthophotomap ranks as a temporary substitute for conventional line maps. The literature cited in respect of the conceptual orthophotomap projects is characterised by a common approach: the concept of a multipurpose map base which is the pictorial record of land use, resources, and integrated survey data. In effect the maps are planned as pictorial data banks.

It is interesting also to examine the planning specifications for the projects listed, as given in Table 1.II. Columns (iv), (viii) and (ix) are of particular interest because of the diversity of specification. Column (iv) gives the constant k of the formula:

$$m_b = k \sqrt{m_k} \tag{1.v}$$

TABLE 1.I

RECENT ORTHOPHOTOMAPPING PROJECTS

Item	Locations	Purpose	Map Scale $1:m_k$	References
1	Australia-Interior	Topographic Base	1:100 000	*Lambert, 1971, 2*
2*	Developing Countries	Mapping by Phases	1:50 000	*Jerie, 1972, 3-17*
3	U.S.A.	General Base Map	1:24 000	***Olsen, 1973, 118***
4	Sweden	Economic (Forest Areas)	1:20 000	*Johannson, 1968, 151*
5	S. Korea	Development	1:12 500	*Visser, 1968, 5*
6	Sweden	Economic Base	1:10 000	*Johannson, 1968, 153*
7	New South Wales	Topographic Base	1:10 000	*Urban, 1973, E1-4*
8	Germany Land Nordrhein-Westfalen	German Base Map	1:5 000	*Voss, 1968, 3*
9	California	Multipurpose	1:4 800	*Ryser, 1973, 128*
10	New South Wales	Topo Cadastral Base	1:4 000	*Urban, 1973, E1-4*
11	New South Wales	Development A [illegible]	1:2 000	*Urban, 1973, E1-4*

* Item 2 is a proposal.

This constant is commonly taken in the range 180 to 300 *for conventional photogrammetric plotting (Förstner, 1968, 107-108)*, and it is interesting to note that only in the cases of items 3 and 7 of what might be called the conceptual orthophotomapping projects is the upper limit exceeded to any considerable extent; together with the JERIE proposal item 2.

Column (viii) gives the number C where C is the ratio Altitude: Contour Vertical Interval, and should be read in conjunction with column (ix) which defines the method of derivation of the contour overlays of the orthophotomap. It should be noted that in no case does C exceed 1000, except when the contours are derived by conventional plotting techniques. Non-conventional contouring was specified in only one case of conceptual orthophotomapping (S. Korea Item 5). Where non-conventional contouring is used in orthophotomapping in projects originally planned for conventional mapping techniques, only in the case of Items 4 and 6 (Sweden) does the C number exceed 400.

The exceptional specification to all current projects is the proposal of JERIE, item 2. In brief he has suggested a concept in which the base topographic mapping of developing countries takes place in successive phases of complexity, the photogrammetric phase of which is based on high altitude super wide angle photography. The initial publications should be orthophotomaps without annotation; followed in subsequent phases with contoured orthophotomaps, next by annotated versions, finally by conventional multicoloured line maps. The contouring should be by dropped line charts produced during the initial phase.

TABLE 1.II

SPECIFICATIONS OF ORTHOPHOTOMAP PROJECTS

Item (i)	Map Scale $1:m_k$ (ii)	Photo Scale $1:m_b$ (iii)	Photo/Map Constant K (iv)	Flight Altitude H(m) (v)	Camera Wide Angle(WA) Super WA (SWA) (vi)	Contour Interval V.I.(m) (vii)	Altitude Contour Ratio C (viii)	Contour Derivation (ix)
1	1:100 000	1: 84 000	266	7400	SWA	20	370	Mixed derivation: includes dropped Lines, Dropped Segments, Digitised contours, Ground Control Interpolation.
2	1: 50 000	1:100 000 1:150 000	447 671	8500 12750	SWA	20	425 637	Dropped Lines
3	1: 24 000	1:120 000	775	18250	WA	-	-	-
4	1: 20 000	1: 30 000	212	4500	WA	5	900	Dropped Lines
5	1: 12 500	1: 37 500	335	5700	WA	10	570	Dropped Lines
6	1: 10 000	1: 30 000	300	4500	WA	5	900	Dropped Lines
7	1: 10 000	1: 48 000 (1:32 000 for Contours)	480 -	7300 4850	WA	- 4	- 1200	- Conventional Plotting
8	1: 5 000	1: 13 000	184	2000	WA	5	400	Conventional plotting
9	1: 4 800	1: 24 000	346	3650	WA	10/20 feet	1200/600	Conventional Plotting
10	1: 4 000	1: 16 000	253	2450	WA	2	1225	Conventional Plotting
11	1: 2 000	1: 8 000	179	1200	WA	1	1200	Conventional Plotting

The Commonwealth of Australia is in a somewhat unique position of development, and of mapping availability. Vast areas of the continental interior are underdeveloped, and the best available maps for planning purposes and for exploration and management of resources are at extremely small scale; complete coverage of the continent at 1:250 000 having been achieved only recently, but with much of the series out-of-date. In early 1973, only some 10% of the total coverage of almost 500 sheets was available with detail revised since 1968, and only about 25% with contours. None of the planned new contoured edition on Australian Map Grid are actually available.

The Division of National Mapping, responsible for geodetic surveying and for the production of topographic maps for Commonwealth purposes, has as its current primary mapping objective the topographic mapping of Australia by the end of 1978 at 1:100 000 scale with 20 metre contours *(Lambert, 1973, 5)*. The series comprises some 3000 sheets for compilation, but many (particularly in the interior), are unlikely to be published at scales larger than 1:250 000. A very large number of the map sheets will be in the form of orthophotomaps (Item 1, Table 1.I), for which the corresponding specifications (Table 1.II) are quite conservative judged by conventional line maps criteria, although the instrumentation involved in the production is extremely sophisticated.

Some areas of the continent are highly developed, in particular the eastern seaboard, where the pace of development has accelerated at such a rate that modern very large scale maps are urgently required as base maps for planners, engineers, developers, and administrators. Thus in New South Wales mapping is in progress at scales 1:10 000, 1:4 000 and 1:2 000 (Items 7, 10, 11 of Table 1.I); and this mapping has been conceptual orthophotomapping from the initial planning stage. Nevertheless the specifications accord with the criteria of conventional line mapping, except that the photograph : map scale ratio in the case of the 1:10 000 orthophotomaps is somewhat outside the normal range.

It is clear that orthophotography is to play a major role in Australian topographic base mapping programmes, but at this period of time the role is still an evolutionary one with many technical problems to be solved. The reaction of the potential map user to an orthophotomap product, compared to the classical cartographic presentation is hardly known, but the urgency of current mapping programmes is so great that completion in a reasonable time scale is not possible by conventional techniques.

It is the purpose of this work to examine some of the problems associated with orthophotomapping at medium scales; in an integrated mapping system in which the successive phases of ground control, aerial triangulation, and photogrammetric processes, all contribute to the accuracy and usefulness of the product.

2. ERRORS OF THE ORTHOPHOTOGRAPHIC PROCESS

2.1

An analysis of the accuracy of differential rectification by orthophotography should not be confined to the image transformation process alone, since orthophotographic production is an extension of the principles of ordinary photogrammetric restitution, and is usually controlled by conventional analogue plotting instruments. To the extent that the data for position location and image scaling is provided, either manually or automatically, by the guidance of a measuring mark in model space - so the control data (measuring mark position) is subject to the errors of any restitution process.

Additionally, the image transfer system utilised in the orthoprojector is a further source of error, independent of the restitution errors. Finally, subsequent treatment of the transferred image, and the physical characteristics of the film base or any derived reproduction medium for presentation of the result, will introduce further errors; analagous to those errors introduced in conventional plotting after transfer from model space to line plot and to cartographic product.

Neglecting those errors introduced by reproduction of the orthophotograph, the sources of error may therefore be classified in four groups which are considered independent of one another:

(i) *Restitution errors:* of the same origin and order of magnitude as any conventional photogrammetric process;

(ii) *System errors:* unique to the orthophotographic process, caused by the departure from a rigorous point-by-point image transfer;

(iii) *Connection errors:* caused if the projection film is not located in the model restitution space, but operates as a connected component either on-line or off-line;

(iv) *Projection film errors:* caused by the lack of flatness of the projection film plane, by instability of the film base, and by processing.

Assumming that some type of elevation data is produced simultaneously with the orthophotograph image transfer, elevation errors additional to (i) are introduced on account of the interpretation and editing or the data; and by the subsequent cartographic treatment to obtain a contour document.

2.2 Photogrammetric Restitution errors

Errors are inevitable in the photogrammetric process, and a complete analysis of the sources of error should include the following factors:

(i) Ground Control: Accuracy of survey control system and method of point fixation. Accuracy of identification in photograph.

(ii) Image errors: Residual (uncorrected) lens distortion, uncorrected atmospheric refraction displacements, film flatness errors, film base instability errors, negative and diapositive processing errors.

(iii) Pass-point errors: If the restitution models are not fully controlled by identified ground controls, the system of pass point determination produces errors. In particular the aerial triangulation method and instrumentation, and the aerial triangulation adjustment procedure.

(iv) Orientation errors: The influence of errors of inner, relative, and absolute orientation on the model point position; and the influence of inner and exterior orientation errors in the orthoprojector if this is a separate unit of the direct projection type.

(v) Projection errors: The influence of the geometric performance of the restitution instrument.

In attempting to estimate the magnitude of errors due to these sources of error, the difficulty is that no general statement can be made on account of the very large number of variables in the possibilities; in particular due to the camera and measuring instrumentation, and to the flight specifications for particular cases. However, a great amount of theoretical investigation of individual physical sources of error has been made, and a large number of controlled experiments have been carried out to confirm theoretical predictions.

AHREND *(Ahrend, 1966)* has summarised the result of many experiments to determine the behaviour and magnitude of individual sources of error. Theoretical investigations of the horizontal accuracy of block adjustment of aerial triangulation by the anblock method have been carried out by ACKERMANN *(Ackermann, 1966)*; and of the vertical accuracy of aerial triangulation by JERIE *(Jerie, 1968)*. Controlled experiments have been carried out to confirm theoretical predictions, in particular by the O.E.E.P.E.

It is possible therefore to estimate the magnitude of errors in extreme cases, and to give some indication of a more general range of errors.

For example, AHREND *(1966, 75)* estimates a plan coordinate mean square error in a model for the case of a universal plotter of the C8 type and a 150 mm wide angle camera, and for the case of full ground control identified by natural points, in terms of accuracy at the plate:

$$m_p = \pm 7.2 \ \mu m \qquad (2.i)$$

and for the corresponding vertical accuracy:

$$m_z = \pm 16.5 \ \mu m = \pm 0.11 \ {}^{o}/_{oo} \ H \qquad (2.ii)$$

AHREND however goes on to say that no allowance has been made for residual terrestial (survey) errors of ground control, or for the effect of refraction.

AHREND'S figure for plan accuracy is almost that used by MEIER *(1966, 80)* in his estimates of theoretical accuracy of the C8-GZ1 system, in which he quotes 8 μm for plan errors inclusive of sources of error excepting 2.2(iii) above, and presumably making no allowance for errors in the control. AHREND'S figure includes an allowance $m_{x,y} = \pm 5$ μm for the influence of the plotting machine, determined from calibration measurements on 20 C8 stereoplanigraphs and the Supragraph; and this allowance may be compared for example at a lower level of precision of the restitution machine, with that of $m_{x,y} = \pm 10$ μm given by SZANGOLIES *(1972, 84)*, determined from factory calibrations of 10 Jena Topocart plotting machines of the topographic type. Adjustment of AHREND'S figures according to the propagation of independent errors, yields the following mean square errors of a controlling instrument of this order:

$$m_p = \pm 11 \text{ μm} \qquad (2.iii)$$

$$m_z = \pm 25 \text{ μm} = 0.17 \,{}^{o}\!/_{oo}\, H \qquad (2.iv)$$

The foregoing figures may be regarded as the *internal or relative* mean square error extremes, due to ordinary photogrammetric restitution errors; but making no allowance for sources of error due to control from 2.2(i) and 2.2(iii). The *external or absolute* precision (m'), which is of great importance in planning mapping projects, is very much more difficult to estimate on account of the wide range of possibilities due to size of area, disposition of ground control, methods and instrumentation for aerial triangulation, and adjustment procedures. It should however be stressed that for most mapping projects at medium and small scales, provision of pass point control for individual models, from fairly large blocks of aerial triangulation, will be the normal procedure rather than fully ground controlled individual models.

As far as plan accuracy is concerned, ACKERMANN has investigated the theoretical horizontal accuracy of adjustment by the Anblock method, of blocks of up to 200 independent models *(Ackermann, 1966, 145-170)*; and this represents perhaps a standard size of block for topographic mapping in developing countries. There is in **any** case only a small dependence on size of block in the Anblock adjustment, providing that the perimeter of the block is well controlled by ground-fixed plan points. ACKERMANN gives the maximum standard deviation of a tie-point in such a block (in the center of the block) as only 1.2 times the standard error of unit weight, and the mean square value for all the tie points as 1.06 times standard error of unit weight. According to ECKHART *(1966)* a standard error of unit weight of 16 μm at plate is assumed for wide angle photographs of 23 x 23 cm on film. The corresponding mean square coordinate error for a block of 200 models is 17 μm at plate.

In Australia until quite recently a great reliance has been placed on strip and simultaneous strip (block) adjustment, by the polynomial form of adjustment due to SCHUT *(1968)*; perhaps owing to the fact that SCHUT'S programs are available without charge and are easily adaptable to various computers, and to user modifications. BERVOETS *(1973, K6)* has recently analysed practical results of aerial triangulations by 11 organisations in Australia engaged in mapping projects, and his analysis gives for the average mean square error of residuals at ground controls after horizontal plan polynomial block adjustment a figure m'_p = 70 µm at plate. BERVOETS however points out that this is only a general impression of the magnitude of precision, as this is a mean figure from blocks averaging 160 models, and of mixed wide angle and super-wide angle systems.

With respect to vertical accuracy of block aerial triangulation, theoretical estimates for planning purposes may be made principally from the work of JERIE *(1968)*. JERIE investigated the theoretical propagation of elevation errors on account of types of camera, number and distribution of ground controls, and dependence on auxiliary data instruments. He remarks that it is not possible to take into account a second set of factors including the quality of photography and the procedure and equipment used for the aerial triangulation; concluding that these factors should be determined by practical tests within an organisation since they should be more or less constant. JERIE calculates for a block of 8 strips by 20 models, with elevation control in every strip at the ends and center, for aerial triangulation without auxiliary data, and for wide angle camera, a mean standard deviation at pass points of 0.36°/ooH with a maximum of 0.49°/ooH, excluding extreme marginal pass points. Interpolating JERIE's figures for a standard block of 200 models, we obtain a mean standard deviation at pass points of 0.42°/ooH.

BERVOETS in his analysis of practical aerial triangulation results in Australia gives a mean square error of ground residuals after polynomial block adjustment, of m'_z = 30 µm at plate, but the blocks are mixed wide and super-wide angle systems, so that the figure given represents a remarkably low range of 0.20 to 0.34^{o}/ooH. The low range is probably due to the fact that the production blocks analysed were unlikely to have been heavily over-determined for elevation controls, all of which would normally have been used in the adjustment transformations, so that the figures quoted are perhaps less reliable as an overall guide than the theoretical predictions of JERIE. We may suggest, as typical of ranges of accuracy for adjusted pass points in a 'standard' mapping block of 200 wide angle models, figures of the following order:

$$m'_p = 17 \text{ to } 70\ \mu\text{m at plate} \qquad (2.v)$$

$$m'_z = 0.20 \text{ to } 0.45^{o}/\text{ooH} \qquad (2.vi)$$

2.3 System errors

2.3.1

System errors are those errors inherent to the orthoprojector image transfer system, the classification **"system"** being due to MEIER *(1968)*, and they are for the most part proportional to the tangent of the angular field (α) of the projection camera. The fundamental cause of the errors is that the image transfer, for practical reasons, cannot be effected on a point-by-point basis from original image to projected image. The exposure element is normally a slit of finite dimensions, essentially a line element, and usually effective as a horizontal line element in the model surface, which is not horizontal in the general case.

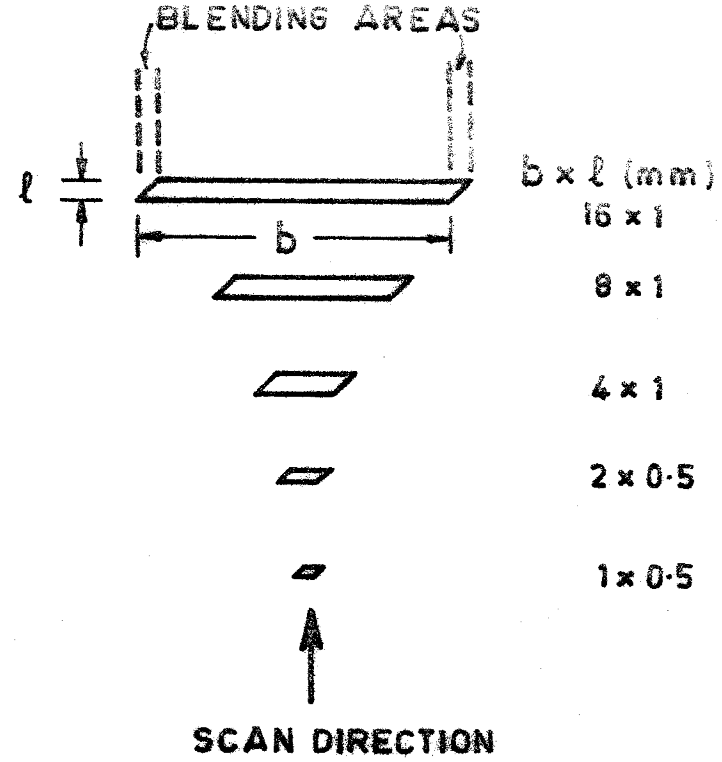

Fig. 2·1: Orthophot Standard Slits

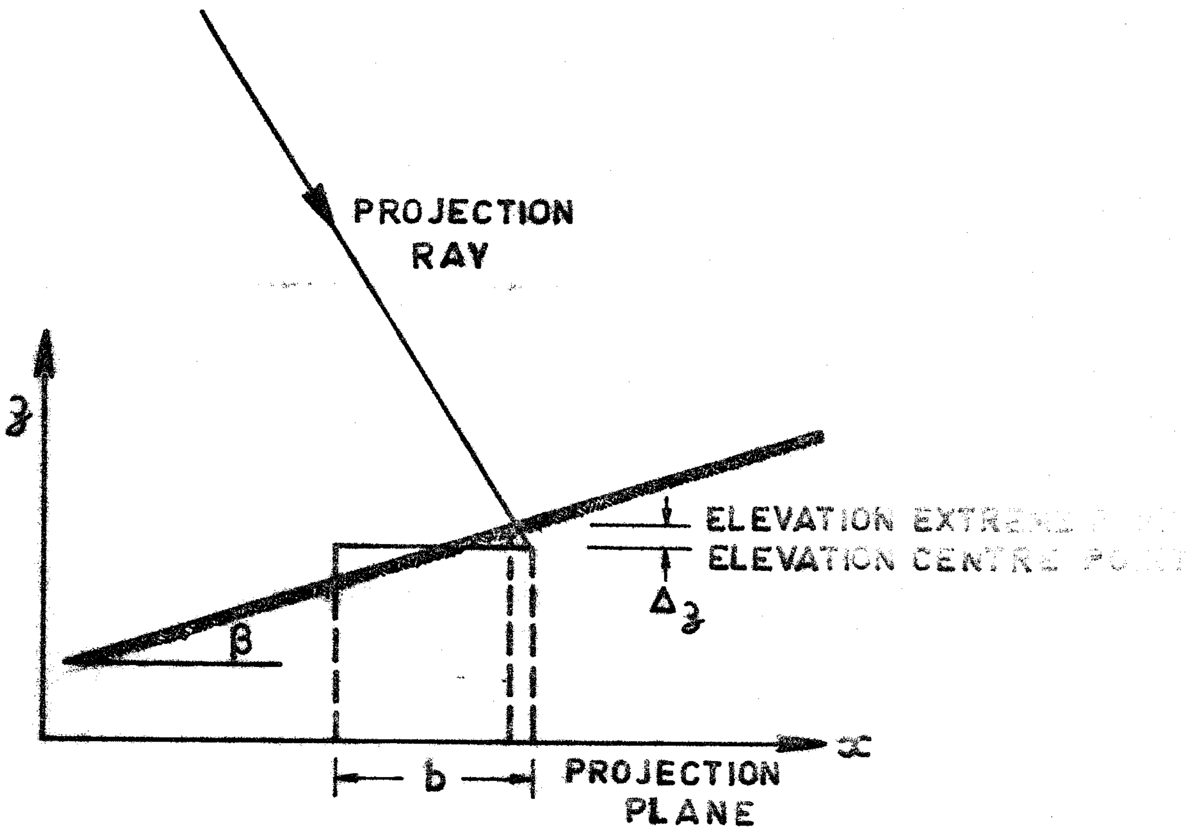

Fig. 2·2: System Error - Slit - Width

Figure 2.1 for example illustrates the available exposure slits for the Jena Topocart-Orthophoto combination. Each exposure slit has finite width (b) and length (l). At each end the slit is diagonally shaped, to provide an exposure blending area in successive scans, as a rectangular shape would result in visually obvious lines of double exposure or gap lines, in the event of the very smallest difference between the slit width and the incremental shift (Δx) between successive scan profiles in the model. Whilst system errors due to exposure slit width can be halved by halving the exposure slit width, each halving of the selected width doubles the operating time for a given scan speed. Clearly selection of optimum slit width for given terrain conditions is a decisive factor in efficient production planning.

System errors occur at the exposure slit, whether the slit is actually in the model surface (direct projection), or in an additional component as in the case of mechanical type plotting machines (non direct image transfer); if the terrain surface at the slit is not horizontal. In the case of sloping terrain across the exposure slit, perpendicular to the direction of movement of scan, even in the absence of observer elevation errors only the centre of the slit defined by the measuring mark position is at correct elevation; and other terrain points within the exposure element are projected with incorrect elevation. Such off-centre points suffer radial displacement away from the nadir or towards it (figures 2.2 and 2.3). The error in elevation Δ_z of an off centre point is a maximum $|\Delta_z|$ at the extreme end of the exposure element, and

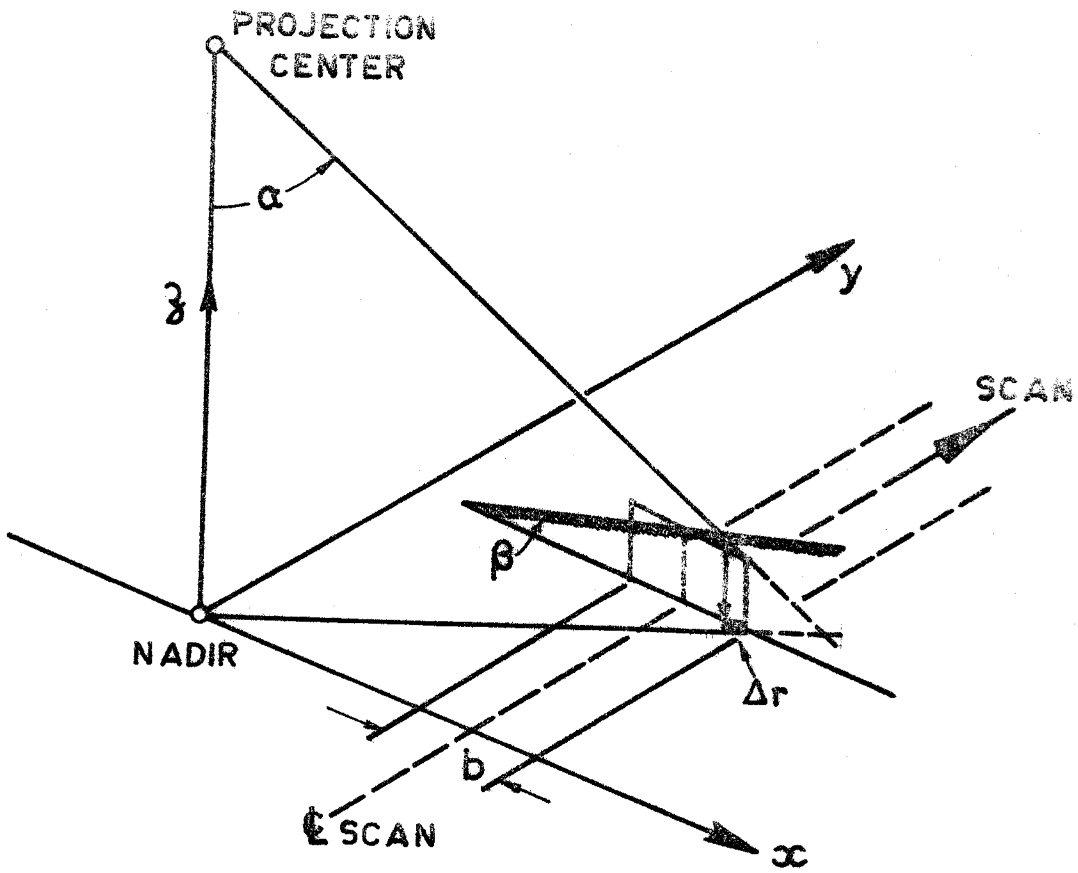

FIG. 2·3: Radial System Error

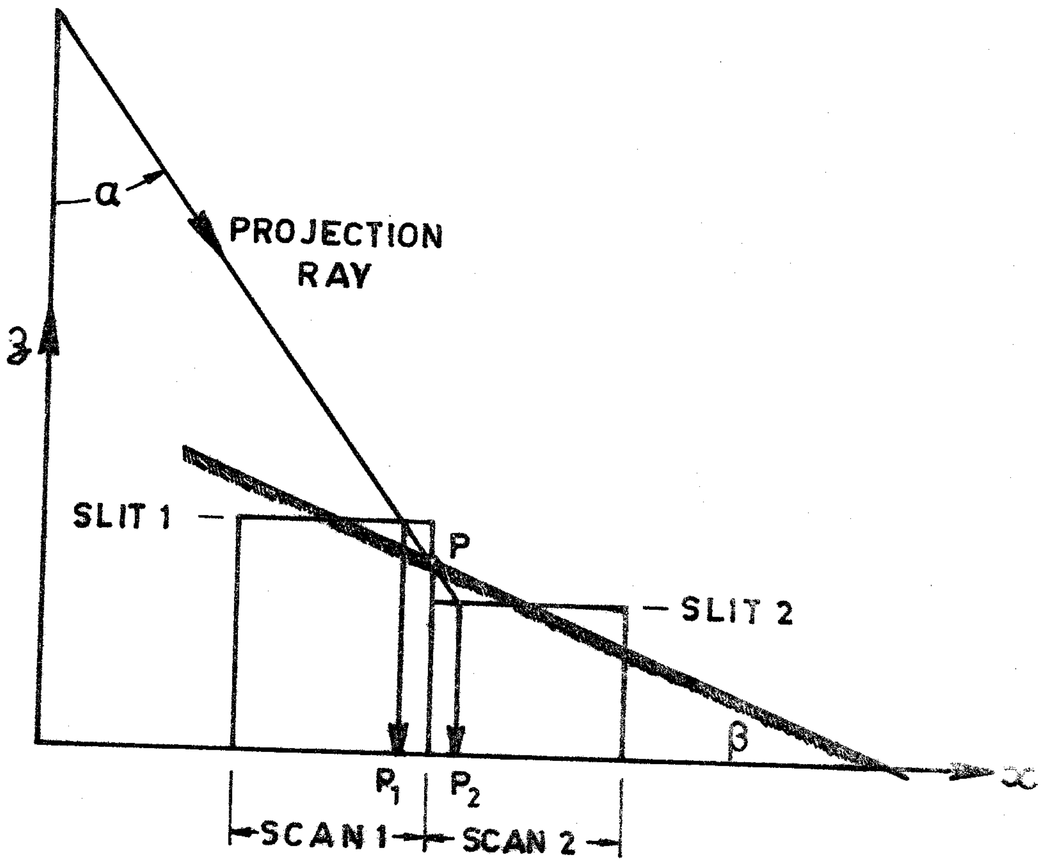

Fig. 2·4: Double Images at Slit Margin

for a transverse ground slope β_x may be taken with a slight degree of over-estimation as:

$$|\Delta_z| = \frac{b}{2} \tan \beta_x$$

The displacement in projected position Δr is however radial to the photograph nadir and proportional to the angular field α of the projection camera, whence

$$|\Delta_r| = \frac{b}{2} \tan\beta_x \tan \alpha \qquad (2.viii)$$

The system error due to slit width is also the cause of profile margin discrepancies in the form of overlaps of detail (points imaged twice) or missing detail (points not imaged) according to the direction of transverse slope. For example in figure 2.4 the terrain surface point P is projected in two successive scans to P_1 and P_2, and in the projection plane these two images are radially separated in the direction of the nadir. For the case of a terrain slope of opposite direction to the projection ray, detail in the scan margin would be missing. The maximum overlap may be taken as twice the maximum displacement (2.viii).

System errors due to slit width may be controlled by appropriate selection of slit width b, but at the expense of increase in scanning time. Other possibilities exist however, particularly when as in the case of the GZ1, the orthoprojector is operated off-line via a profile storage device. In such a mode of operation it is possible to carry out the scanning operation in the restitution plotter at a wide scanning increment Δ_x during which phase the plotter is linked to a storage unit SG1, in which each scan line is scribed as a profile on a 24 x 30 cm glass plate *(Meier, 1968, 61)*. Subsequently in off-line operation the storage plate is scanned in a scanning unit LG1 which is able to operate the orthoprojector at a scanning speed of 10 mm/sec in the projection plane, changing the projection distance according to the elevations recorded on the profiles. Furthermore a smaller incremental shift Δ_x may be selected, so that the width of the scan in the projection may be reduced to as little as one sixth of the profile interval used in the restitution plotter. Control of these additional intermediate profiles is by automatic linear interpolation of elevations across the recorded profiles.

An additional possibility with the GZ1 is the use of the *optical interpolation system* using fibre optics *(Brunnthaler, 1972, 95)*. With this attachment it is possible in effect to tilt the exposure slit according to the transverse terrain slope. A ring of fibre optics is placed around the slit of the orthoprojector with its base parallel to the projection plane, perpendicular to the directions of the optical fibres. The upper surface of the optic ring is shaped to contain gradients from horizontal to 35° slope. The appropriate slope is placed in the path of the projection rays by automatic interpolation of the recorded elevations across the scanning path.

In spite of the fact that the interpolating element is made of fibre optics, there is no loss of image quality, since with 16 µm fibres the resolution of the fibre optic ring is almost 30 lines per mm in the projection plane, increasing to as much as 90 lines per mm if 6 µm fibres are used *(Hobbie, 1969, 226)*.

In the absence of any correction device, control of system error due to slit *width* should be achieved in the production planning stage, by appropriate selection of exposure slit for terrain conditions. Figure 2.5 indicates the maximum displacement $|\Delta_r|$ which will occur for combinations of slit width and mean transverse terrain slopes β_x, for a scanning area of 200 mm (y) by 100 mm (x) at picture scale. Slopes in particular directions may be estimated from the work of NEUBAUER *(1969, 180)*, who investigated the frequency distribution of ground slopes (slopes in the fall line). Not taking into account unusual geomorphological formations, the fall line is found to be independent of azimuth; so that for a particular direction such as the transverse scan direction the relationship between mean transverse slope β_x and mean overall slope β may be expected to reach:

$$\tan \beta_x = \frac{\tan \beta}{\sqrt{2}} \qquad (2.ix)$$

2.3.ii

Slopes in the direction of scan produce no significant error in location of images, on account of the very short length of the exposure slit (excepting that an error may occur on account of observer profile error). Image quality may however deteriorate, due to projected image movement because of the movement in elevation of the slit during the period of transition of the slit through a projected ray (figure 2.6). For an angular field angle α_y in the model space YZ plane, radial direction $\hat{\gamma}$ in the XZ plane, slope β_y (in the direction of scan), and length of slit l, the image movement W is given by:

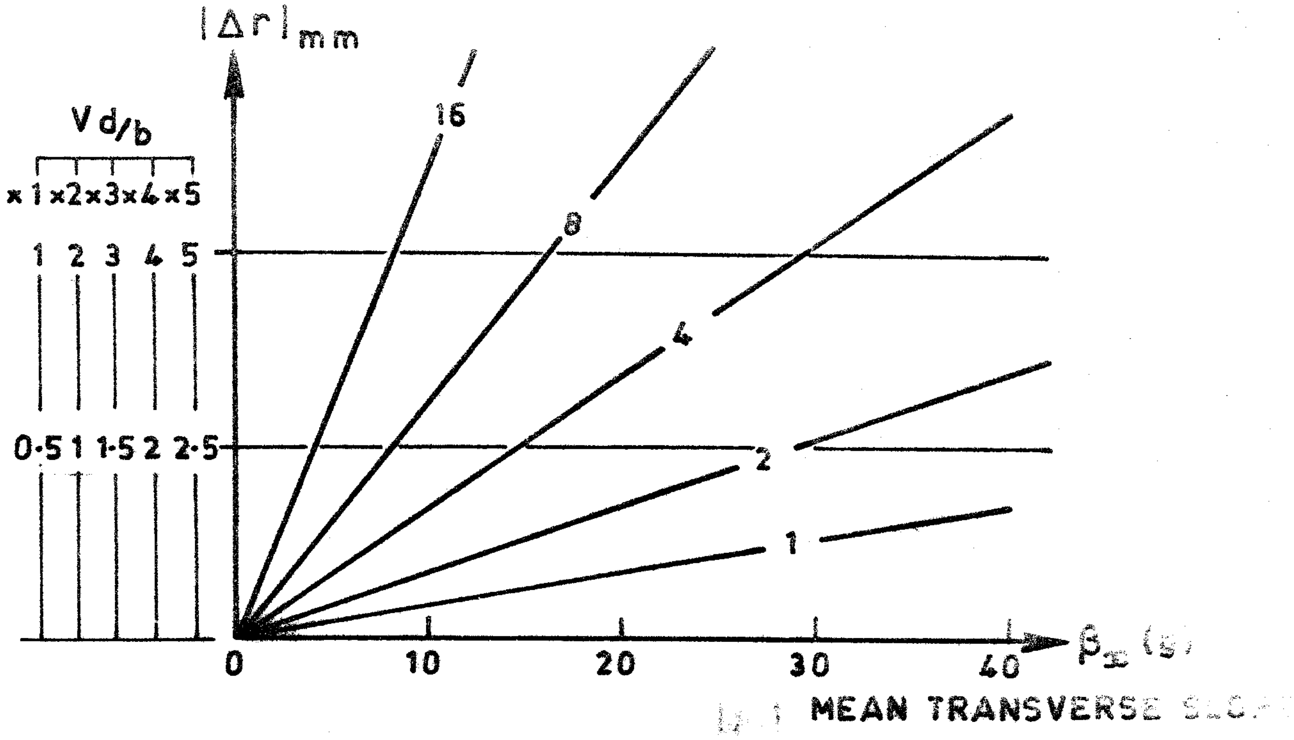

MAXIMUM RADIAL DISPLACEMENT $|\Delta r|_{mm}$ FOR SCAN AREA
100 mm. x BY 200 mm. y (AT PLATE) FOR 150 mm CAMERA
Vd/b : MAGNIFICATION RATIO FROM PLATE TO ORTHOPHOTO

Fig. 2·5

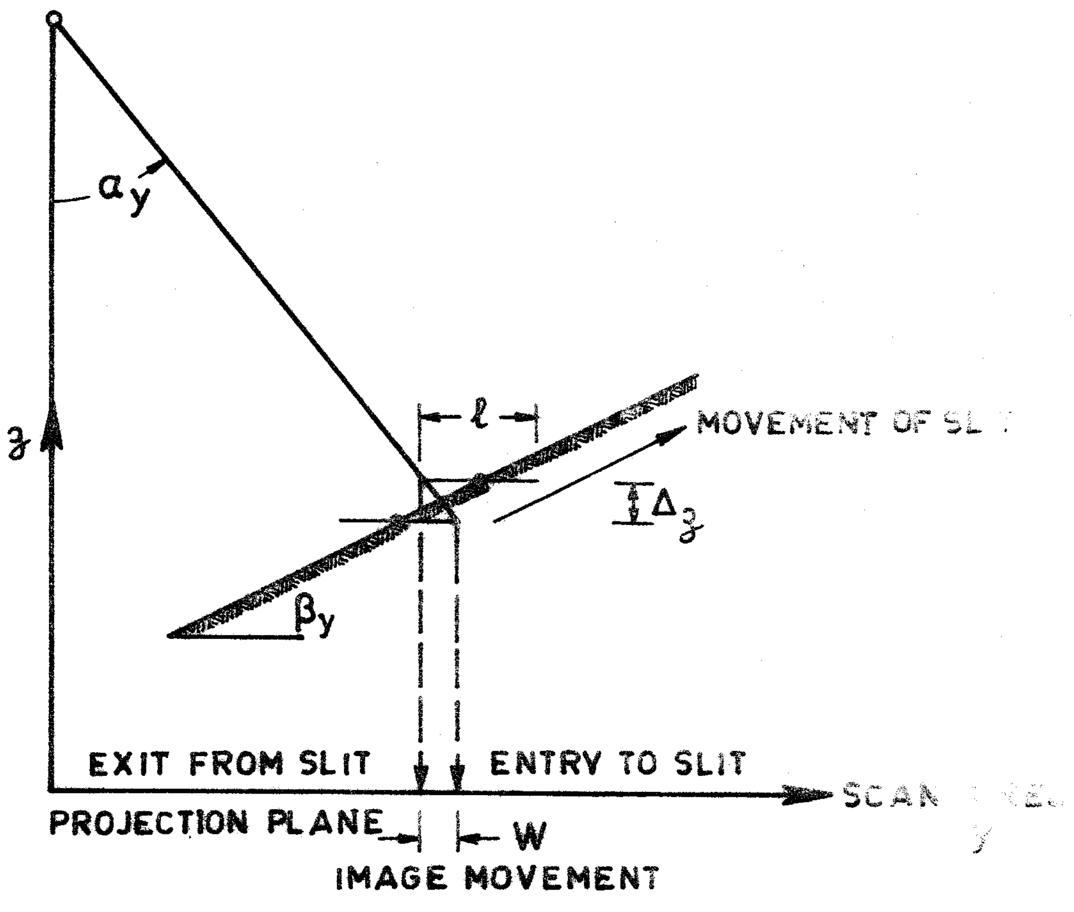

Fig. 2·6: Image Movement Due to Slit Length

$$W = 1 \left(\frac{\tan \alpha_y - \tan \beta_y}{1 - \tan \alpha_y \tan \beta_y \cos \gamma} \right) \qquad (2.x)$$

MEIER shows *(Meier, 1966, 91)* that a tolerance limit of 0.4 mm for image movement at the scale of the plate is just reached inside the maximum plotting area of a 23 x 23 cm wide angle photograph, for the case of a 1 mm length slit and 25° slope away from the projection ray. Again, control of image movement should be achieved at the planning stage by appropriate selection of slit *length* for prevailing terrain slopes. In the case of the JENA Orthophot , special slits are available for mountainous terrain in the following lengths:

Width	Length
4 mm	0.5 mm
4 mm	0.25mm
2 mm	0.25mm

2.4 Scanning Errors

2.4.i.

Scanning errors are due to incorrect elimination of x parallaxes by the observer, so that the measuring mark is not at correct elevation. It is clear that they should not be classified as 'system' errors, since such an error is commonplace in any normal restitution method, and thus the errors are restitution errors. In the case of flat terrain, an elevation error Δ_z results in a planimetric displacement Δ_r radial from the nadir as a function of the angular field α (figure 2.7):

$$\Delta r = \Delta z \tan \alpha$$

MEIER *(1966, 83)* considers that in the case of sloping terrain, and the dynamic scanning mode of operation, the error in z is made up of two components. One is a constant C_c expressing the fact that an error will be made even when the mark is stationary, for which MEIER estimates a mean square value of $0.1^o/_{oo}Z$. The other part is variable dependent upon the velocity of scanning V_B, the ground slope in the scan direction β_y, and the reaction time C_t which is taken by the observer to convert visual stereoscopic information into the appropriate Δ_z correction of the measuring mark. Accordingly, (figure 2.8), the mark and the exposure slit travel forward a distance $V_B.C_t$ during the reaction interval, and the corresponding elevation error Δ_z taking into account the constant error, is:

$$\Delta_z = V_B.C_t.\tan\beta_y + C_c \qquad (2.xii)$$

Equation (2.xii) then represents the error in elevation due to the scanning process, and the corresponding planimetric displacement is:

$$\Delta_r = \tan\alpha\,(V_B.C_t.\tan\beta_y + C_c) \qquad (2.xiii)$$

From (2.xii) we may derive the mean square error in elevation in any concurrently produced elevation record such as a drop line chart, in terms of speed in the image plane V_B, camera focal length f in mm, and mean slope β_y in the scan direction as:

$$m_z(^o/oo) = \pm\sqrt{\left[\left[\frac{1000}{f}.\tan\beta_y.V_B.C_t\right]^2 + C_c{}^2\right]}$$

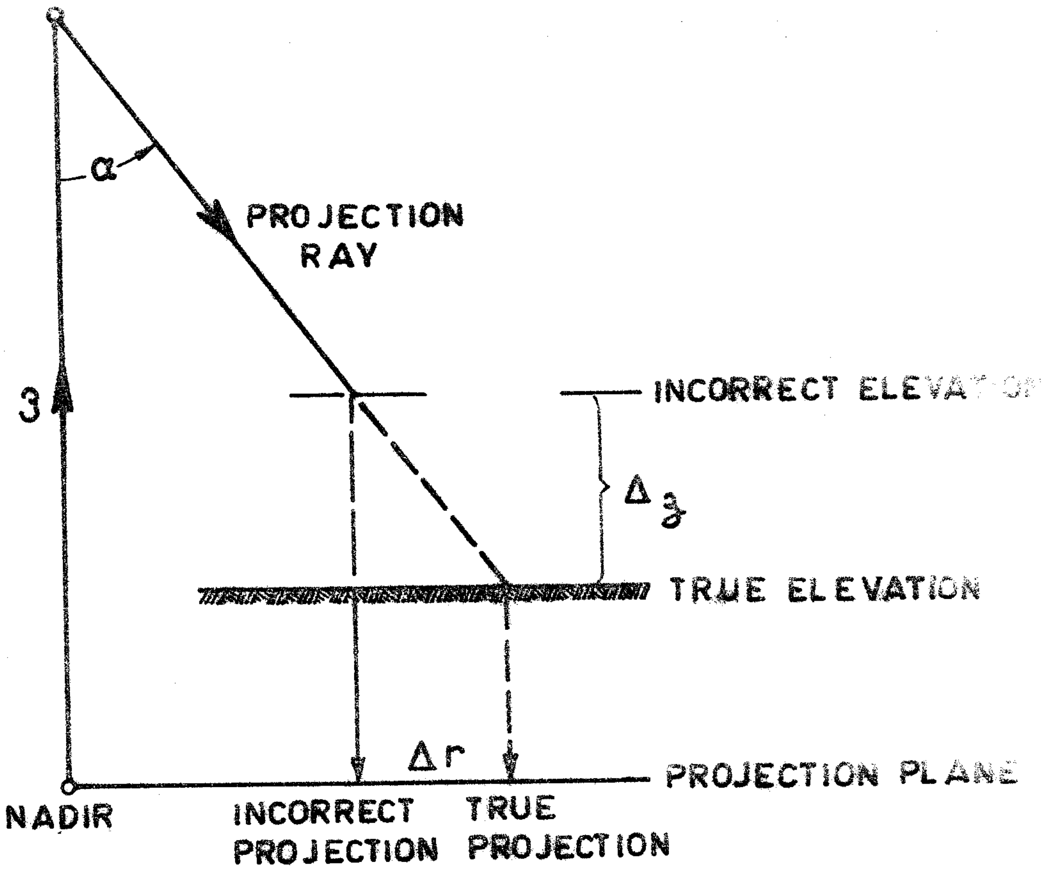

Fig. 2·7: Radial Displacement Due to Observational Scan Error.

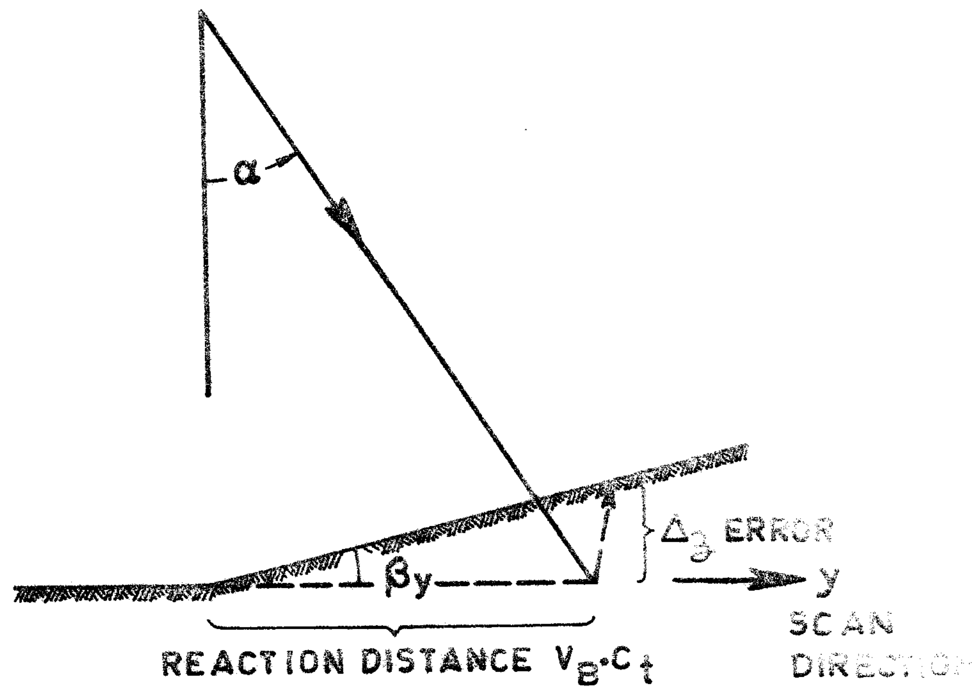

Fig. 2·8: Elevation Error Due to Reaction Time.

MEIER *(1966, 84)* gives a graph of this relationship with arguments maximum slope and image plane speeds 1-4 mm/sec, using $C_t = 0.16$ sec, and deriving a range of m_z of 0.2 - 0.6‰ Z

2.4.ii

In making estimates of theoretical accuracy for particular cases, it is important not to confuse the same sources of error, and for this reason the writer prefers to remove the constant part C_c from MEIER's formulae, since this is strictly a usual restitution error and is accounted for in equations 2.1 to 2.iv. The question also arises as to the general validity of equations 2.xii and 2.iii. Whilst it seems very reasonable that errors of this type should take place when *changes of slope* are encountered during the scan, it also seems reasonable to assume that on uniform slopes the operator will respond with correct elevation rate of change after an initial adjustment of elevation; so that only the usual elevation errors will be made on average, with irregular errors whose frequency depends on the frequency of slope changes in the terrain rather than the actual slope.

2.5 Connection errors and projection film errors

2.5.i.

Connection errors occur when the projection film is not located in the model space, as it is for example in the case of the Bean Orthophotoscopes. In the case of an off-line direct-projection system such as the GZ1, the possibility arises of incorrect setting of the exterior orientation elements of the projection camera, but the errors due to this source will be negligible if correct procedures are followed, as the effect of very small tilt setting errors has little influence in planimetric position. Care must be exercised in the fine setting of kappa so that the recorded profiles and the scan direction are correctly aligned. The major error possibility lies in incorrect transfer of Z (magnification control) due to mechanical tolerances, causing a planimetric displacement proportional to angular field: $\Delta Z . \tan \alpha$. MEIER *(1966, 80)* estimates a mean square coordinate error of the order of ±0.030 mm in the orthophoto due to this cause.

The flatness of the film platform surface, the degree of efficiency of the electrostatic tightening of the film, and the scaling of the film also contribute to planimetric errors. Film deformation errors arise from processing of the exposed film, but differential errors amounting to a non-uniform scale change are negligible in the case of a polyester base film, since unlike film in a serial camera there is no tension in one direction due to film advance. Uniform scale changes may be estimated to give a mean square error of ± 5 µm in the scale of the aerial photograph *(Ahrend, 1966, 66)*. There may in any case be no real significance in the case of uniform scale changes, depending on the subsequent reproduction techniques for the orthophotograph. If the treatment involves only contact reproduction techniques, the planimetric scale error will have no significance in position location if the orthophotograph is combined with a grid or a scale bar correspondingly adjusted; so that the error will only be noticeable in matches with adjacent sheets. In the case of reproduction involving process camera work, the orthophoto negative will in any case be rescaled. VISSER *(1968, 8)* concludes from his tests of GZ1 that flatness of table surface, tightening of film, and deformation of film together contribute to planimetric mean square coordinate errors of ± 0.07 mm in the scale of the orthophoto, corresponding to ±25 μm in the scale of the aerial photograph for his enlargement setting.

2.5.ii

In the case of on-line projection not in the model space, such as takes place in the Jena Topocart, connection errors are negligible provided that the optical and mechanical system is correctly calibrated and aligned; so that the measuring mark position coincides with the centre of the exposure slit throughout a scan run. As the optical transfer axis is orthogonal to the projection film, no error takes place in dependence of the angular field. However as the optical transfer is non-direct projection, so no optical rectification of the images within the exposure slit takes place; and the possibility arises of scale variations and of ϕ tilt image rotations within the exposure slit, which will be discussed in 3.9. The film flattening in the exposure plane is mechanically enforced within a film cassette, with the theoretical possiblity of affine deformation of x direction relative to y direction as the film is advanced across the cassette shutter in incremental Δx steps. However the writer has not been able to detect any significant differences between x and y residual errors at control points in his series of tests, which might be accounted for by affine deformation of film. It seems reasonable only to allow for uniform scale changes in theoretical predictions.

3. CHARACTERISTICS OF THE TOPOCART-B-ORTHOPHOT-OROGRAPH INSTRUMENT COMBINATION

3.1

The JENA Topocart B plotting machine of topographic classification evolved from the earlier model Topocart C *(Cimerman and Tomasegović, 1970, 150)*. The differential rectifier Orthophot A **was** introduced in 1965, originally as a component of the stereotrigomat universal instrument system, an improved version Orthophot B being introduced in 1968. The first combination of the Orthophot with the lower order plotter Topograph appeared in 1969. The current version, which also provides for drop line chart drawing with the drawing head Orograph, has been used in the tests described in the work (plate 1).

3.2

The plotter Topocart B is an extremely versatile equipment of rather unusual mechanical design features, and is capable of very high restitution precision for an instrument of this classification. For plotting purposes only, as distinct from orthophotography, it is possible to plot from negatives or positives on glass, film, or paper; over an extremely wide range of focal lengths of camera (C_k = 50 mm to 215 mm). The range of z movement permits the following magnification ranges ($V_{m/b}$) between plate and model for the usual camera types:

Super wide angle 88 mm:	0.8	to	2.2
Wide angle 115 mm:	0.6	to	2.7
Wide angle 150 mm:	0.5	to	2.1
Normal angle 210 mm:	0.3	to	1.5

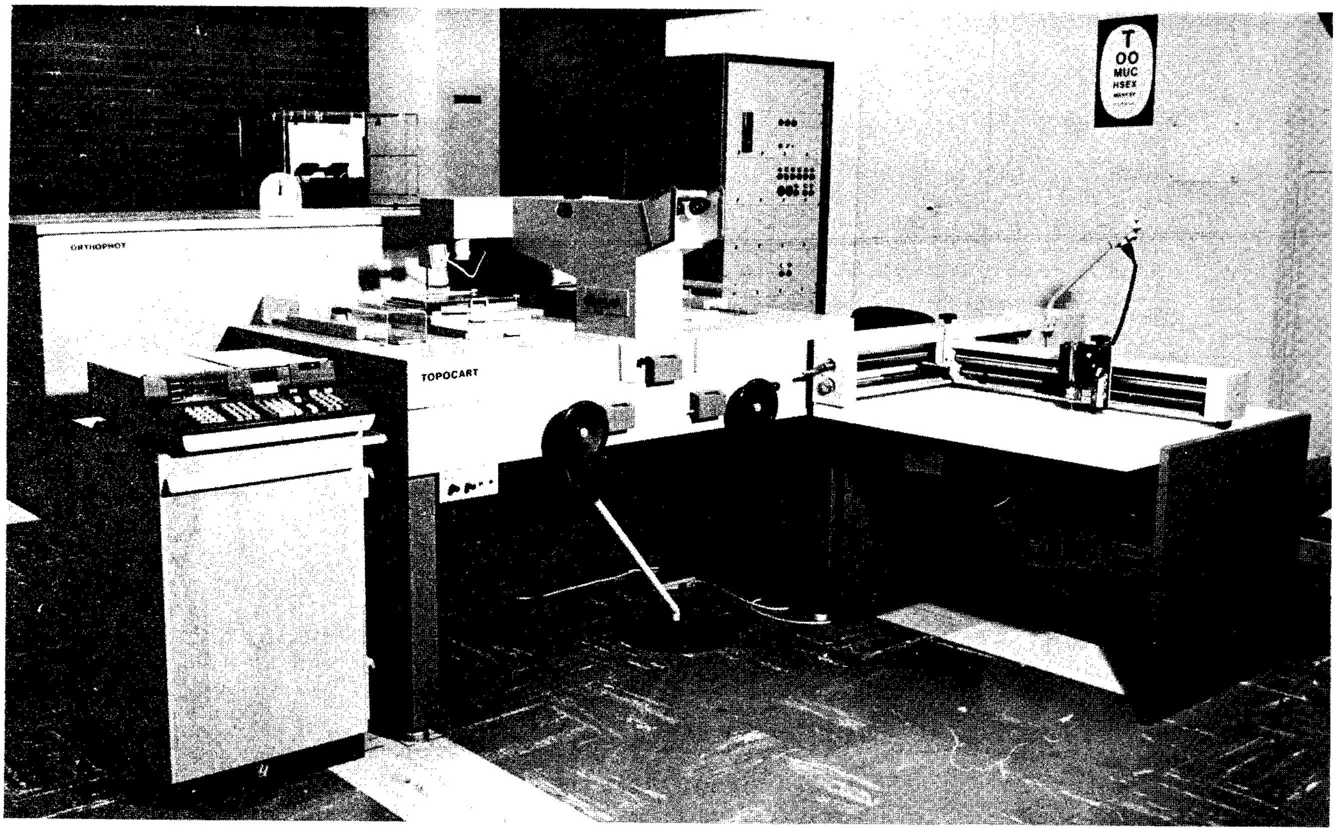

Topocart-Orthophot-Orograph with HP9810A

desk calculator

PLATE 1

The ratio from plate to map scale ($V_{k/b}$) may be selected by transmission gears to the drawing table in a total range 0.1 to 10 times. Lateral and longitudinal tilt of the camera ω and ϕ may be accommodated to ±5g. The connections to x and y handwheels, and to z foot disc are interchangeable, and any two drives may be transmitted to the drawing table; making it possible to plot from terrestial photographs for both terrestial topographic and close-up photogrammetry; and to plot profiles and cross sections from aerial photography.

Mechanical coordinate counters can be read directly to 0.01 mm in the model, and may easily be set to specific numbers and reversed in direction, so that the plotter may readily be used for numerical applications. The x, y, z output shafts can be fitted with digital encoders without difficulty.

3.3

The plate carriers are mounted horizontally on x and y carriages, but are not capable of physical tilt rotations in the usual manner of plotting cameras, other than kappa rotations. Instead the transformation between each pair of plate image coordinates x'y', and the corresponding model coordinates xy, is realised through analogue computers for each photograph carrier system. The computers take the form of lineals or straight-edges, arranged to rotate in horizontal planes around a verical axis of rotation below each carrier system. The spatial direction for each image is first projected into corresponding directions in xy and yz planes, represented by corresponding horizontally stacked x and y lineals on each side The spatial coordinates x and y corresponding to each partial image, are transformed by the lineals into image coordinates

$x'y'$, which may be in a photograph tilted by angles ϕ and ω in nature. The transformation for each plate carrier is rigorous according to the following equations for perspective transformation:

$$x = \frac{[(C_k.\cos\omega - y'\sin\omega)\sin\phi + x'\cos\phi]}{(C_k.\cos\omega - y'\sin\omega)\cos\phi - x'\sin\phi}.z \qquad (3.i)$$

$$y = \frac{(y'\cos\omega + C_k.\sin\omega)}{(C_k.\cos\omega - y'\sin\omega)\cos\phi - x'\sin\phi}.z \qquad (3.ii)$$

Equations 3.1 and 3.ii are respectively equivalent to 1.iii and 1.iv. The horizontally stacked lineals on each side thus perform the functions of mechanical computing rectifiers for each corresponding pair of plate images. Auxiliary lineals capable of being fixed at angular displacements permit the ϕ and ω rotations to be set separately for each side. For base scaling setting bx, the right space point is translated relative to the left, and additionally at the right space point it is possible to set a translation movement by'', controlled by micrometer drums so that y parallax measurements can be made. Movement in z is effected by foot disc and drive to a z carriage which supports guides for x and y movement carriages. Additional relative movement of the right x and y carriages corresponds to a translation base component bz'', divided for each space direction lineal into components bz_x'' and bz_y''. Since the spatial direction for each projection ray is separated into projections in xz and yz planes, the camera constant C_k is accordingly separated into components C_{kx} and C_{ky} on each side. It is therefore possible to set different constants for x and y directions at the plate, by which affine errors due to differential film shrinkage may be compensated.

A complete description of the plotter and in particular the mechanical computers, is given in the appropriate instrument handbook *(VEB Carl Zeiss Jena, 1971)*.

3.4

The Orthophot B differential rectification unit is rigidly attached to the rear of the Topocart plotter in a cast box-section frame, entirely enclosed in removeable panels. Access to the interior is provided through a door panel, in order to permit the insertion and removal of a film cassette so that the scanning operation may be carried out on line to the plotting machine, in a room under normal lighting conditions. The film cassette (10, fig. 3.1) consists of a casing with a hinged lid, enclosing a film carrier so that the cassette is completely light proof. On the underside of the casing there is a slotted aperture extending the entire length of the cassette, covered by a shutter blind, which can only be released mechanically when the cassette is in operating position within the Orthophot. Micro switch contacts ensure that the scanning operation cannot be commenced with the shutter closed.

The film carrier is a cylindrical drum, to which one edge of the y direction of the film is firmly fixed by spring-loaded pin clips. The film sheet is drawn tightly over a film stage through felt jaws, as the drum rotates for each incremental Δx step during the scanning operation. A gear at the end of the axis engages with the step switch mechanism (9, fig. 3.7), and transmits the Δx increment to the film carrier. The drum diameter of the cassette is designed for a film thickness of 0.20 mm, but film in the range 0.15 to 0.25 mm can be used without focussing difficulties. The maximum size of film which

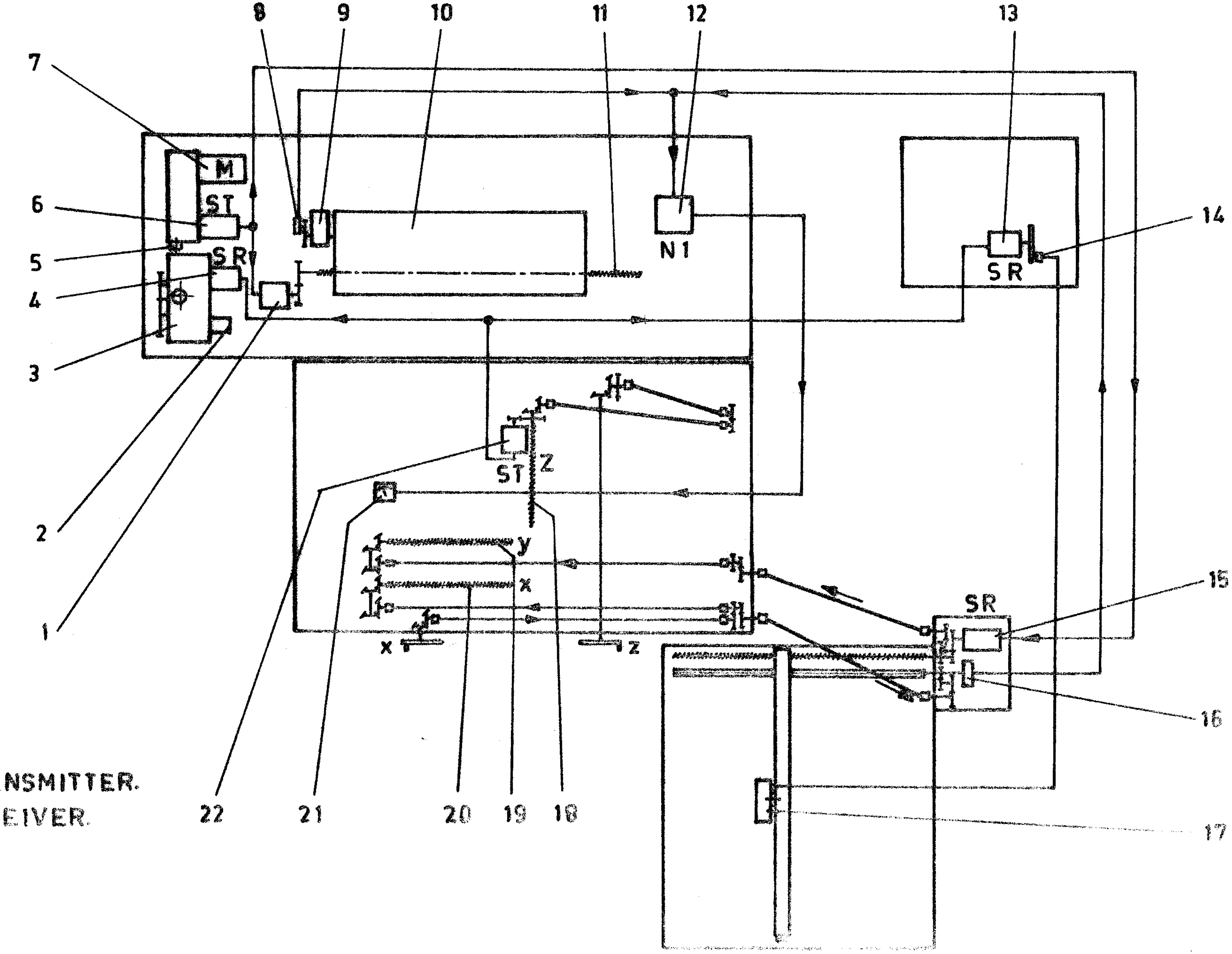

M: MOTOR.
ST: SELSYN TRANSMITTER.
SR: SELSYN RECEIVER.

[illegible] – Orthophot – Orograph[illegible] can be inserted is 600 mm (x direction) by 750 mm (y direction). However about 50 mm at each side in x direction is required to attach the film in the cassette, and about 20 mm must be allowed in the y direction at the starting end, so that the effective maximum film format is 500 mm (x) by 730 mm (y). The image magnification control permits magnification possibilities from original picture to orthophoto ($V_{d/b}$) within the range 0.7 to 5 for flat terrain; but for a scanning area of 100 mm x by 200 mm y in the picture scale, corresponding to full usable format, the maximum enlargement $V_{d/b}$ is 3.65 times in one operation of scanning; corresponding to the maximum effective orthophoto film format. In order to utilise the $V_{d/b}$ upper limit of 5, the scanning operation must be carried out in two phases for the upper and lower portions of the picture.

3.5

During scanning the cassette carriage is activated by a y spindle (11 fig. 3.1), to move backwards and forwards in the y direction across the slit diaphragm (14 fig. 3.2). A motor (7 fig. 3.1), the speed of which is stabilized, and which can be controlled in an overall ratio of 1 : 9; drives a y selysyn transmitter (6 fig. 3.1), via a gear which changes the speed in two stages. The y selsyn transmitter is connected by cable to receivers on the y spindle of the cassette carriage (1 fig. 3.1), and on the drawing table (15 fig. 3.1). The drawing table receiver is in turn mechanically connected through gear wheels and lead screw to the Orograph drop line drawing head (17 fig. 3.1), and to the y spindle in the Topocart

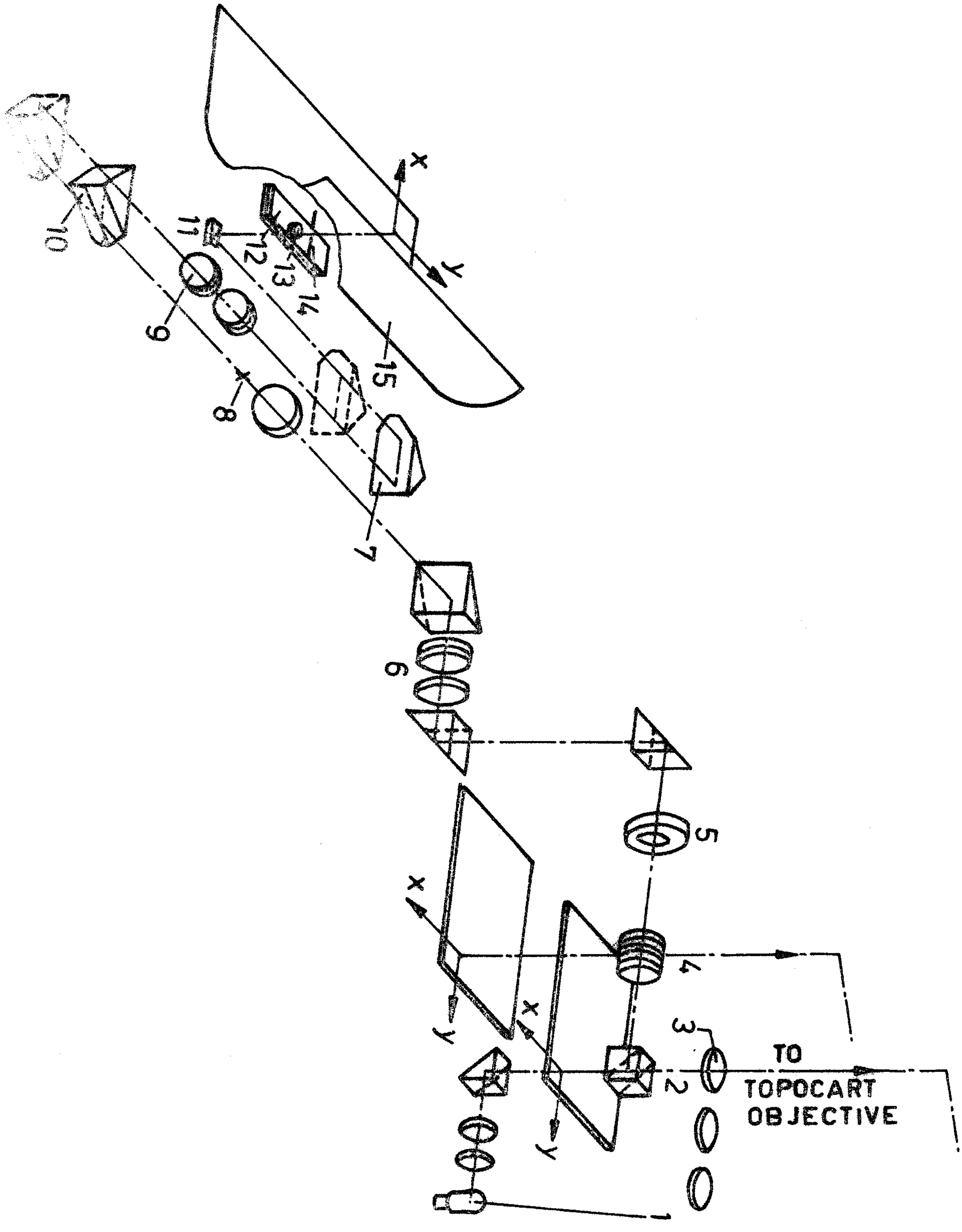
1
2
3
4
5
6
7
8
9
10
11
12
13
14
15
x
y
TO
TOPOCART
OBJECTIVE

(19 fig. 3.1); so that the cassette, drawing table, and model y drives are continuously coordinated.

In order to be able to adapt scan speed to terrain conditions, y scan speed can be varied by the operator during the scan by finger tip control; in a ratio of 1 : 3 of a selected basic speed within the overall 1 : 9 ratio of the drive motor. Basic scan speed is adjusted to a suitable mean value, by a trial scan at varied speeds through the most difficult terrain area of the photograph, before the operational scanning commences. Speeds of 0.7 to 2.0 mm/sec in the picture scale are recommended for difficult terrain, and 1 to 3 mm/sec for simple terrain. Multiplication of these speeds by the overall magnification factor $Vd/_b$ gives speed in the rectification plane; and reference to figure 3.3 shows the appropriate basic speed setting (controlled by potentiometer as a fixed setting), the appropriate y selsyn gear stage fast or slow, and the variation of speed possible under operator control during the scan.

As film exposure is proportional to y scan speed, speed variation during scan would normally result in exposure changes with consequential density variations in the developed film. In order to compensate this, a variable density grey wedge is placed below the slit diaphragm (12 fig. 3.2), which is automatically moved to appropriate transmission density when the operators variable speed control is adjusted. The ability to achieve constant film exposure over a wide range of scan speed by finger-tip control, is a very desirable feature of on-line orthophoto production.

3.6

The Δx increment necessary to move from one scan profile to the next, is activated by a mechanical step switch mechanism. The increment is selected by a numbered control knob, corresponding to the slit width placed in the diaphragm aperture, and activates adjustable stops at the step switch mechanism.

The transmission of the increment to the drawing table and thence to the plotter, is effected by a Wheatstone bridge as measuring element. A generator potentiometer (8 fig. 3.1) transforms the Δx increment at the step switch mechanism to an analogous electrical resistance. A receiver potentiometer (16 fig. 3.1) is fixed at the drawing table gears. As the Δx increment is released by the step switch mechanism at the cassette, at the limit of each y scan by an end limit switch, so the Wheatstone bridge becomes unbalanced. The operator then carries out an x movement using the x-handwheel of the Topocart, which adjusts the receiver potentiometer until zero balance of the bridge is restored. Exact balance is indicated by a null indicator (12, fig. 3.1) visible from the observers operational position.

3.7

Contrary to the original Stereotrigomat system, the right hand photograph in the topocart is the photograph differentially rectified. The illumination source for projection is a fan-cooled 12 V. 100 w. halogen lamp (1 fig. 3.2), directed through the right hand diapositive. The visual observation ray path is interrupted by a beam splitting prism (2 fig. 3.2), and two lens element systems (4 and 6, fig. 3.2) produce through two deflection prisms, a real exactly twice-magnified intermediate image of the photograph image at a point 8 fig. 3.2. This intermediate image is again brought to an image at the film stage in the cassette, through two roof prisms (7 and 10, fig. 3.2), a projection lens (9 fig. 3.2) between the roof prisms, and a final deflection prism 11 fig. 3.2. The roof prisms are mechanically coupled by a Peancellier inversor, so that the prisms shift towards or away from one another along the optical axis of the projection lens of focal length f_e. Each position of the inversor and of the roof prims corresponds to a certain magnification of the projected image at the rectification plane, compared to the twice magnified intermediate image. The extra focal distances m and m^1 from the focal points of the projector lens, to the intermediate image point and to the rectification plane respectively, are coordinated by the Peancellier inversor, so that correct focussing corresponding to the Newtonian lens law $m.^1m = f_e^2$ is achieved. The corresponding principal distance a and projection distance a^1 give the imaging ratio:

$$V^{d}/_{b} = \frac{a^1}{a} \qquad (3.111)$$

This imaging ratio must be continuously varied according to terrain elevations on the centre line of the scan profile, in order that photograph images at non-uniform scale due to elevation differences are brought to the required uniform orthophoto scale. Control of magnification is provided by the parameters c_k of the camera constant, and variable z in the Topocart model, also taking into account the intermediate double magnification, and the magnification factor $Vd/_m$ from model to rectification plane:

$$Vd/_b = \frac{a^1}{a} = \frac{z}{C_k} \cdot Vd/_m \qquad (3.iv)$$

Control is achieved by a self-balancing potentiometer computing bridge, on the transmitter side of which the variable ratio $Vd/_b$ is simulated by the analogous ratio of the resistances of a set of linear potentiometers. The z component resistance is presented through a helical potentiometer variable by movement of the z spindle, multiplied by the magnification factor $Vd/_m$ set at the Orthophot by interchangeable gear wheels. Additionally a correction to the z resistance on account of the b_z" base component if any, is set by a second potentiometer at the Orthophot. The variable camera constant c_k also represented by a resistance, is set on a counter at the Orthophot as the resistance of a further helical potentiometer. A linear potentiometer is coupled by gears to the projection-side roof prism of the Pencellier inversor, the movement of which is controlled by servo motor activated by any current in the computing bridge. A movement in z at the plotter produces a drive to the servo motor until zero balance is restored at the computing bridge, when there is coincidence between the computed scale and the imaging scale set by the inversor.

3.8

The z selsyn transmitter (22, fig. 3.1) providing the z data for control of magnification, is also utilised for control of the Orograph dropline drawing head for presentation of elevation data. A separate z selsyn receiver(13, fig. 3.1) is placed in the electronic control cabinet, the rotary movements of this receiver acting on an optical pulse generator scanned by a photoelectric device. The analogue to digital converter transforms the input shaft rotations into electric pulse sequences which show the magnitude and direction of each change in elevation. For each revolution of the input shaft, the pulse generator supplies 625 pulse changes, one such pulse corresponding to 0.001 mm change in the elevation of the floating mark in the plotter model. An output signal generator (14, fig. 3.1) energizes an alternating current magnet in the drawing head (17 fig. 3.1) at appropriate contour intervals which may be selected. Contour intervals are selected by placing an adaptor plug, identified by a number equivalent to the contour interval in terms of model scale millimetres, into the electronic control cabinet. A large number of such plugs are available in the range 0.03 to 5.08 mm, equivalent to metre and feet intervals for standard metric and imperial map scales.

The drawing head is designed to contain a vertical plunger into which is fixed a steel scribing needle. The alternating current magnet causes the scribing needle to oscillate at right angles to the direction of movement of the drawing head (y scan direction) at 100 Hz frequency. The pulse generator

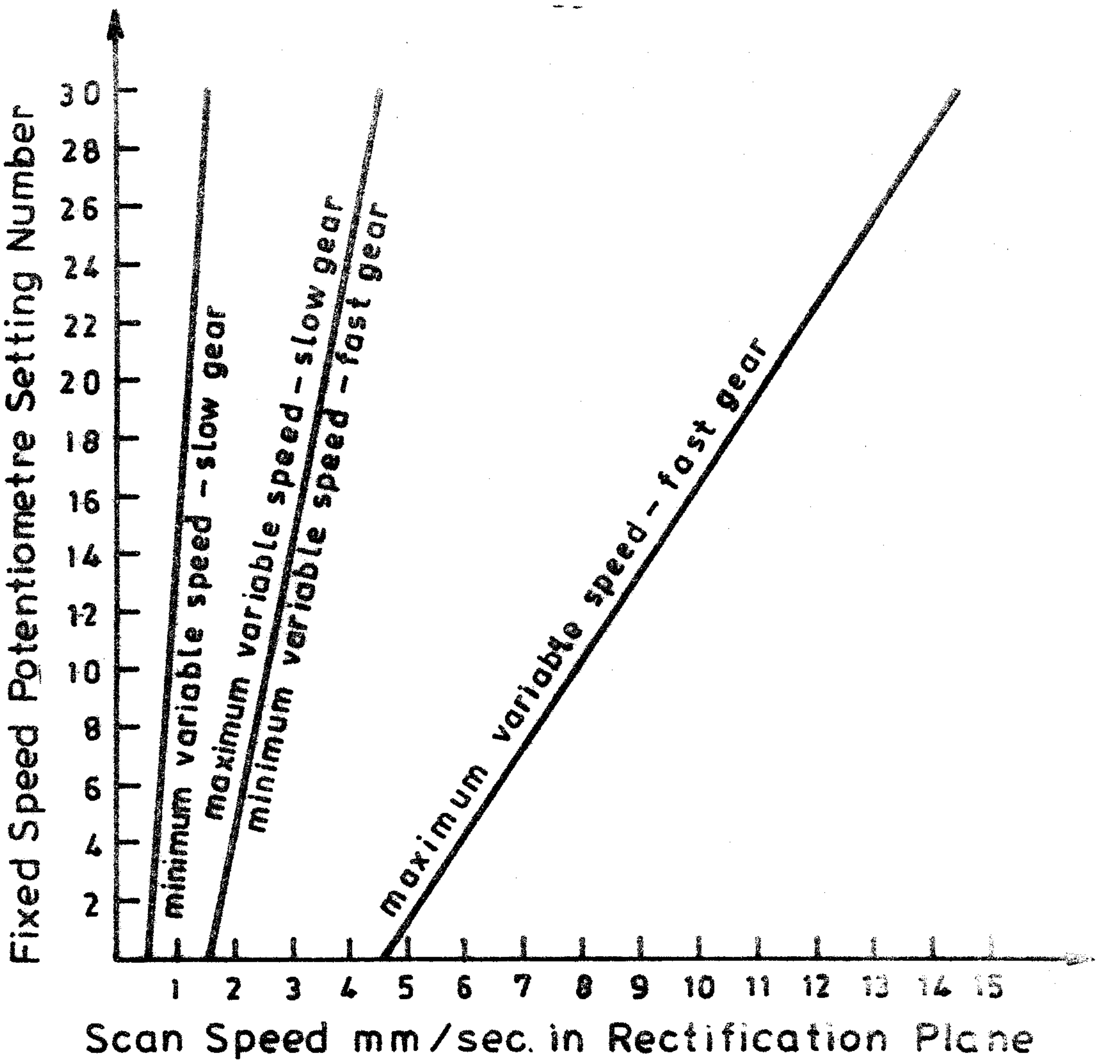

FIG. 3·3. SCAN SPEED CONTROL POSSIBILITIES

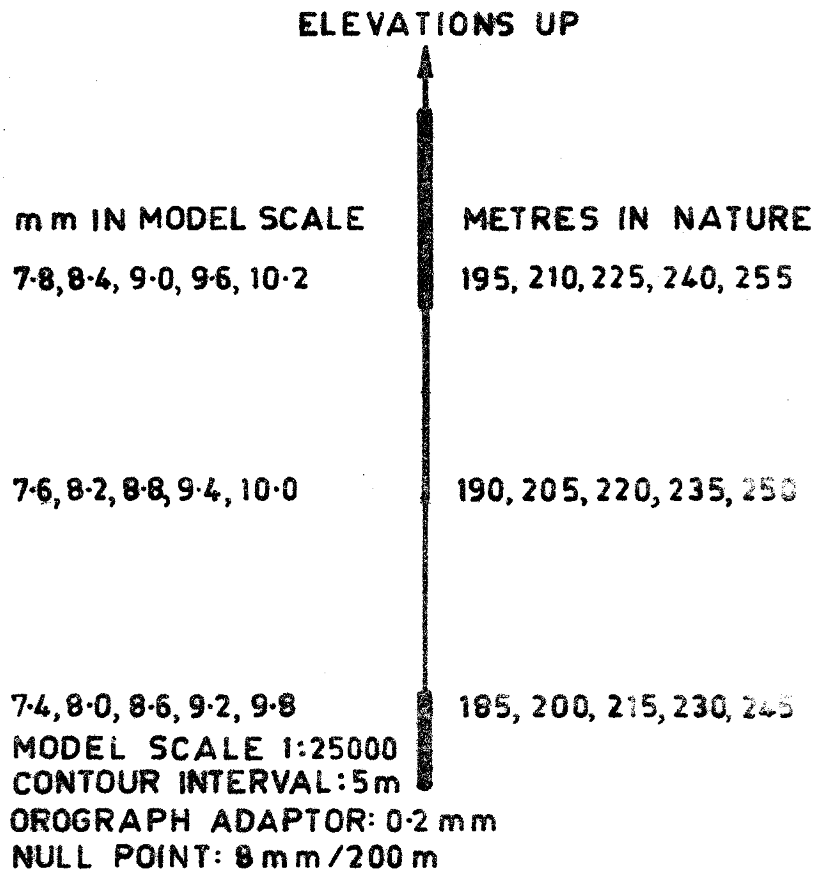

FIG. 3·4. CONTOUR ZONE DROP LINES PROD[illegible]
BY OROGRAPH

feeds two different voltage signals corresponding to two different amplitudes of the needle to the magnet. Including a condition in which there is no input signal, the result is that three different line thicknesses are generated, the centre thickness of which is adjustable at the drawing head relative to the other two. Each line length then represents a band width horizontally of a particular zone between two contours. It is necessary to identify the starting point of a sequence of lines, and this is done by nulling the Orograph with the model z counter set at a selected whole number. The first line in the upwards direction is then the finest line thickness. For the case of the scribing needle, the line thickness of the thin line is 0.1 to 0.2 mm depending on the grinding of the needle point. The thick line is dependent on the setting of the magnet with respect to the scribing plunger and should be 0.8 to 1.0 mm. The medium line may then be adjusted to provide clear differentiation. The scribing needle is intended to be used in conjunction with emulsion coated glass plates as drawing medium, but in the tests described in this work a ball point pen was substituted, and the drawing medium used was a five-sheet laminated white drawing card with a smooth finish. The most suitable ball point was found by experimentation to be a black fine point 'Jumbo' refill by Papermate. The white card was found to be more suitable than drafting film, which tended to fill the ball housing of the ball point with plastic residue. Figure 3.4 illustrates the identification of contour zones in a particular case.

3.9 Non-direct image transfer errors

In direct optical image transfer by reprojection such as takes place in the Bean Orthophotoscopes and the GZ1, scale variations and image rotations due to photographic tilts are optically rectified by reprojection; so that if no observer errors or system errors are made (flat terrain conditions), the projected images are perfectly rectified. In the case of the non-direct image transfer system of the Topocart, the magnification control by the inversor allows only for change of scale of image due to elevation differences. Scale variations due to ω and ϕ tilts are illustrated in fig. 3.5, showing the distortion of an orthogonal square grid in flat terrain. As the movement of the exposure slit of width b is in the y direction of the plate, it is seen that an ω tilt causes uniform scale change along the slit width, but the scale varies during the scan according to y plate coordinate. The effect of ϕ tilt is to cause scale variation proportional to x coordinate, i.e. non uniform along the slit width; and additionally a rotation of images within the slit.

Corrections must be made for the effect of the scale variation within the exposure slit, as otherwise displacement of detail would occur on the slit margins, causing overlaps and missing details. The non-uniform effect of the ϕ scale variation is negligible within the small slit widths, taking into account the small tilts possible in a plotter designed for near-vertical photography, but correction must be made

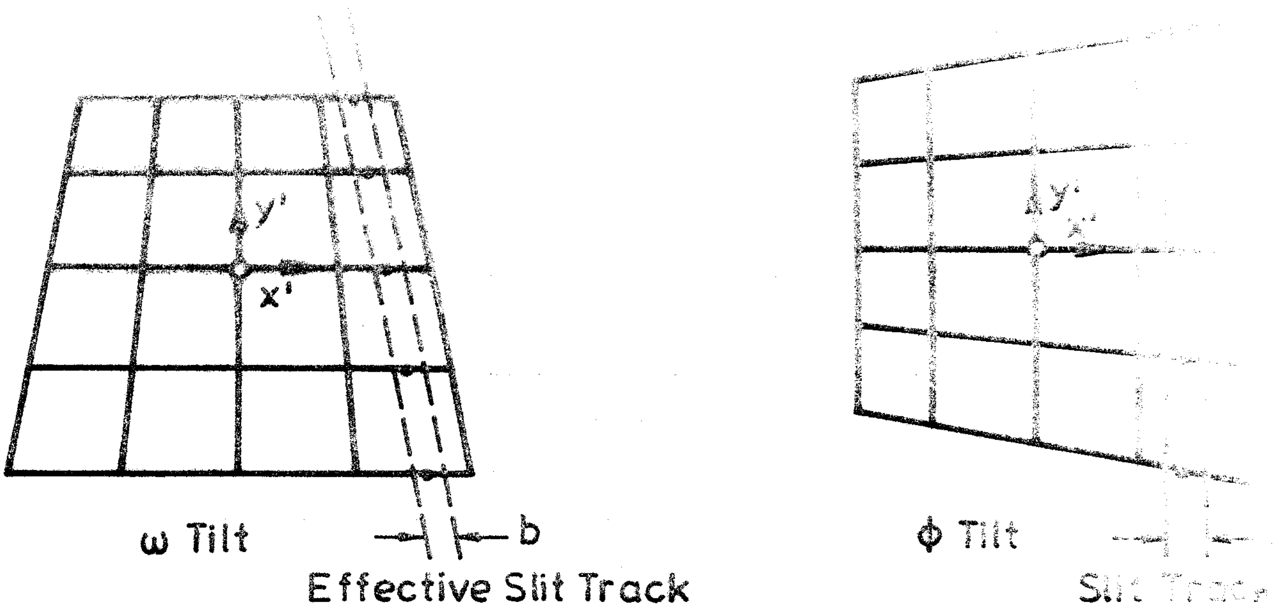

FIG. 3·5. EFFECT WITHIN EXPOSURE SLIT OF SCALE VARIATIONS DUE TO TILTS

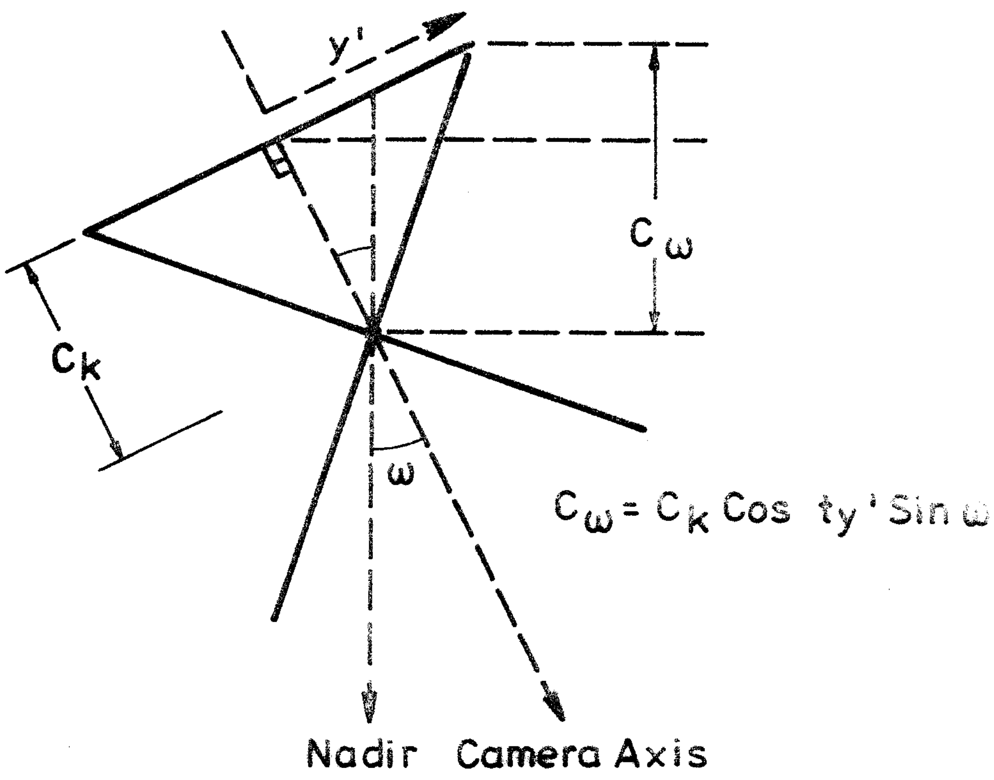

FIG. 3·6. CORRECTION OF C_k FOR ω TILT SCALE VARIATIONS for the mean scale at the centre of the slit due to x position. Figure 3.6 illustrates how correction may be achieved for ω tilt by adjustment of the camera constant C_k, by substitution at the magnification computing bridge of a camera constant C_ω, which represents the constant of a perfectly vertical camera in the same spatial position, and which would produce the same scale of image as the tilted camera.

$$C_\omega = C_k \cos\omega + y' \sin\omega$$

Similarly for ϕ tilts:

$$C_\phi = C_k \cos\phi + x' \sin\phi$$

And for the combined effect of the tilts $(\omega + \phi)$ we may substitute an adjusted camera constant $C_{(\omega+\phi)}$; for plate coordinates x' y' from the right hand plate centre as origin:

$$C_{(\omega+\phi)} = C_k \cos\omega \cos\phi + y' \sin\omega + x' \sin\phi \qquad (3.v)$$

The function $C_k \cos\omega \cos\phi$ is easily computed from the tilt values read at the plate rotation arcs; or may be applied as a correction Δ_{ck} from tables provided, in which Δ_{ck} is always a negative correction:

$$\Delta_{ck} = Ck \cos\omega \cos\phi - Ck$$

The correction Δ_{ck} is made to the Ck counter at the Orthophot (Fig. 3.7).

For the residual correction to C_k due to image coordinate position x'y', a "special tilt compensator for large tilts" may be provided which is attached beside the right plate carrier carriage. Swivelling rulers are manually set to the rotation angles ω, ϕ read from the arcs, and the position of the plate relative to the rulers determines the plate coordinates x'y'. The appropriate corrections are computed by this analogue computer, and transmitted as resistances by two potentiometers which continuously add the resistances to the resistance representing C_k at the computing bridge magnification control. If this residual correction to C_k is not made, the mean saale error within an exposure slit is:

$$\pm \left(y' \frac{\sin \omega + x'}{C_k} \sin \phi\right)$$

For the case of y' max = x' max = r; and for a slit width b; the displacement Δrx at the edge of the slit in x direction is:

$$\Delta r_x = \pm \frac{r.b.(\phi + \omega)}{2C_k}$$

Table 3.I gives limit values for $(\phi + \omega)g$ which result in maximum displacements $\pm \Delta r_x$ of ±0.1 mm in the Orthophoto, for the case of a 150 mm wide angle camera with maximum scan area 100 mm(y) by 200 mm (x) in the photograph scale, for different overall magnification factors $Vd/_b$ from photograph scale to orthophoto scale.

$V_d/_b$	1x	2x	3x	4x	5x
Slit Width mm					
1	19.1	9.5	6.4	4.8	3.8
2	9.5	4.8	3.2	2.4	1.9
4	4.8	2.4	1.6	1.2	1.0
8	2.4	1.2	0.8	0.6	0.5
16	1.2	0.6	0.4	0.3	0.2

TABLE 3.I Limit Values $(\phi+\omega)g$ for 150 mm Camera

3.10

The rotation of images due to ϕ tilt is not corrected, but should be minimised by appropriate choice of slit width after orientation is completed, at which stage ϕ of the right plate may be read from the ϕ"arc. The rotation is evident as a y displacement at the slit margin, effective proportionately from the slit center, as the center point is always correctly located by the model point location in the plotter. For the total y displacement (dy) in image position at the plate of an image with respect to plate center as origin of coordinates, we have in terms of plate scale displacement:

$$dy = \frac{x.y}{C_k} . d\phi$$

The relative displacement for a small increment dx is:

$$d(dy) = \frac{y}{C_k} . d\phi.dx$$

Whence the displacement Δry over an incremental distance of half slit width is:

$$\Delta ry = \frac{b.y.d\phi}{2.C_k}$$

And the displacement in the orthophoto at magnification $Vd/_b$ is:

$$\Delta ry = \frac{Vd/b.b.y.\phi}{2.C_k}$$

Clearly the maximum displacement Δry, is the same amount as the maximum displacement Δrx (due to scalar errors if the tilt correction device is not used), for the same given conditions, i.e. y max = 100 mm at plate. It follows that Table 3.I may also be used to determine the limit value $\phi(g)$ for a maximum displacement Δry of ± 0.1 mm at slit margin for the case of a 150 mm wide angle camera.

4. TESTS OF ORTHOPHOTOGRAPHIC PLANIMETRIC AND ELEVATION ACCURACY

4.1

In this section a review is given of the procedures and results of the principal experimental tests reported, concerning the accuracy of orthophotograph production techniques, and an outline is presented of the objectives and experimental work carried out during the investigation. There is always some difficulty in comparing photogrammetric experimental work, because of the variable factors involved; in particular the differences which occur in photographic instrumentation and flying altitude, the variable ratios possible in the plotting and orthoprojection equipment, the system variations such as scan speed and slit width, and of course in the terrain conditions. Furthermore the test controls are of variable accuracy and may be derived from ground marked signals, or from higher-precision photogrammetric work; and the results are not always presented in a uniform manner. Where possible the results published by the experimenters have been reduced in the case of planimetric errors, to mean square vector (position) error m_p in millimetres at the orthophoto scale; and also the corresponding error m_{pb} in micrometers at the common base of original picture scale. In the case of vertical errors the results are given in terms of parts pro mille flying altitude ($^o/_{oo}Z$). The tests are reviewed in approximate chronological order of publication, and are separately given as planimetric tests identified by the letter P, and elevation tests identified by the letter E. Whenever possible the relevant variable factors are given:

flight altitude	:	Z
original picture scale number	:	m_b
model scale number	:	m_m
orthophoto scale number	:	m_d
orthophoto slit width (m.m)	:	b
model scan width if applicable	:	b_m
scan speed in original picture scale	:	V_B mm/sec

4.2 Planimetric Accuracy Tests

4.2.i Test Series 1P

NEUBAUER *(1964)* presented the first numerical data on accuracy after evaluation of four orthophotos of the REICHENBACH test field. Instrumentation for the tests was a C.8 Stereoplanigraph directly coupled to GZ1. The range of relief ΔZ in the models tested amounted to about 20%Z.

m_b	m_d	Z	$Vd/_b$	V_B	b
8500	3000	1275	2.83	1.7	4

Check points	m_p	m_{pb}
60 signalised per orthophoto	±0.12mm	42 μm

m_p (points near slit centre) : ± 0.11 mm

m_p (points near slit margin) : ±0.14 mm

MEIER *(1966, 81)* comments that the small differences between errors at the centre of the slit and errors at the margin, confirm that it is not only the system errors which have to be taken into account, but above all the scanning error.

4.2.ii Test Series 2P

JOHANSSON *(1968, 55)* reported on tests in which a standard orthophotomap sheet of the 1:10 000 Economic Map of Sweden was tested in planimetry by comparison of 98 points, check coordinates of which were determined by measurements in a Wild A7 plotter. The map sheet composed of 3 orthophoto models covered a relatively hilly woodland area with elevation differences of 3.7%Z. The plotter instrumentation was both C.8 and Stereometrograph, and GZ1 Orthoprojector in the storage mode.

m_b	m_m	m_d	Z	$V_d/_b$	b_m	b
30000	15000	10000	4600	3	4	1

Check points	m_p	m_{pb}
98 photogrammetric	+0.20 mm	67 µm(similarity transform)
	±0.18 mm	60 µm(affine transform)

The measurements in the A7 were assumed to have a planimetric standard error of about ±0.05 mm, and the coordinatograph of about ±0.03 mm, so that the following reduced errors are obtained for the total orthoprojection method:

m_p	m_{pb}
± 0.19	63 µm
± 0.17	57 µm

4.2.iii Test Series 3P

MEIER *(1968, 82)* published the results of tests carried out by Rikets Allmäna Kartverk of Stockholm on 9 orthophotomap sheets; believed to be produced by the C8 - GZ1 combination:

m_b	m_d	$V_{d/b}$
10000	4000	2.5

Check points	m_p	m_{pb}
75	±0.16 mm	66 µm
95	±0.15 mm	59 µm
91	±0.18 mm	72 µm

m_b	m_d	$V_{d/b}$
30000	10000	3

Check points		
24	±0.37 mm	123 µm
36	±0.19 mm	63 µm
65	±0.37 mm	123 µm
66	±0.19 mm	63 µm
58	±0.29 mm	97 µm
67	±0.19 mm	63 µm

MEIER comments that in these tests, the theoretically estimated magnitude of residual errors in orthophotos made with the GZ1 was confirmed.

4.2.iv Test Series 4P

FÖRSTNER *(1968, 111)* reported on further tests made in the Institut für Angewandte Geodäsie, of the REICHENBACH test area, additional to those of NEUBAUER (test series 1P). A total of 44 orthophotos were prepared from which the coordinates of some 6000 signalised points were measured by coordinatorgraph:

m_b	m_d	Z	$V_{d}/_{b}$	b
8000-12000	3000(?)	1200-1800	2.83-3.6	2-4

Check points	m_p
6000 signalised	±0.16 mm (similarity transform to all points in each sheet)
	±0.20 mm (transform to 5 controls per sheet with change of scale)
	±0.24 mm (transform to 5 controls without change of scale)

The tests were carried out with C8 and GZ1 directly coupled, using variations of slit width $\bar{b}$; and also variations of base-height ratio of 0.3 and 0.6 as a method of control of maximum projection angle in the x direction. FÖRSTNER comments that orthophotos prepared with a slit width of 4 mm show a mean square error which on average exceeds by 10% those taken with a slit width of 2 mm; and that orthophotos produced from a base ratio of 0.6 show a mean square error which on the average exceeds by 5% those produced with a base ratio of 0.3. He also comments that the influence of the magnification ratio $V_{d/b}$ is practically negligible, but it should perhaps be noted that the range tested was only 27% different.

4.2.v Test Series 5P

VISSER *(1968, 10-22)* has reported on several tests of the REICHENBACH test field with a C.8 directly coupled to GZ1.

<u>First test model</u>

m_b	m_m	m_d	Z	$V_{d/b}$	V_B	b
12000	10000	4000	1825	2.4	1.3mm/sec	4

Check points

	m_p	m_{pb}
5 Controls, and 54 checks (signalised)	±0.20	83 µm

<u>Second test model</u>

m_b	m_m	m_d	Z	$V_{d/b}$	V_B	b
8500	5000	2500	1275	3.4	0.74mm/sec	4

Check points	m_p	m_{pb}
5 controls, 55 checks	±0.22	65 µm

<u>Third test</u>

Conditions as for the second test, but variable speeds with two different observers:

	Observer No. 1		Observer No. 2	
V_B	m_p	m_{pb}	m_p	m_{pb}
0.74	±0.17	50 μm	±0.14	41 μm
0.97	±0.17	50 μm	±0.16	47 μm
1.47	±0.20	59 μm	±0.15	44 μm
2.20	±0.18	53 μm	±0.24	71 μm
2.94	±0.17	50 μm	±0.16	47 μm

VISSER comments that the results show a high correlation for the same observer between tests at different speeds, due to the influence of the system errors and the common errors of snap-marking of the signalised points; but that the scanning error appears to be almost independent of speed, in contrast to the formula of MEIER given in equation 2.xiii.

4.2vi Test Series 6P

ACKERMANN *(1969)* investigated errors in very large scale orthophotomaps. From original scale photographs of 1:4000 an orthophoto was produced at 1:1250, subsequently enlarged with a process camera to 1:1000. The total magnifications factor from picture scale to map ($V_{k/b}$) is thus 4. The orthophotomap image details were compared with corresponding details of photogrammetric line maps, 10 500 individual checks being made. The extreme scale conditions of this test result in large system errors and scanning errors, because of the possibility of very large elevation differences being present in images within the exposure slit.

m_b	m_d	m_k	$V_{d/b}$	$V_{k/b}$
4000	1250	1000	3.2	4

	m_{pk}	m_{pb}
Various details at ground level:	±0.20-0.46mm	50-115 μm
Objects with large perspective errors, e.g.:		
Bridge crossing valley	5.3 mm	1325 μm
Roof corners	2.5 mm	625 μm

4.2.vii Test Series 7P

FLEMING *(1973, 55)* published the results of planimetric accuracy tests, in which Contractors to a government agency produced orthophotographs of the same areas using different instrumentation : Zeiss GZ1, Jena Orthophot, SFOM 693, Kelsh Orthophotoscope, and Hobrough Gestalt Photomapper. The tests were performed from three different photographic scales in areas of various types of relief as follows:

a. Low relief area : $\Delta Z < 1\%Z$; m_b 19 000, 8 test models.
b. Medium relief area: ΔZ 4%Z; m_b 38 000, 7 test models.
c. Mountainous relief area: ΔZ13%Z; m_b 50 000, 10 test models.

Details are not given of the relevant restitution parameters, but the results are presented in terms of mean square errors at original photographic scales. The error checks were made at 25 points per orthophoto, the positions of which were determined by photogrammetric measurements in a Wild A7 plotter:

	m_{pb}
Low relief area :	40 - 60 μm
Medium relief area :	30 - 60 μm
Mountainous relief area:	60 -270 μm

FLEMING points out that the largest errors (270 μm) were recorded for a test in which a model was scanned with slit width inappropriate to terrain (large system errors). Apparently there was no correlation between tested accuracy and instrumentation. In the cases of the low and medium relief areas, the errors corresponded in magnitude with the theoretical predictions of MEIER *(1966)*. Comparing the errors with U.S. Map Accuracy Standards for a standard in which 90% of points checked should be within ±0.05mm of line position; it followed that the orthophotos of low and moderate relief areas could be used at $V_{d/b}$ ratio of 5.5 times, whereas for mountainous areas the maximum allowable $V_{d/b}$ ratio would be 1.5 times.

An additional feature of this test series was that a number of map marked points were positioned in tree cover at maximum field angles in the models. It was shown that systematic radial displacements could be detected at these points in orthophotos produced by automatic electronic correlation, in contrast to the manually-scanned orthophotos.

4.3 Vertical Accuracy Tests

4.3.i Test series 1E

MEIER *(1966, b)* published the first numerical accuracy data on contours produced from drop-line charts, obtained concurrently with orthophotos. Meier compared the derived contours with a contour plot of WALDMATT area, produced by conventional photogrammetric techniques. 136 check points were selected on contour lines of the photogrammetric plot of an area of 0.25 km^2, and the interpolated errors of the drop-line derived contours were classified by groups of terrain slope, varying between 3 and 50%. The instrumentation was Zeiss C8 and GZ1 directly coupled. The contour interval of the drop-line signals was 5m ($2.8^o/_{oo}Z$), equivalent to a C number (see 1.4) of 360.

m_b	m_m	m_d	Z	$V_d/_b$	VB	b
12000	10000	5000	1800	2.4	1.38mm/sec	4

Meier's test confirmed dependency of elevation errors upon terrain slope, as postulated in his analysis of errors of the GZ1 system (see 2.4.i), obtaining for the mean square error in elevation:

$$m_z = \pm(0.58 + 2.82 \tan \beta)m$$

Elimination of the errors due to normal photogrammetric plotting, gave for the errors due to orthoprojection scanning:

$$m_z = \pm(0.56 + 2.64 \tan \beta)m$$
$$= \pm(0.31 + 1.47 \tan \beta)^o/_{oo}Z$$

Meier comments that the results of the test are in general agreement with his prediction of errors, and that they satisfy the specifications for both mean and maximum errors of the German Base Map 1:5000.

4.3.ii Test Series 2E

HAMPEL *(1967)* produced an orthophoto at a scale of 1:2500 of BURLADINGEN area, with elevation differences of 5%Z and slopes of 0-190%. Profile drop-line charts were produced without conversion to contours, and compared with eight profiles surveyed in the terrain, arranged parallel to the orthophoto profiles. Comparison was made at 98 profile points, also arranged in slope groups. The drop-line signal changes were made at contour intervals of 2.5m ($2^{o}/_{oo}Z$), equivalent to C number 480. C8 and GZ1 were directly coupled.

m_b	m_m	m_d	Z	$V_d/_b$	VB	b
8000	5000	2500	1200	3.2	1.56mm/sec	4

The error of elevations was found:

$$m_z = \pm 0.6\text{m} = \pm 0.5^{o}/\text{oo}Z$$

Hampel found no dependency of elevation error on account of slope.

4.3.iii Test Series 3E

JOHANSSON *(1968, 156)* published elevation accuracy data concurrently with planimetric test series 2P. Elevation errors were determined by the comparison of check points obtained from measurements in Wild A7 plotter. Drop line signals were produced at contour intervals of 5m ($1.1^{o}/_{oo}Z$), equivalent to

C number 920. Comparison was made at 134 points interpolated from the derived contours. The production parameters are identical with those of test series 2P.

The errors of elevation were found:

all tested points: $m_z = \pm 1.7m = \pm 0.37^{o}/_{oo}Z$,
points in open areas: $m_z = \pm 1.6m = \pm 0.35^{o}/_{oo}Z$,
points in forest areas: $m_z = \pm 2.0m = \pm 0.43^{o}/_{oo}Z$

Dependency upon terrain slope was apparently not tested, but a contour plot was also produced by purely conventional plotting on Wild B8 plotter, and also tested. The accuracy of the two plots was of about the same order, except that in the case of points in forest areas, the B8 results were somewhat better with $m_z = \pm 0.33^{o}/_{oo}Z$. Reduction of the errors of the orthoprojection contours by the estimated error of the measurements in Wild A7, results in a figure of $m_z = \pm 0.35^{o}/_{oo}$ for all tested points.

4.3.iv Test series 4E

VISSER *(1968, 10-27)*, also tested elevation accuracy concurrently with the same test models as used in planimetric test series 5P, where the production parameters may be found.

First test model

The selected profile interval was 5m ($2.7^{o}/_{oo}Z$), corresponding to C number 365.

55 ground points interpolated from contours:

$m_z = \pm 0.74$ m $= \pm 0.41^{o}/_{oo}Z$

Second test model

The selected profile interval was 2m ($1.6^{o}/_{oo}Z$), corresponding to C number 637:

$m_z = \pm 0.37$ m $= \pm 0.29\ ^{o}/_{oo}Z$.

This test was carried out at VB 0.74 mm/sec, and subsequently repeated with scan speed VB 1.5 mm/sec:

$$m_z = \pm 0.47 \text{ m} = \pm 0.37\ ^{o}/_{oo}Z.$$

In the same test model, a profile was selected and scanned at five different speeds, twice at each speed. The repeatability of profiling at speed was judged on the basis of the differences of the errors between pairs of profiles scanned at the same speeds. 131 check points were compared, derived from static profile measurements in Zeiss C8. The absolute accuracy of profiling was determined by comparison of individual profiles against the static measurments.

Visser concluded that the results were almost the same for all speeds over the complete V_B range of 0.74 - 2.94 mm/sec. The absolute errors varied from m_z ±0.12 to $0.32^{o}/_{oo}Z$ over three groups of slope at all speeds. In the case of irregular broken terrain (but with only slight slopes of 2-3%), the errors were significantly worse, and in this case a significant constant error of $0.5^{o}/_{oo}Z$ was apparent.

The same test model was completely scanned by two different operators at five different speeds. Contours were derived, and height errors found at 56 ground check points by interpolation from the contours. As average, Visser found:

$$m_z = \pm 0.56 \text{ m} = \pm 0.43^o/_{oo}Z$$

Visser comments that the tests on both profiles and derived contours showed that the errors were almost independent of scan speed, and that it appeared that actual slope was not as significant as changes of slope.

4.3.v Test series 5E

ACKERMANN *(1969)* concurrently with his very large scale planimetric test series 6P, produced a drop line chart with 1 m contour interval ($1.7^o/_{oo}Z$), corresponding to a C number of 600. Interpolated contours were drawn at an interval of 0.1 metre. 263 points were compared with contour lines from photogrammetric conventional plotting:

$$m_z = \pm 0.22\text{m} = \pm 0.37^o/_{oo}Z$$

4.3.vi Test Series 6E

HOBBIE *(1969, 225)* repeated the WALDMATT model test of series 1E (MEIER), using the same instrument production parameters except that the C8 and GZ1 were not directly coupled, but used in the storage mode of operation (see 2.3.i). The purpose of the test was to investigate the efficiency of the Zeiss Electonic Contourliner system for GZ1, in which a series of dots are generated across the scan path by cathode ray tube, at contour intervals derived by interpolation from the stored profile information. The resulting array of dots has the appearance of lines of contours. Comparisons were made with 201 arbitrarily chosen points combined in slope groups, compared to a conventional contour plot assumed to be free of error. Hobbie found:

$$m_z = \pm[(0.6 \pm 0.2) + (1.3 \pm 0.6) \tan \beta] m$$

$$= \pm[(0.33 \pm 0.11) + (0.72 \pm 0.33) \tan \beta] ^{o}/_{oo} Z$$

Hobbie comments that these results represent a considerable gain in accuracy over the corresponding figures of test series 1E produced from drop lines.

4.3.vii Test Series 7E

SCHNEIDER *(1970)* carried out a comprehensive series of tests, the purpose of which was to examine both the quality and accuracy of contours derived from drop-line charts; especially in terms of orthophoto scale 1:5000 and the specifications of the German Base Map 1:5000. The tests were carried out at two levels of significance: namely the accuracy of the profile signals, and the accuracy and quality of the derived contours. A number of variable parameters were tested, such as speed of scan, slit width, observer influence, land slope influence, landcover influence, and to a rather limited extent the influence of picture scale. Instrument combinations used were Zeiss C8 and Zeiss Planimat, coupledto Orthoprojector GZ1.

The number of separate tests is such that it is not possible to give the production parameters for each, but for example Schneider found very close agreement with Meier's test series 1E under similar conditions.

Schneider concluded that for profile signals, as far as the scanning error is concerned:

(a) of all parameters slope is the most significant,

(b) the difference between observers was of little influence,

(c) the scan direction had little influence.

As a general conclusion, Schneider found that derived contours satisfied both the mean square and maximum specifications for the German Base Map 1:5000; except that in the cases of fast scanning speeds V_B of 2.5 and 3.3 mm/sec in ground slopes below 5g, the tolerances were exceeded. He found that the accuracy of signals does not necessarily correspond with derived contour accuracy, commenting that in drawing the contours a kind of adjustment takes place. Schneider found little significance in slit width, except in so far as elevation details between profiles may be completely missing.

4.3.viii Test Series 8E

SCHMIDT-FALKENBERG *(1970)* carried out a series of tests in some respects similar to those of SCHNEIDER (series 8D). His purpose was to examine the suitability of drop-line chart derived contours, particularly from the view point of completeness of representation of land-forms, as well as accuracy, for the German Base Map 1:5000. The principal tests were carried out in the REICHENBACH test field, with slopes up to 17°, mean slope 7°. The variable factors tested included those of profile interval, picture scale, and observer. Elevation errors were measured by interpolation from contours, at 69 randomly distributed check points surveyed on the ground. The instrumentation was Zeiss C8, and GZ1 in storage mode of operation. The contour interval of the drop lines was 2.5 m, and the speed of scan V_B 1.3 mm/sec.

Falkenberg found the following errors, in which m_z is the arithmetic mean of the mean square errors for the number of tests stated:

m_b	m_d	Z	C	$V_{d/b}$	m_z	Number of tests
8000	5000	1200	480	1.6	±0.5m (.41$^o/_{oo}$Z)	5
12000	5000	1800	720	2.4	±0.6m (.33$^o/_{oo}$Z)	11
20000	5000	3000	1200	4.0	±1.1m (.37$^o/_{oo}$Z)	4

Falkenberg made a particular study of the grouping of errors by slope values, in order to determine whether or not slope errors confirmed to a law of the type attributed to KOPPE (1902). KOPPE postulates that errors in elevation on maps are dependent on slope with the following relationship, in which a and b are constants, β is ground slope, and V_z is an error in elevation:

$$V_z = \pm (a + b \tan \beta) \qquad (4.1)$$

Falkenberg investigated the errors of each test in terms of linear correlation between errors and the corresponding slope, and also in terms of the distribution of errors. As a general conclusion he found no confirmation whatsoever of a Koppe type law. Falkenberg considered however that his results were in general agreement with those of HAMPEL (test series 2E), and also that the requirements of the German Base Map were satisfied, in spite of the fact that the tolerances for this map are stated in terms of a Koppe type law.

4.4 Characteristics of previous tests

4.4.i

Planimetric errors in the tests summarised lie within the range m_p ±0.12 to 0.46 mm in the orthophotograph, corresponding to a range m_{pb} ± 42 to 123 μm at plate; excluding the results from mountainous terrain (test series 7P) and those with large perspective errors (test series 6P). An analysis of the production variables shows that there has been a marked preponderance of tests at the large scale end of the mapping range, and in particular an emphasis on tests designed to show the suitability of orthophotography for the German Base Map series 1:5 000. All of the tests except those of FLEMING (test series 7P) have been of a single orthoprojection system (GZ1), and practically all have used a single restitution plotter (Zeiss C8 Stereoplanigraph) of the highest standard of precision.

All of the tests can be considered tests of the internal accuracy of orthoprojection, based either on error-free control, or alternatively on photogrammetric control in which allowance is made only for the accepted restitution errors of single models. In large-scale mapping it is quite a normal procedure to provide complete control for each mapping model, and in the production of the orthophotomaps it may be quite usual for a single photograph (two models) to constitute a single large-scale map sheet. Such a procedure ensures that the orthophotomap composed of the two joined orthophotographs, has uniform photographic contrast, so that there is little or no evidence of a join line *(Urban, 1973)*. It is therefore reasonable to assume that large-scale orthophotomaps should have errors of the order of the range disclosed by the summarised tests.

For medium and small-scale mapping however, normally the individual models will be oriented in the orthophotographic productions phase on control established from an aerial triangulation block. Furthermore separated models will provide orthophotographs which will be fitted to a control sheet so that several such components comprise one mapsheet. Significant errors may occur on account of the errors in the pass point control. The question of absolute accuracy in the geodetic sense is not important, because separate blocks of aerial triangulation pass points will be constrained in relation to one another by perimeter controls of suitable precision. Accuracy within the individual blocks, and the relationship of pass point errors between separated models within the block and within the map sheet, is of more importance. In this work the errors of position and elevation within a block of triangulation are referred to as the *external* errors of a model or orthophotograph (m_p', m_z'), as distinct from the errors within a single orthophotograph, referred to as the *internal* errors (m_p, m_z). Perhaps there is an anomaly in the fact that the majority of tests are concerned with the most precise product of mapping technology: namely the large scale map in a European environment; whereas many authorities have stressed the importance of this new mapping technique in terms of the mapping problems of underdeveloped countries, where medium and small scale mapping is the primary objective.

4.4.ii

Test results on the accuracy of elevations is obtained in the tests either from drop line profiles, or from the derived contours. The range of results is $m_z = \pm 0.3$ to $0.5^{o}/_{oo}Z$, plus in some cases a dependency on ground slope of the order of $(1 \text{ to } 1.5)^{o}/_{oo}Z \tan \beta$. It is interesting to note that dependency on slope is confirmed in about half the tests, but not in the remainder. Test confirmation of dependency on scan speed is also divided in opinion. From the viewpoint of planning criteria it is interesting to note that the test parameters in terms of C number are rather uniformly moderate, in the range 360 - 650. Only in the case of test series 3E at 920, and in one model of series 7E at 1200, do the C numbers approach what may be considered more usual criteria for conventional medium and small scale mapping. It is also notable that the landforms of the test areas, in those cases where drop lines have been converted to contours, are not particularly complex; being characterised by regular slopes and rather simple drainage patterns. The suitability of the drop line system for derivation of contours in complex irregular landforms, at medium and small scales, cannot be confirmed from the published tests.

4.4.iii

Few details are given in the tests regarding the time taken and methods used, to derive contours from the graphical data. This is particularly important because it could be the decisive factor for production planning of the contouring process, especially if the process is not only time-consuming but also a technically demanding procedure in the case of complex terrain landforms. Furthermore if there is a very wide range of possible times depending on land forms, then it becomes extremely difficult to forecast and plan an efficient production line between the phases of photogrammetric work, cartographic work, and reproduction. We have to look elsewhere than to the tests for data on this important factor, and there appears to be a wide range of opinion.

VOSS *(1968, 7)*, in an article on the production of 1:5 000 orthophotomaps in North Rhine-Westphalia, estimates that about four days are required for a two model mapsheet in the case of medium-high mountains; for the interpolation of contours from profiles produced by GZ1. This figure of about 14 hours per model in such a case, does not include the fair drawing (or scribing) of the derived contours, for which he estimates a further 3 days per map sheet. LAMBERT *(1971)* estimates 2 hours per model as an average figure for interpolation of contour segments produced by B8 Stereomat, adding that the figure could vary from 20 minutes in flat terrain to 8 hours in difficult mountainous terrain. Comparing these figures, one should bear in mind that contour segments are short portions of contours correctly oriented within the scan width, so that we may presume that the interpolation problem is rather easier than the problem with continuous profile line signals in which the signal change points are always perpendicular to the scan direction. SZANGOLIES *(1973, 155)* states that "the quickest and least expensive method for producing contour line plans is now as before and despite certain doubts, the derivation of contours from dropped lines." He estimates that the derivation of the contours from dropped lines takes 0.5 to 4 hours for one model.

It may well be that the question of production time for interpolation, is the crucial factor regarding the viability of drop line profiles as a contouring procedure, particularly as the procedure of direct scribing is now so widespread with conventional contouring. In such a case the machine compilation plot is substantially a fair drawing requiring only editing, the addition of contour numbers, and retouching. A production process in which orthophotos are produced separately on one instrument, and contouring by conventional methods on another, such as that described by URBAN *(1973, E2)* may therefore lend itself to more efficient production planning.

4.5 Objectives of test programme

A Zeiss Jena Topocart B and Orthophot, together with drop line profile Orograph accessory, was delivered to the School of Surveying of the University of New South Wales in September 1971. Unfortunately some damage occurred to lineals of the right-hand projection system in transit, and replacement and satisfactory installation was not completed until November 1972. After study of the types of orthophotography tests published, a test programme was devised within the concept of an integrated mapping system in which the orthophotomap is the topographic base at medium scale. The concept was one in which planning criteria for production were to be deliberately based on extreme limits rather than conventional conservative limits. In particular the relationship between original picture image scale and orthophotomap scale; and the altitude/contour interval; were both to be beyond normal conventional limits. The following factors were considered to be desirable objectives:

(a) Control for the orthophotograph production models should be provided by pass points from an aerial triangulation block;

(b) test models should be selected in which the landforms were of different types; one with features in which system errors could be expected to be quite marked, and in which landforms would test the suitability of drop line profiles for complex terrain patterns, and one in conditions of relatively flat terrain,

(c) tests should be conducted over a wide range of scan speeds and slit widths;

(d) results should be evaluated in terms of both internal and external errors;

(e) elevation errors should be tested in terms of accuracy of profile signals and also derived contours;

(f) drawing times for the interpolation of drop line signals and the derivation of contours should be determined;

(g) correlation should be tested between errors and variable production and terrain parameters.

Further details of the test block and models are given subsequently, but at this stage it should be stated that a block of wide-angle photography was selected as a test area, in which a number of ground controls were provided. An independent model triangulation was carried out, and adjusted to provide pass point control for the production phase. The orthophotograph scale was selected as 1:25 000 from 1:60 000 original photography. Two models were selected as test models within the central strip of the triangulation block, one of terrain including irregular broken landforms, and one of substantially flat terrain. The two models were separated within the strip by three models between them, so that the separated test models were as far distant from one another as would be possible in a single map sheet at publication scale. The map distance from extreme west edge of one model to extreme east edge of the second was 900 mm.

In the case of the model of irregular terrain (model A), tests were carried out at slit widths of 2, 4, 8 and 16 mm; each test at fixed scan speeds V_d in the orthophoto of 2, 4, 6 and 8 mm/sec, and also at a variable speed at operators personal choice. In the case of the flat terrain model (model B), tests were carried out only at 8 and 16 mm slit widths at a fixed speed of 4 mm/sec. Individual tests are identified by test labels consisting of two digits, the first of which consists of the slit width, and the second of which identifies the scan speed. Model B tests are prefixed by the letter B. The complete test programme with identification labels is shown in Table 4.I.

TABLE 4.I

TEST LABEL IDENTIFICATION

1:25 000 Orthophotomap Test Programme
Fowlers Gap Arid Zone Research Station, New South Wales

(i) Planimetry Tests

Model A, Broken Terrain

Orthophoto Scan Speed V_d:	2	4	6	8mm/sec	Variable
Image Scan Speed V_B:	0.83	1.67	2.5	3.33	
Slit Width b mm					
2	2/0	2/1	2/2	2/3	2/4
4	4/0	4/1	4/2	4/3	4/4
8	8/0	8/1	8/2	8/3	8/4
16	16/0	16/1	16/2	16/3	16/4

Model B, Flat Terrain

8	B/8/1
16	B/16/1

(ii) Elevation Profile Signal Tests

2/0	2/1	2/2	2/3	2/4
	4/1			
	8/1			
	16/1*			

(iii) Elevation Derived Contour Tests

2/1

4/1

8/1 (and B/8/1)

16/1*(and B/16/1)

Table 4.I Cont.

Camera : RC5a, 115 mm wide angle.		Altitude :	6875 m
Picture scale $1/_{m_b}$:	1/60 000.	Contour Interval :	5 m
Model scale $1/_{m_m}$:	1/25 000.	C number :	1375
Orthophoto Scale $1/_{m_d}$:	1/25 000.		

*Test 16/1 contour interval was 10m, C number 688.

5. GROUND SURVEYS IN TEST AREA, AND AERIAL TRIANGULATION OF MAPPING BLOCK.

5.1 Fowlers Gap Arid Zone Research Station

Fowlers Gap Station is a 39000 ha property leased by the University of New South Wales, situated about 110 km north of the City of Broken Hill in the extreme west of New South Wales. The University operates the property as an Arid Zone Research Station, the average rainfall being 193 mm per annum, the principal areas of research being concerned with the pastoral industry in an arid environment. Research projects have been initiated in such diverse fields as vegetation studies, land system surveys, water resources, marsupial studies, and climatology. Until 1970 the best available mapping of the area was in the form of aerial photograph mosaics with no elevation information, and this was quite inadequate to the needs of many research workers.

In April 1970 the N.S.W. Minister of Lands agreed that his Department would assist in the production of a two-sheet 1:25 000 multicoloured topographic map of the Station, contoured at 5 m interval. Control for the photogrammetric mapping had previously been provided by the School of Surveying as a final-year student class exercise. Fig. 5.1 shows the triangulation network established at that time, by breaking down from major geodetic stations to a lower-order density by classical triangulation methods. The 14 triangulation points established in the network were subsequently permanently beaconed with tubular steel tripods,

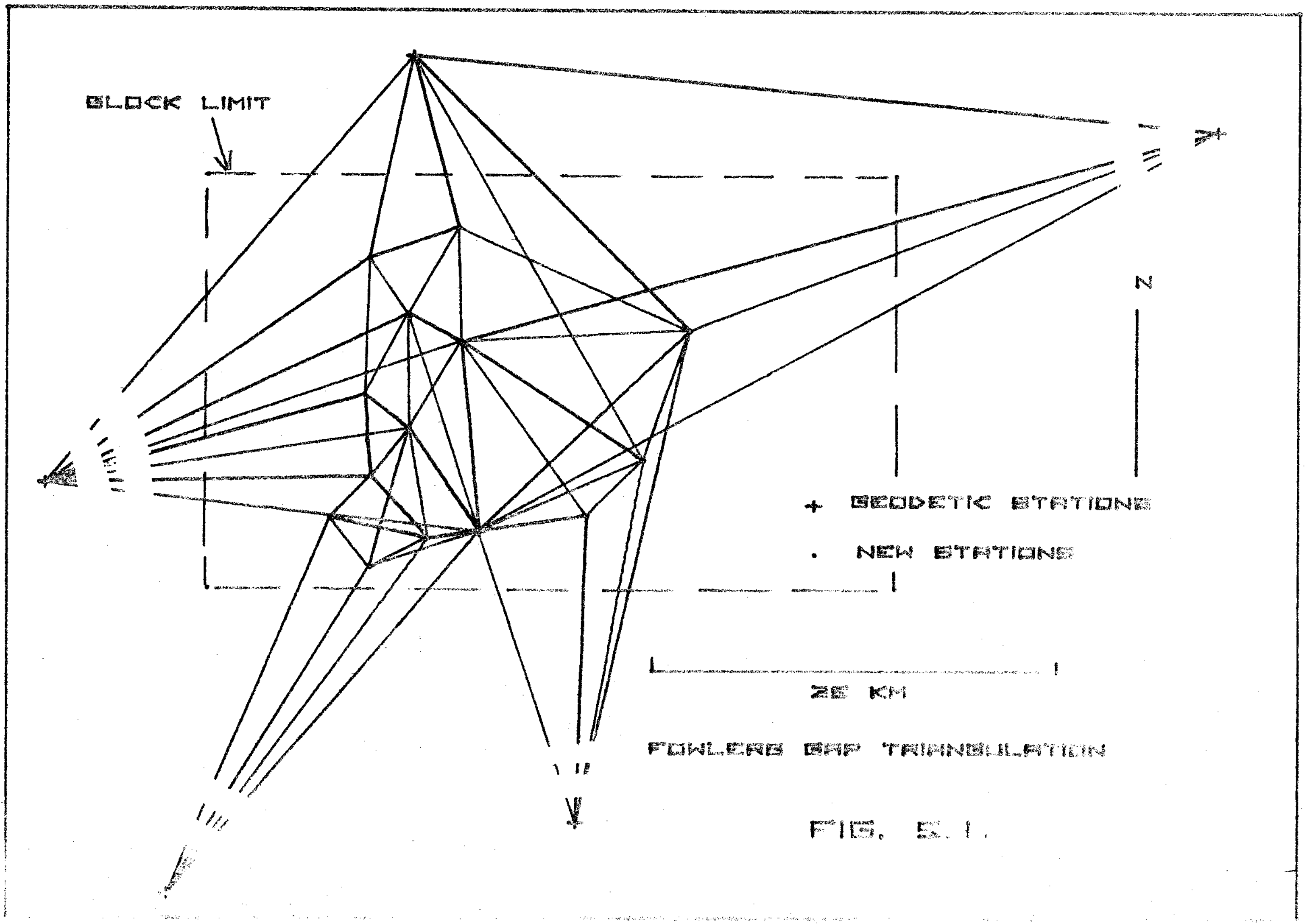

FOWLERS GAP TRIANGULATION

FIG. 5.1.

and since the original 6 geodetic stations within a 40 km radius of the property were also beaconed, the area was unusually well controlled to a density not common in the less developed interior of Australia. The triangulation network was connected by spirit-levelling from two stations to a line of geodetic levelling which followed the highway traversing the Station. Four rounds of horizontal angles, and of reciprocal vertical angles, were observed with 1" theodolites on all lines of the network; which was adjusted by a programme for the adjustment of networks by the parametric method devised by Dr. J.S. ALLMAN of the School of Surveying. The trigonometrical heighting network was adjusted by condition method by Mr. M. MAUGAN of the School of Surveying. The precision of the adjusted coordinates of the network stations is estimated to be a standard error in plan coordinates of ±0.04 m, and for elevations ±0.05 m.

5.2 Aerial Triangulation Block Ground Surveys

The requirement to provide photogrammetric control for the mapping project referred to in 5.1, together with the ready availability of small scale photography, prompted the writer to consider the suitability of the area for research work in orthophotographic mapping. The only other possiblity of a well controlled test block in Australia was photographed by Super Wide Angle photography, for which unfortunately no instrumentation was available within the University for the execution of the aerial triangulation phase. The photography of the Fowlers Gap area consisted of strips of 115 mm wide angle photography by Wild RC5a camera of 180 x 180 mm format; photographed in April 1965 at an altitude of 6875 m, picture scale 1:60 000. In the extreme north of the Station, a strip at the same scale had been photographed in September 1968 immediately after the network triangulation observations, and the photogrammetric control in this strip had been premarked. The marks consisted of crosses of black and yellow polythene pinned to the ground, of material 3 m wide (50 μm at picture scale), and of limb length 6 m (100 μm at picture scale). 8 such premarked controls had been positioned, and all were subsequently verified in the photography. At the same time as the northern strip was photographed, 8 additional strips had been photographed at altitude 2875 m, picture scale 1: 25 000. This photography was therefore available for photo identification purposes at larger scale than the mapping photography; and also made it possible to carry out certain parts of the projected test programme with greater precision than possible with the mapping photography, in particular the testing of accuracy of profiles and derived contours, and the provision of photogrammetric check points.

A block of 3 strips each of 10 models of the 1:60 000 photography was selected for the aerial triangulation phase. Whilst small in terms of production medium scale mapping blocks this limitation was to a large extent dictated by the necessity to carry out much of the work single-handed. It is felt that the block is large enough to simulate a standard mapping block and to provide useful data on the problems associated with orthophotographic mapping projects. In principle the fundamental control for the block was planned to consist of 6 fully controlled points, 3 each on the perimeter of the top and bottom strips, and additionally 4 points of elevation data only, in the centre strip containing the test models (fig. 5.2).

Including the fundamental block controls, a total of 58 fully controlled points were fixed by ground surveys, of which 8 were the premarked points in the northern strip. 31 of the points were distributed throughout the block, and 27 were provided in the two selected orthophotograph Models A and B. These latter points, 14 in Model A and 13 in Model B, were located in such positions as to provide 4 ideally situated controls for each of the 1:25 000 picture scale overlaps falling within the mapping photography models A and B.

All surveyed points except these within the orthophoto models were fixed by resection and trigonometrical heighting, as the open nature of the terrain traversed by foothills of the Great Barrier Range of relative elevation 200 m, and the presence of a number of beaconed triangulation points, was well suited to such procedures. The 31 resection points were fixed by 1 or 2 man survey parties in 19 days working time, with the 2 man parties averaging 2 points per day. The limitation on working speed was imposed not so much on account of cross-country travelling time, but by the necessity under Australian summer conditions to observe horizontal angles early in the morning or late in the evening, when the effects of heat haze and shimmer are minimal.

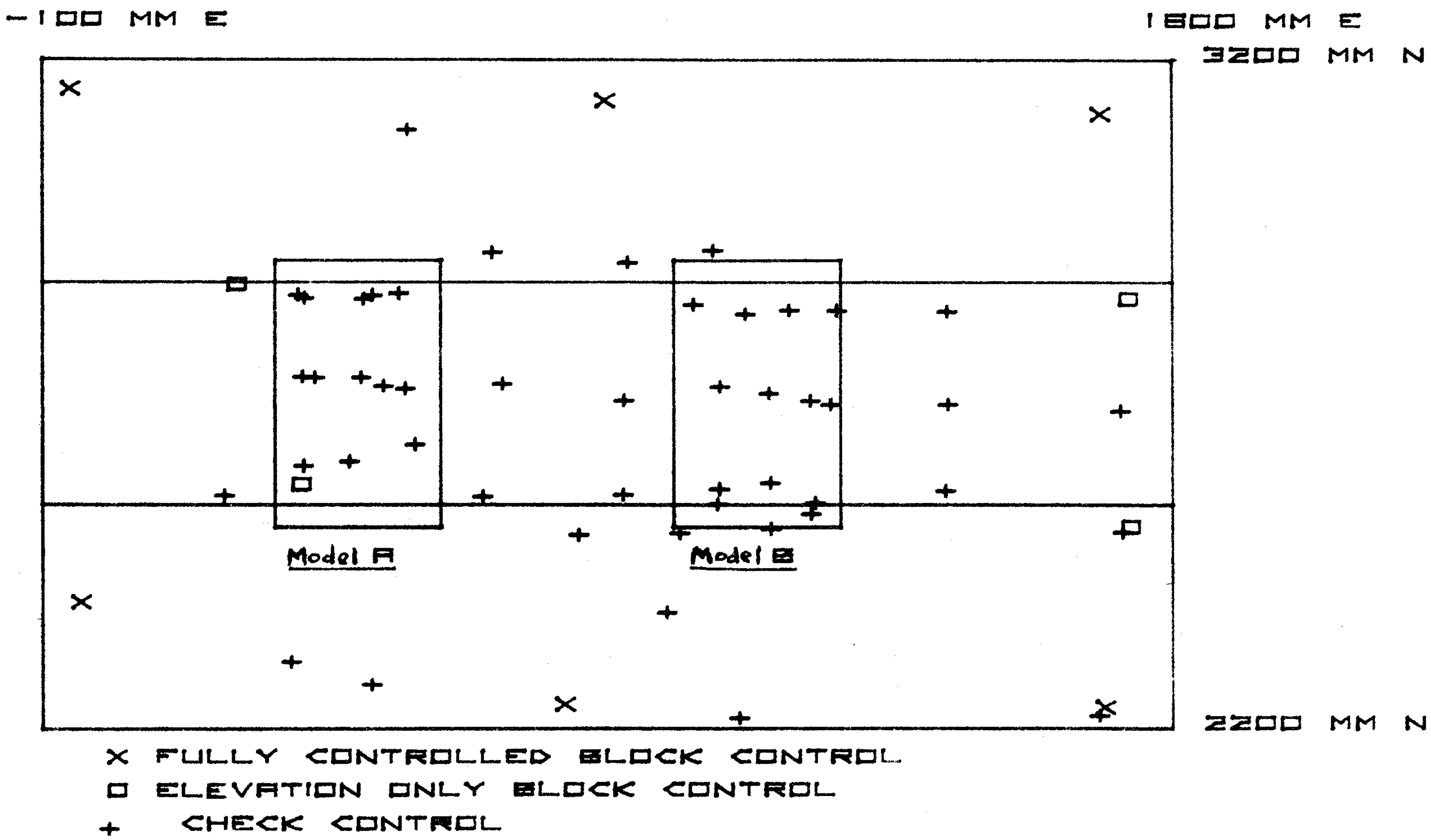

FIG 5.2 LAYOUT OF CHECK CONTROLS

Conversely elevation angles (non-reciprocal at resection points), should be measured in the period ±2 hours around midday when the diurnal variation in the vertical refraction angle is minimal *(Brown, 1968, 52)*.

All resection points were fixed from a minimum of 4 triangulation points, usually 6, using 1" theodolites and 4 rounds of angles. Connection to a suitable identifiable photographic point was then normally made by a very short radiation usually measured by steel tape, and with some form of check made on the radiation, such as a two leg traverse from the resection point. Identification of the selected photographic control point was made on the 1:25 000 photography, and supported by a field book sketch of the immediate area.

The 14 points in model A and the 13 in model B were surveyed using an electronic distance meter, Hewlett Packard Distance Meter 3800A. The survey work has been reported by ROBINSON *(1972, 143)*. As the instrument is graduated in non-SI units, these units are used in the following description.

The Hewlett Packard Distance Meter 3800A is a short range distance measuring instrument weighing 30 lb including power pack. The instrument uses a gallium arsenide diode, to emit an infra red carrier wave. The range of the instrument is quoted as 10,000 feet in ideal atmospheric conditions, and 7,500 feet in normal conditions using 3 prisms (of the AGA type). The readout system comprises a manual null, which has a maximum unambiguous reading of 9999.998 feet. The least count of the readout is 0.002 feet, although the reading may easily be interpolated to .001 feet.

The instrument is mounted on a yoke which can be adapted for the tribrach systems of Wild, Kern and Zeiss theodolites. The power supply is a 12 volt lead acid or nickel cadmium internal battery or a 12 volt external battery. The power is supplied to the measuring head through a power pack, which contains an atmospheric control unit. This control unit has a dial graduated from -50 to ±100 where these figures represent a parts per million (p.p.m.) correction to the distance for any variation in atmospheric conditions from standard. A table is supplied so that users can read off the p.p.m. setting by entering with the temperature, in degrees fahrenheit and pressure in inches of mercury or feet above sea level.

Two traverses were executed by a 3 man party within models A and B, referred to as traverses A and B, each starting and terminating at a network control point. Traverse A consisted of 6 lines with a total length of 25 000 feet, the traverse closing with a vector coordinate error of 0.72 feet (scale error 1:35 000), and angular misclosure of 14 seconds of arc, and an elevation closure of 1.21 feet calculated from simultaneous reciprocal vertical angles observed along every line. The range of temperature and pressure during the measurements was 66°F to 84°F, and 29.1 to 29.2 inches of mercury. Traverse B consisted of 7 lines with a total length of 33 000 feet. The traverse closed with a vector coordinate error of 0.56 feet (scale error 1:59 000), an angular misclosure of 2 seconds of arc, and an elevation closure of 0.67 feet. Several long radiations were measured during the course of the traverse to photographic control points, and checked at the control point end by a minimum of two directions observed to triangulation points. The two longest radiations were:

(a) 10 500 feet measured after a thunderstorm at a temperature of $70^{o}F$ and a pressure of 28.9 inches of mercury. The atmospheric conditions for this measurement were ideal, and no difficulty was experienced during the measurement.

(b) 10 600 feet measured at 1900 hours in temperature of $69^{o}F$ and pressure 29.3 inches of mercury.

During all measurements three reflectors were used except on one line of 8000 feet, for which six prisms, giving an increase of about 10% in return signal strength, were used.

The 14 traverse stations occupied, and the 27 photographic controls fixed, were surveyed by a 3 man party in 6 working days with dawn to dusk working. The superiority of E.D.M. as a method for photographic control purposes, even in an area eminently suitable for classical triangulation procedures, was clearly demonstrated in this survey. Three factors are of particular importance:

(i) Speed of reconnaissance, free from restrictions imposed by the necessity to obtain clear sight-lines to a number of fixed points. It is usually always possible to place controls in ideally located photographic positions.

(ii) Freedom from the severe limiations imposed by observing restrictions for horizontal and vertical angles. It is always possible to shorten the line length and continue working under difficult lighting conditions.

(iii) The ability to obtain reliable elevations by simultaneous reciprocal observations along the lines.

Analysis of the computations for all of the surveyed controls gives an estimated precision expressed as a standard error at the photograph controls of:

$$m'_p = \pm 0.2 \text{ m}$$

$$m'_z = \pm 0.3 \text{ m}$$

However as all of the points were subsequently snap marked using Zeiss Snap Marker for the aerial triangulation photographs, and Wild PUG4 for the orthophotograph diapositives, the estimated precision at the diapositives has been reduced to ± 0.6 metres for both plan and elevation, resulting in the following figures for control accuracy at picture scale 1:60 000 .

$$m'_{pb} = \pm 10 \ \mu m$$

$$m'_z = \pm 10 \ \mu m \ (0.09^{\circ}/ooZ) \qquad (5.1)$$

5.3 Experimental Work in Perspective Centre Calibration

5.3.i

The aerial triangulation phase was to be executed by the method of Independent Models, using a Wild A.8 precision plotter. At the time of execution (1969-1970), very little literature on perspective centre calibration had been published, and therefore a considerable amount of work was carried out on this topic, which to some extent paralleled work being carried out simultaneously elsewhere.

Aerial triangulation by the method of Independent Models, sometimes called semi-analytical triangulation, has become a popular procedure because modern Precision plotters such as the Wild A-8, Zeiss Planimat, and Zeiss Stereometrograph can be used in dual-purpose roles both as traditional cartographic plotters, and also for aerial triangulation observations. In large photogrammetric organisations this promotes efficient and flexible planning of production from plotters in this category, in contrast to the situation of recent times, when aerial triangulation was the reserve of the more expensive and relatively fewer Universal plotters, or analytical systems using comparators. There is little doubt that precision plotters can achieve measuring accuracies of the same order as the Universal machines. In small organisations the practical advantages of carrying out all work on one type of machine are extremely attractive.

The basic requirements of a plotter capable of independent model triangulation are that it must be possible to carry out a relative orientation, and it must be possible, as in the case of the classical procedure, to register the coordinates of pass points.

In the observation procedure two successive models are separately set up by relative orientation only, i.e. at arbitrary scale and exterior orientation. The connection between successive models is achieved in the computational absolute orientation of a new model, through transformation into the coordinate system of the previous model, by the control data provided by common pass points *and the common perspective centres.*

5.3.ii

The computational problem may be written as the transformation:

$$\begin{Bmatrix} X' \\ Y' \\ Z' \end{Bmatrix} = \lambda.M. \begin{Bmatrix} X'' \\ Y'' \\ Z'' \end{Bmatrix} + \begin{Bmatrix} \Delta X \\ \Delta Y \\ \Delta Z \end{Bmatrix}$$

in which λ is a scale factor, M is a 3 x 3 orthogonal matrix in which the elements are functions of 3 rotations κ, ϕ and Ω around Z, Y and X axes respectively, and ΔX ΔY ΔZ are translations giving 7 unknowns. X' Y' Z' are the coordinates in the first (fixed) model, and X" Y" Z" the coordinates in the next model.

By analogy with the empirical absolute orientation of a plotter in a cartographic role, there is no difficulty in the solution for the 6 unknowns λ, κ, Ω, ΔX, ΔY, ΔZ, from a minimum of 2 separated pass points in the small common overlap between models, for which full coordinates are known in both systems; *but there is no solution possible for ϕ unless a common third point is available which is non-collinear with them,* because the joined models would be free to rotate in ϕ around the axis joining the pass points, which is nearly a Y axis.

The best solution for ϕ is given by a third common point which is as far as possible from the pass point axis, *and this common point is the perspective centre of the common plotting camera between the two models,* which is the right camera of one model, and the left camera of the successive model. Clearly for the determination of ϕ, *only the X coordinates of the perspective centres are required with precision,* but because the procedure is computational the

Y and Z coordinates must also be known at least approximately. The point is of interest however, because it will be shown that the X (and Y) coordinates can be determined without being influenced by errors in the determination of Z.

Since the perspective centres must be known in the model coordinate system, *in principle each model should be set up in a condition in which the coordinates of the perspective centres remain invariant*, so that any element which moves a perspective centre should not be disturbed. In such a case it will usually be sufficient to determine perspective centre locations by calibration immediately before and after a complete task of several models comprising a strip or block. In some plotters however the locations of the perspective centres change during relative orientation, e.g. in the Planimat because the axes of rotation of ϕ and ω do not intersect the projection cardan; and in the PG2 where the element $b\Phi$ is essential for relative orientation; and in such cases the locations must be determined in every model observed.

The precision to which the coordinates of the perspective centres can be determined is a matter of importance both for practical reasons and from a theoretical point of view. In the first place the stability of the centres will have a direct bearing on the frequency of calibration, and in the second place the method of effecting the mathematical join between models is influenced.

TRINDER *(1971)* has remarked that in the well-known method of SCHUT *(1967)* and THOMPSON *(1959)*, the perspective centres common to two models are made to coincide. His conclusion is that the perspective centre are thus given a variance of zero, apparently on the assumption that they are determined with infinitely greater precision than the coordinates of common model pass points. Published experimental work such as that of LIGTERINCK *(1970)*, STEWARDSON *(1972)*, and EBNER and WAGNER *(1972)*, does not support this assumption, and it would seem more appropriate to introduce suitable variances for common pass points and common perspective centres into the transformation. The recent Independent Model programme of the Institute of Photogrammetry of the University of Stuttgart assigns the same weight to perspective centres as to model pass points.

5.4 Methods of Determination of Perspective Centre Coördinates.

5.4.i

There are three methods available for use in the determination of perspective centre coordinates, one of which requires essential special equipment, the second of which requires at least a calibrated reseau or grid plate for the observation, and the third which requires no extra equipment and is completely general. The methods are respectively referred to in this work as (i) Vertical Space Rod Method, (ii) Spatial Resection Method, and (iii) Spatial Intersection Method.

5.4.ii Vertical Space Rod Method

In principle special equipment is provided to enable each space rod in turn to be placed vertical in the plotter, either by means of magnetic bubble levels (Zeiss PLANIMAT) or by means of auto-collimators (PG2, PG3). When this position is achieved, the space rod is moved vertically until a calibrated mark on the space rod is viewed through a microscope. Recording of the X Y position of the projection centre is made immediately, and the Z is obtained by adding the known calibrated distance of the annular mark along the space rod to the actual Z reading of the model point which may be in an arbitrary datum selected below the lowest point of the strip surface. The mark will usually be offset from the perspective centre by some constant amount which will be taken into consideration.

The advantage of the method is that it is extremely quick and is thus eminently suitable to those plotters in which the perspective centre must be determined in every model, because Relative Orientation has altered the position of the perspective centres in model space. EBNER and WAGNER *(1972)* conclude that their experimental work shows that this method gives better results in the case of wide angle photography than the spatial resection method, and that in the case of ultra-wide-angle that the results are about the same. The method is not however of general application because of the requirement for special equipment.

5.4.iii Spatial Resection

This method requires the use of a calibrated reseau or grid plate on which at least 3 non-collinear points are observed at a constant Z value, and the model space XY coordinates of these points registered. Initial approximate values $X_c Y_c Z_c$ of the projection centre are required. The discrepancies dX, dY, between the measured coordinates and computed ideal projected coordinates are inserted in linearised correction equations of the form:

$$v_X = dX_c + \frac{X}{Z}.dZ_c + \frac{XY}{Z}.d\omega - \left(\frac{X^2 + Z^2}{Z}\right).d\phi + Y.d\kappa - dX$$

$$v_Y = dY_c + \frac{Y}{Z}.dZ_c + \left(\frac{Y^2 + Z^2}{Z}\right).d\omega - \frac{XY}{Z}.d\phi - X.d\kappa - dY$$

The problem will usually be overdetermined and solution of the normal equations by a least squares method gives corrections dX_c, dY_c, dZ_c to the assumed perspective centre coordinates, and $d\omega$, $d\phi$, $d\kappa$ to the initial settings of the orientation elements. The corrections are applied and the solution iterated until the changes in the corrections are not significant.

The major drawback of this method apart from the fact that a grid plate is required, is that the errors of inner orientation Δx_o Δy_o Δc are assumed to be zero when such will rarely be the case. These errors arise from three sources: firstly the placing of the grid plate on the register plate in the plotting camera, secondly the inner orientation errors of the fiducial marks of the register plate, and thirdly the location errors of the plateholder, and this latter error will change according to which plotting camera an individual plate holder is placed in.

5.4.iv Spatial Intersection

The method of spatial intersection, which has been that used in this work, has the advantage that it is completely free from errors of inner orientation and requires no special equipment whatsoever; so that it may be used for example with observation points defined by photographic images, by artificial photographic points such as artificial pass points, by register plate marks, or by grid points. It is therefore eminently suitable in production since perspective centre determination can be made at any phase of the triangulation procedure even when models are set up for observation if for some reason this should be considered desirable.

The observed points are observed at two different Z levels in the plotter (Z' and Z"), separated by as great a measured Z distance as possible for the configuration of points and the working ranges of the plotter. The intersection $X_cY_cZ_c$ is defined by the intersection of two or more lines joining corresponding points at different levels. The collinearity equation for the perspective centre and two corresponding points is given by:

$$\frac{X_c - X''}{X'' - X'} = \frac{Y_c - Y''}{Y'' - Y'} = \frac{Z_c - Z''}{Z'' - Z'}$$

or in matrix notation:

$$\begin{pmatrix} -(Z''-Z') & 0 & (X''-X') \\ 0 & -(Z''-Z') & (Y''-Y') \end{pmatrix} \begin{pmatrix} X_c \\ Y_c \\ Z_c \end{pmatrix} = \begin{pmatrix} -X' & X'' \\ Y' & Y'' \end{pmatrix} \begin{pmatrix} Z'' \\ Z' \end{pmatrix}$$

There are 3 unknowns $X_cY_cZ_c$ and each pair of points gives two equations so that the problem is solved with one observed pair of corresponding points in which both X and Y coordinates are observed, and one pair for which either X or Y are observed. In practice usually 6 points are fully observed at both levels, and it seems logical to select points at standard relative orientation and pass points locations.

It is interesting to note that although $X_cY_cZ_c$ are normally determined simultaneously by actually measuring the Z level shift (Z"-Z'), that any arbitrary values may be assigned to Z" and Z' *and the numerical solutions for X_cY_c are not altered,* but of course the Z_c value changes. The problem may in fact be approached as if it were a two dimensional problem, by assuming that the observations are made in one Z plane and reducing the collinearity equations to

$$\frac{X_c - X''}{X'' - X'} = \frac{Y_c - Y''}{Y'' - Y'}$$

It follows that the precision of determination of X_c and Y_c is not influenced by the determination of Z_c or the measurement of (Z"-Z').

5.5 Restoration Stability of Perspective Centre Calibration

There is now available a reasonable amount of test data on the question of the precision of perspective centre determination on particular instruments. A matter of interest however, for which no data was available, is the extent to which the perspective centres may be regarded as stable, *provided that all orientation elements and coordinate initialisations which affect the positions are returned to the calibration state.*

In general, any instrument in which the relative orientation elements move the perspective centre must include a calibration in every model. In principle any instrument in which this is not so, may be returned to a particular calibration state by careful setting of appropriate datums on any variable outside the plotting cameras which either physically or effectively changes the coordinates of the centre. If the number of variables is large however the restoration of the calibration condition is poor.

The Wild A-8 instrument has the least number of variables which affect perspective centre position, particularly if the base carriage X and Y scales are used for coordinate reading, as must be done if no automatic registration device is available. The variables are 3:

Z_o (Z column and Glass Scale initialisation)

bx (Base Setting)

Φ_o (Common Longitudinal Tilt Datum).

The only modification to the instrument was the addition of an index mark on the Φ wheel axis and the axis bearing to define Φ_o. The instrument was then returned to standard calibration state by setting a bx value of 160 mm (for wide angle photography), setting ϕ_o, and setting Z_o by bringing the Z column main reading to 300 mm with the Z lead screw index mark aligned. A 1:5 000 metric glass scale was set to zero at this position so that XYZ coordinates could be read in similar units (as the XY scales are in 2 mm units).

A test was carried out in which 10 separate calibrations were made by 15 point spatial intersection method over a period of 7 days. Before each calibration the variable elements were deliberately moved off by large amounts and then brought back to datum positions. Each test included small random inner orientation errors of the grid plates used. In two tests relative orientation elements ϕ and ω were given large inclinations. The observations were computed both as 6 point and 15 point intersections. The abbreviated results for the left camera are given in Table 5.1 in terms of micrometers at the plate (i.e. model enlargement 1).

TABLE 5.1

Restoration Stability from 10 Calibrations

	6 points			15 points				15-6		
	c_{X_L}	c_{Y_L}	c_{Z_L}	c_{X_L}	c_{Y_L}	c_{Z_L}		Δc_X	Δc_Y	Δc_Z
m.s.e.	14	15	11	13	14	11	mean	+ 4	-1	-8
spread	44	52	37	39	44	33	max	+12	-7	-10

It was concluded that the instrument could be restored to calibration condition with some degree of confidence. The test supported the results of other workers that observations to more than 6 points are hardly warranted. It should be noted that the 3 maximum differences between computed coordinates from 15 and 6 point observations all occurred in different calibrations for the ΔX, ΔY, and ΔZ differences.

A simple modification to an A-8 plotter has been designed to facilitate rapid restoration of predetermined calibrations, and this modification is still under test. A spacing block of mild steel about 65 mm in length is inserted at the Φ lead screw base plate under the left hand camera, and this takes the weight of the upper plotting cameras when Φ is rotated to a reading below 100.00 g. Restoration to calibration parameters for Φ is very easily achieved, and tests are in progress to determine the precision.

5.6 Computation Methods of the Intersection Problem

5.6.i Form of the Equations

For each point observed at the two levels Z' and Z" two equations are formed:

$$-(Z'' - Z')X_c + (X'' - X')Z_c = X''Z' - X'Z'' \qquad (5.ii)$$

$$-(Z'' - Z')Y_c + (Y'' - Y')Z_c = Y''Z' - Y'Z'' \qquad (5.iii)$$

Where X" Y" and X' Y' are the measured coordinates and $X_c Y_c Z_c$ are the coordinates of the perspective centre. Z", Z' and the measured coordinates contain observational errors, and residuals vx", vy", vx', vy', vz", vz' are therefore introduced into the equations.

Equation (5.ii) becomes:

$$(Z' + vz' - Z'' - vz'')X_c + (X'' + vx'' - X' - vx')Z_c$$
$$= (X'' + vx'')(Z' + vz') - (X' + vx')(Z'' + vz'')$$

Equation (5.iii) takes identical form except that X and vx are replaced by Y and vy.

If the equations are expanded and products of residuals ignored the following result is obtained for the X equation:

$$(X' - X_c)vz'' + (X_c - X'')vz' + (Z_c - Z')vx'' + (Z'' - Z_c)vx'$$
$$+ (Z' - Z'')X_c + (X'' - X')Z_c + (X'Z'' - X''Z') = 0$$

Approximate values of $X_cY_cZ_c$ are therefore required in order to form the coefficients in the equations. If n points are observed at both levels, a set of 2n equations of this type is obtained.

The equations have the form Av + Bx + C = 0 where A and B are rectangular matrices, while v, x and C are the vectors of residuals, perspective centre coordinates, and constant terms respectively.

The least squares solution of the equations is:

$$x = - [B^T(AGA^T)^{-1}B]^{-1} B^T(AGA^T)^{-1}C \qquad (5.iv)$$

$$v = - GA^T(AGA^T)^{-1} (Bx + C) \qquad (5.v)$$

where G is the matrix of weight coefficients of the observations.

The variance-covariance matrix of the perspective centre coordinates is given by -

$$\sigma_{xx} = \sigma_o^2 \, [B^T G^{-1} B]^{-1}$$

where the unit variance $\sigma_o^2 = \dfrac{v^T G^{-1} v}{r}$ and r is the number of redundancies. If n points are observed then $r = 4n - 6$ (for two level observations).

It is clear that even when only a few points are observed, the vectors x and v cannot be solved on a small programmable calculator from equations (5.iv) and (5.v). A program was therefore written for the IBM 360, and was used to compute a large number of intersections. This program was devised by Mr. L. BERLIN of the School of Surveying, who collaborated with the writer in perspective centre calibration experiments.

5.6.ii Relative Precision of Coordinates

In forming the G matrix, the assumption was made that the observed X and Y machine coordinates had equal precision. One cannot however assume that the precision of the Z settings will be the same. This is because the Z setting is an observation of a different type, in which no pointing is made with the measuring mark. For a correct least squares solution of the Z coordinate of the P.C. the absolute values of the weight coefficients are not important. Multiplication of the G matrix by an arbitrary scalar will yield the same solution. However it was expected that the *relative* precisions of the Z setting and the X, Y coordinate measurements would affect the Z coordinate of the perspective centre.

The situation is analogous to the adjustment of a geodetic net in which both angles and distances have been measured. The result obtained will depend on the ratio of weight coefficients of the angles to the distances.

The relative precision of the Z setting to the X, Y measurements could be determined empirically, but this was found to be unnecessary. A large number of 6 point and 15 point calibrations, made on the Wild A-8 steroplotter, were processed using widely different ratios for the estimated precisions. *The perspective centre coordinates were found to agree to within a few micrometers irrespective of the ratio used, as can be seen by Table 5.II.*

It is significant that the determination of X_c and Y_c for a perspective centre is not affected by the precision of the Z setting values, nor by the actual range of Z used between the levels. If the centre coordinates are to be used only for the solution of common Φ longitudinal tilt between models, and not for the solution of the other six unknowns, then only X_c is required with precision.

5.6.iii Computation on a Desk-Top Calculator

Equations (5.ii) and (5.iii) can be treated as if they were observation equations in which the right hand sides are the "observations".

The set obtained will have the form:

$$Ax = b$$

and the least squares solution, will be

$$x = (A^TA)^{-1}.A^Tb$$

The result obtained is *identical* to the result obtained using equation (5.iv) but the computation is much easier because only 9 registers are required for the elements A^TA and A^Tb. This computation method is therefore recommended when the precision of the coordinates is not required.

To show that the above equation yields the same solution for X as equation (5.iv), let AV = U, where U can be regarded as the vector of corrections to a set of "quasi" observations, then:

$$U + BX + C = 0$$

for which the least-squares solution is :

$$X = -(B^TG_1B)^{-1}B^TG_1^{-1}C$$

where G_1 is the variance-covariance matrix of U.
Now $G_1 = AGA^T$ where G is the variance-covariance matrix of V and therefore $X = -[B^T(AGA^T)^{-1}B]^{-1}B^T(AGA^T)^{-1}C$ which is the same as equation (5.iv).

TABLE 5.II

Example of an intersection computed with different absolute values of estimated variances, and different ratios of estimated variances

Estimated σ_{xx} (σ_{yy})	Variances σ_{zz}	Ratio $\frac{\sigma_{zz}}{\sigma_{xx}}$	Perspective Centre Coordinates X_c	Y_c	Z_c	Computed Variances $\sigma_{x_c x_c}$	$\sigma_{y_c y_c}$	$\sigma_{z_c z_c}$	Observation Points
$(5\mu m)^2$	$(5\mu m)^2$	1	240.0275	200.1522	150.0247	.00005	.00004	.00032	6
$(10\mu m)^2$	$(10\mu m)^2$	1	.0275	.1522	.0247	.00005	.00004	.00032	6
$(5\mu m)^2$	$(50\mu m)^2$	100	.0275	.1522	.0215	.00005	.00004	.02340	6
$(10\mu m)^2$	$(100\mu m)^2$	100	.0275	.1522	.0215	.00005	.00004	.02340	6
$(5\mu m)^2$	$(5\mu m)^2$	1	.0213	.1516	.0247	.00002	.00001	.00021	15
$(10\mu m)^2$	$(10\mu m)^2$	1	.0213	.1516	.0247	.00002	.00001	.00021	15
$(5\mu m)^2$	$(50\mu m)^2$	100	.0213	.1516	.0215	.00002	.00001	.01725	15
$(10\mu m)^2$	$(100\mu m)^2$	100	.0213	.1516	.0215	.00002	.00001	.01725	15

5.7 Execution of Aerial Triangulation Phase

The aerial triangultion of the mapping block was executed by Independent Model method, using a Wild A.8 plotter for model measurements. The 180 mm diapositive plates were prepared with arbitrarily selected artificial pass points, by snap marking with Zeiss snap marker at image positions ±80 mm (y) from plate centre, with an additional point close to centre. Apart from checking that the pass points did not lie on disturbing image details, no attempt was made to associate the pass points with identifiable image details. Points were identified only on one diapositive for each point, except that every alternate outer pass point in the centre strip was transferred to lateral strips to serve as tie points. Ground controls were also snap marked.

The models were relatively oriented with perspective centre variable parameters as defined in 5.5, restored to standard calibration positions. The bx setting of 160 mm gave model scales of approximately 1:25 000, so that the triangulation was carried out at about the same scale as the subsequent orthophotographic mapping. Coordinates were read directly from X and Y carriage scales and micrometers, as encoders were not fitted. A glass 1:5 000 elevation scale was used for Z readings to give same scale XYZ coordinates, as the carriage lead screws are 2 mm pitch and the XY scale graduations are physically 2 mm divisions. All points were measured twice without uncoupling the freehand movement of the model point, and estimation of coordinate micrometer drums made to 0.001 (X,Y), and to 0.005 on the Z scale.

The average time for complete measurement of a model from initial insertion of diapositives was 2 hours. Due to interruptions of normal academic work when the plotter was required for other purposes, it was not possible to carry out the triangulation continuously. Frequent recalibrations of perspective centre coordinates were therefore made, using the intersection method, and observing to the six pass points within a model. Such a calibration at two levels, with manual recording, takes only about 45 minutes. As each new model was observed, the connections to the previous model were tested using program INDEMODFORM (appx. A), prepared by the writer for Hewlett Packard Model 9810A desk calculator. A desk calculator used in such a role operates virtually as a computer on-line to the plotter, average time for a model connection solution being about 45 seconds.

5.8 Aerial Triangulation Results

For the reasons discussed in 5.3.ii, connection of Independent Models by a computational process in which perspective centres are joined as if they were error free, is undesirable. Program INDEMODFORM was therefore prepared for the strip formations, a characteristic of the program being that perspective centres and model pass points are treated with the same weight. As a check however, the same model data was processed through SCHUT's program *(1967)*, on the University of New South Wales IBM 360 computer. Table 5.III gives the comparison between the two methods of strip formation, in terms of micrometers at plate scale 1:60 000. The figures given are the mean square errors of the residual half-discrepancies from mean coordinate positions at the join points, i.e., half the residuals between each join point after transformation. Separate figures are given, firstly for all joins including perspective centres, secondly for model pass points only. In the former case the discrepancies using SCHUT program are zero at perspective centres. For the first case there is hardly a significant difference for Δx and Δy, but an improvement of 8 µm Δz with INDEMODFORM. In the second case, an improvement takes place of 10 µm in Δy and 13 µm in Δz.

After strip formation, the strips were subjected to block adjustment using the program referred to in 2.2, *(SCHUT, 1968)*. The program is essentially a strip adjustment in which height corrections are parabolic functions of specified degree in the planimetric coordinates, and the planimetric adjustment is a conformal transformation of specified degree in the planimetric coordinates. The block adjustment is an iterative procedure in which each strip is transformed in turn, using as control points any ground controls and tie points with overlapping strips. As the iterations proceed, the updated values of tie points are used as ground controls. SCHUT comments *(1968, 2)* that as a rule ten iterations of a block adjustment are ample to obtain the desired degree of convergence.

TABLE 5.III

Mapping Block Triangulation

Discrepancies according to treatment of model joins

µm at plate 1:60 000

TYPE	HOLDEN INDEMODFORM STRIP FORMATION				SCHUT STRIP FORMATION		
Strip Formation (108 joins)	(incl. perspective centres)	$m_X 3$	$m_Y 24$	$m_Z 19$	$m_X 4$	$m_Y 26$	$m_Z 27$
½ discrepancies at join points	(model points only)	$m_X 4$	$m_Y 20$	$m_Z 19$	$m_X 5$	$m_Y 30$	$m_Z 32$
Block Tie Points (12 ties)	$m_{(XYZ)}$	9	15	16	10	18	25
½ discrepancies	$\Delta_{(XYZ)}$ maximum	14	33	30	16	36	42
Ground Control Residuals (58 points) after block adjustments to 6 full and 4 elevn. controls	$m'_{(XYZ)}$	25	31	25	28	32	34
	$\Delta_{(XYZ)}$ maximum	62	81	69	67	96	82
		m'p 40 µm			m'p 43 µm		
		m'z 0.22$^{0}/_{00}$%			m'z 0.30$^{0}/_{00}$%		

In the case of the mapping block, adjustment was computed with 2nd degree planimetric corrections, and 2nd degree longitudinal and lateral height corrections. The solution was iterated nine times, at which stage examination of changes in successive coordinates of selected points indicated that convergence was satisfactory. The computation was carried out using strip coordinates computed both from INDEMODFORM and SCHUT programs. Table 5.III also gives results for mean square errors at tie points for both solutions, and the final residual errors at all check ground controls, maximum values also being given. The improvement in Δy and Δz residuals, as indicated in the strip formation results, is maintained to a limited extent at all stages, but particularly in Δz.

The accepted results, give for the checked precision of the mapping block at plate:

$$\begin{aligned} m'_p &= \pm 40\ \mu m \\ m'_z &= 0.22\ {}^{o}/_{oo}Z \end{aligned} \qquad (5.iv)$$

In comparing these figures with those of the estimates (2.v) and (2.vi), it is seen that the plan error is almost at the mean of the range, and the elevation error at the lower end of the range. However the block is smaller than a usual mapping block.

5.9 Aerial Triangulation Errors in Test Models

The errors of the derived aerial triangulation coordinates (X'Y'Z') within test models A and B were separately analysed. The analysis was performed using program ABSOR (appx. A), also prepared by the writer for HP9810A desk calculator. The coordinates X'Y'Z' were subjected to an analytical absolute orientation, by comparison with the known ground coordinates (XYZ) of the 14 ground controls in model A and the 13 in model B. For the sake of convenience, all geodetic coordinates used from every phase of the test programme from aerial triangulation onwards, were arbitrarily scaled to equivalent millimetres at orthophotographic scale 1:25 000 and shifted to arbitrary local origin, see fig. 5.2. The model errors are given in table 5.IV. The model errors were in general rather better than in the block as a whole, but within model A there was a rather systematic tendency in the plan coordinates, only 3 of the X' and Y' coordinates having negative errors, with the remainder having positive coordinate errors.

TABLE 5.IV

Analysis of errors of aerial triangulation coordinates within test models

(a) Model A

	$\Delta\Omega$:	-0.6c
	$\Delta\Phi$:	-2.0c
	$\Delta\kappa$:	-0.2c
	Scalar:	$-0.16^{\circ}/_{oo}$
Translation	ΔX:	+0.022 mm
"	ΔY:	+0.045 mm
"	ΔZ:	+0.004 mm
	m'_x:	±21 μm (at plate)
	m'_y:	±26 μm "
	m'_p:	±33 μm "
	m'_z:	$\pm 0.16^{\circ}/_{oo}Z$

(b) Model B

	$\Delta\Omega$:	+1.7c
	$\Delta\Phi$:	+0.0c
	$\Delta\kappa$:	+0.2c
	Scalar:	$+0.10^{\circ}/_{oo}$
Translation	ΔX:	+0.005 mm
"	ΔY:	+0.014 mm
"	ΔZ:	-0.009 mm
	m'_x:	±17 μm (at plate)
	m'_y:	±20 μm "
	m'_p:	±26 μm "
	m'_z:	$\pm 0.25^{\circ}/_{oo}Z$

6. EXECUTION OF TEST PROGRAMME

6.1 Selection of production parameters for tests

6.1.1

The mapping photography of 1:60 000 scale offered several possibilities of choice of orthophotograph scale in the combination Topocart-Orthophot. As a general principle the tests were to be carried out at maximum possibilities, rather than to be influenced by conventional mapping criteria. The maximum enlargement from plate to model scale is determined by available Z range for a particular classification of camera, as given in 3.2. In the case of 115 mm wide angle camera the maximum enlargement model scale from plate scale ($V^m/_b$) is 2.7, and thus the maximum rational metric model scale is 1:25 000 ($V^m/_b = 2.4$). The connection from Topocart to Orthophot is through a range of mechanical gears, but practical limitations are imposed by overall range of magnification from plate to orthophotograph $V^d/_b$ as given in 3.4; since for a scanning area equivalent to 100 mm (x) by 200 mm (y) at plate maximum $V^d/_b$ is 3.65 in a single scanning operation. Taking $V^m/_b$ as 2.4, the gear connection possibilities to the Orthophot inversor control permitted choice of either 1 or 1.25 magnification from model to orthophoto, for an overall $V^d/_b$ of either 2.4 or 3, orthophoto scales 1:25 000 or 1:20 000. The former scale gives a value for the constant k of formula (1.v) $m_b = k\sqrt{m_k}$ of about 380, and the latter of about 425, both figures being well above conventional mapping limits. Orthophotograph scale of 1:25 000 was selected, as this is a more usual standard medium mapping scale.

6.1.ii

Choice of appropriate contour interval for profile signals for the production of drop line charts is conditioned by the availability of Orograph adaptor plugs (3.8) for a particular model scale; but is influenced also by the terrain conditions and the elevation ranges within the test areas. Model A of broken terrain contained a total range of elevation of about 100 m, Model B of relatively flat terrain a range of only 20 m. In the latter case a choice of contour interval of 20 m or 10 m would have proved quite inadequate for tests of contouring possibilities in flat terrain, and thus a choice of 5 m seemed appropriate. In the former case the area contained several hill slopes of the order of 20 g, and in such slopes a contour interval of 5 m would result in planimetric separation of profile signals and contours, of only 0.62 mm at orthophoto scale 1:25 ooo. However the mean slope of the model was estimated from the slopes at all check points as 3 g, resulting in a mean planimetric separation of about 4 mm at orthophoto scale. Considered in terms of Contour/Altitude ratio C numbers for a flight altitude of 6875m, the contour interval of 5 m gives C number 1375, and contour interval of 10 m gives C number 688. The larger number was deliberately selected for the majority of tests in accordance with the principle of working to maximum possibilities. However it would clearly have been absurd to attempt such a small profile interval in Model A in the case of spacing of profiles at Δx 16 mm, since anomalies would be created in attempting to join corresponding profile signals with a mean planimetric separation along the profiles of 4 mm. In all tests therefore except 16 mm slit width tests in Model A, the selected contour interval was 5 m; and in the case of the exceptions the contour interval was 10 m (table 4.1). Orograph adaptor plugs of ΔZ interval 0.2 mm and 0.4 mm were available for the model scale 1:25 000.

6.2 Description of test model A in broken terrain

Model A was an area of about 5½ by 10 km, with total elevation range of about 100 m, and ground slopes in the fall lines to a maximum of 20 g, mean ground slope at 56 points 3 g. The centre area of the model is characterised by a broadly undulating perched stony plain, with shallowly incised dendritic drainage; draining through a rather sandy tract up to 200 m wide, towards the east. Above the main drainage tract there are rounded gravel hills, with slopes to 6 g, and some minor limestone outcrops of local elevation 15 m. Vegetation in this area consists of bladder saltbush *(atriplex vesicaria)* and grasses, with the drainage tracts generally bare. The north section of the model was more rugged with some ranges of massive sandstone of rather rocky crests and faces, with local elevations to 50 m, including one very steep peak: "Butlers Peak:. Vegetation includes saltbush and grasses, and fairly extensive cover of mulga trees *(acacia aneura)*. The western side of the model is rather stony

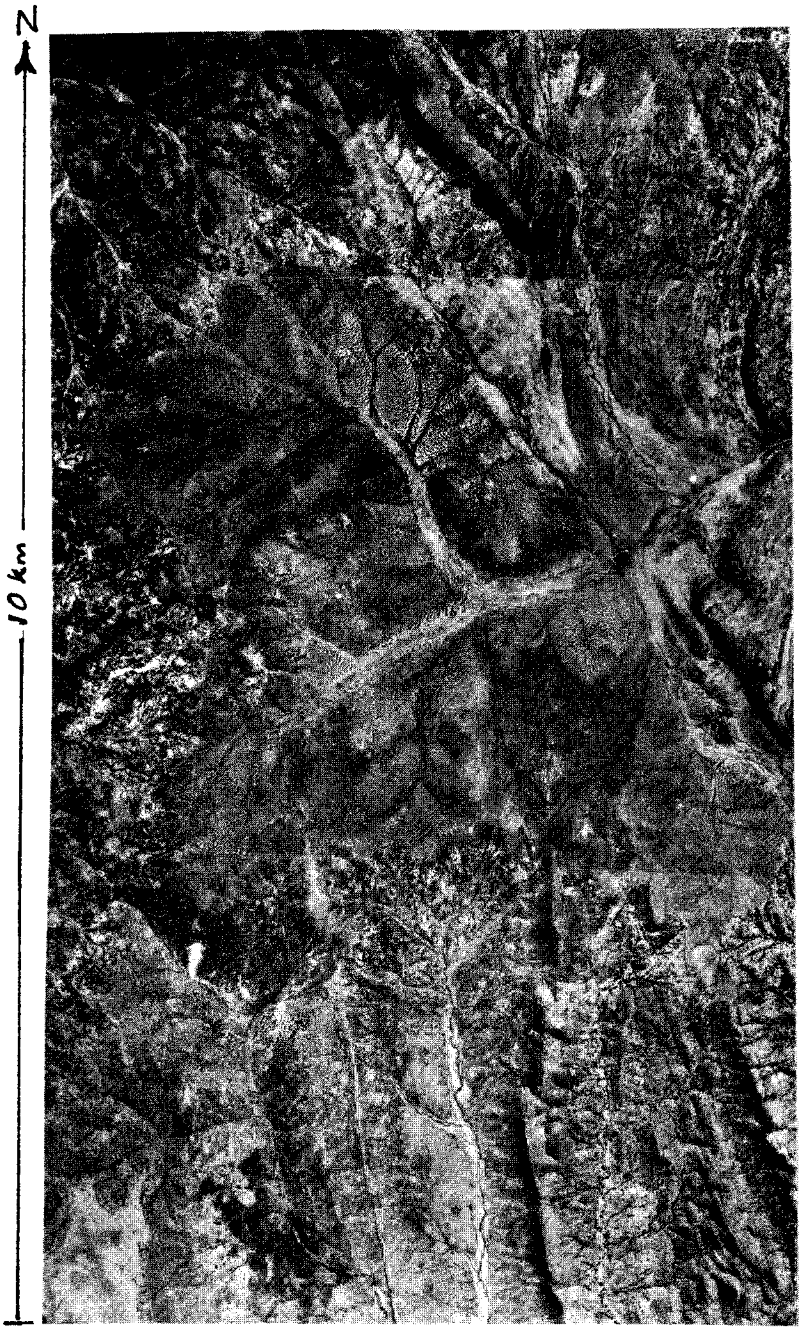

Model A (0506) of broken terrain,
at plate scale 1:60 000.

PLATE 2

undulating country with a dense dendritic drainage, severely gullied in many places, and draining to the west. The south eastern part of the model contains high sandstone ridges of local elevation to 50 m with prominent outcrops of quartzite, and low rounded hills with an extremely complex pattern of incising trellis drainage, draining to the south. A striking feature is a long high sandstone ridge some 200 m wide, running almost northwards, and thus parallel to the y (scanning) direction of the model. This model was expected to present a severe challenge to the principle of drop line derived contours, in view of the geomorphology of the area, and the complex drainage pattern, draining to all principal directions. Model A is pictured at plate scale 1:60 000 in plate 2.

6.3 Description of test model B in flat terrain

Model B was also an area of about 55 km^2, but quite different in character, since the total elevation range was only 20 m with an almost uniform slope from south-western corner of the model to north-eastern, of the order of 0.15 g. The area consisted principally of a flat to the east of a 1 km wide floodplain, with a main trenched creek 10 m wide passing diagonally across the north-western part of the model. The main creek was rather indefinite in many places, with several sinuous braided sandy channels. In the flat there were many hard bare claypans, and rather ill defined drainage zones. The vegetation consisted of saltbush and abundant perennial grasses, and scattered and isolated prickly wattle *(acacia victoriae)*. Model B is pictured at plate scale 1:60 000 in plate 3.

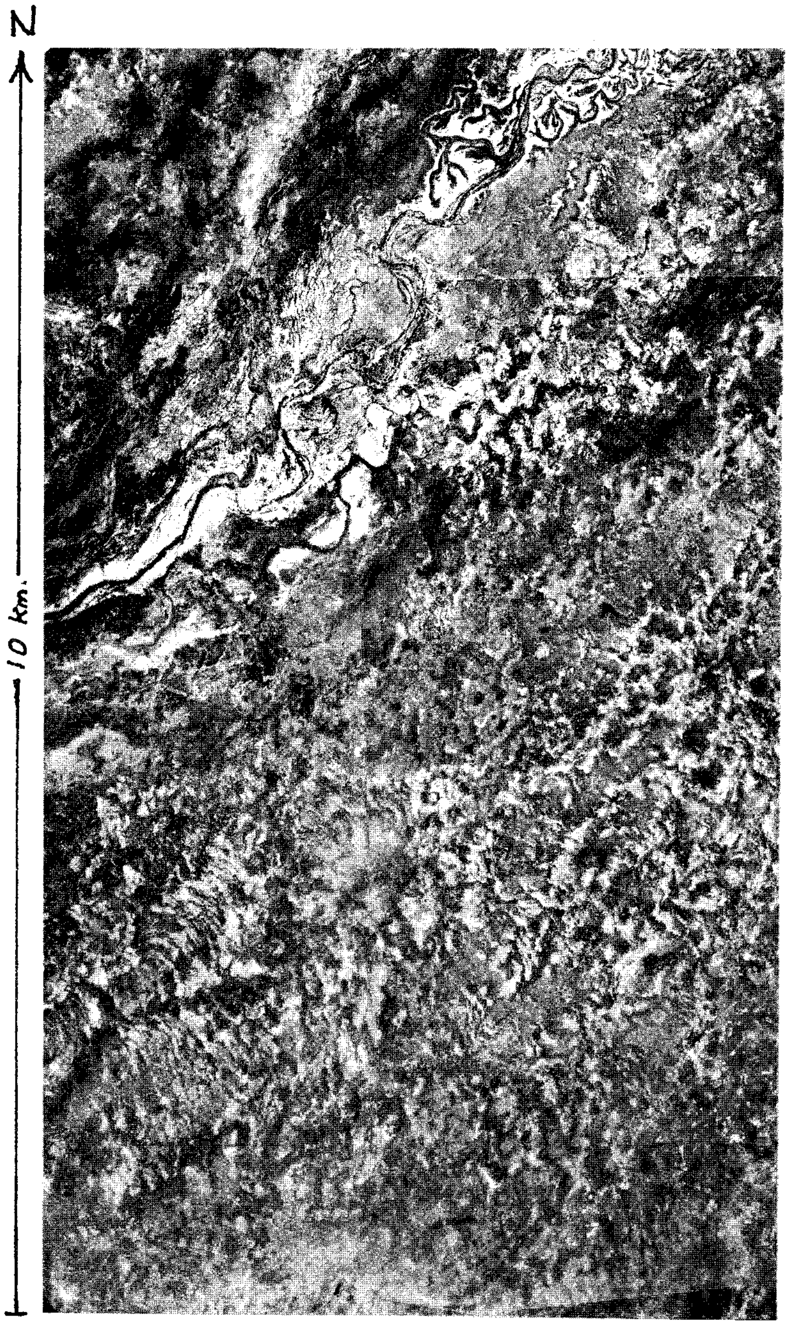

Model B (0910) of flat terrain,
at plate scale 1:60 000.

PLATE 3

6.4 Provision of additional photogrammetric test points

Since only 14 ground check points were provided in model A, and 13 in model B, additional check points were provided in both models by photogrammetric methods. The area of each orthophotograph model was also covered by six overlaps of 115 mm wide angle photography at plate scale 1:25 000 from altitude 2875 m (5.2); and the location of ground controls enabled each of these larger scale overlaps to be set up on 4 ground control points. Additional photographic controls were selected and marked by Wild PUG4 Point Transfer Device, both on the 1:25 000 diapositives and in one plate of a set of 1:60 000 diapositives to be used for the orthophotography. The 1:25 000 plates were set up in Wild A.8 plotter at model scale 1:10 000, and the new points measured for XYZ coordinates with three observations to each mark, together with the ground controls. The mean observed coordinates were transformed analytically to the ground control system, through HP 9810A program ABSOR (appx. A). The residual errors at the ground controls after transformation, enabled an estimate to be made for the precision of the new points of ±0.5 m for both plan and elevation. It was assumed therefore that the new points had the same precision at the mapping photography scale as the surveyed control points, as given in equation (5.1). The location of all controls in both models, totalling 56 in Model A and 50 in Model B, is shown in the plan vector error figures in 7.

6.5 Operation of the test programme

Table 4.1 gives a schedule of the test programme. In Model A, twenty tests were run at four slit width sizes and with five speed variations. Four of the speed variations were tests in which the speed was quite constant throughout the scan. The fifth variation was a variable speed scan at operators discretion, and in each of the four variable speed test subsequent analysis of total time and line length showed that the average speed achieved was about 2.6 mm/sec in the orthophoto, equivalent to 1.08 mm/sec at plate. In every test a drop line chart was produced by Orograph. It was not intended to analyse all of these charts, but since their production involved very little extra work, superfluous charts were produced in order to gain experience in the technique; and in particular to provide spare charts for experiments in contour drawing.

A record of production times, and of setting values of variable controls such as exposure lamp intensity, was maintained on a panel fixed to the drop line charts, examples of which may be seen in annexure 1. The item 'scan time' refers to the total scanning time from the moment at which the cassette shutter is opened, until the cassette shutter is finally closed. This time includes the time required to move from one scan line to another, but excludes any short non-operational period, when the operator momentarily rested. The item 'completion time' includes operator rest periods, and work carried out after cassette closure. This work includes the identification of control points, marginal notes, and in principle the provision of 'guide contours' and spot heighting of salient points by conventional plotting techniques.

The identification of control points is essential because the chart cannot easily be placed in orientation in a similar manner to a conventional mapping plot prior to commencing work, owing to the mechanical operations necessary in starting the scanning procedure. The chart however remains in registration with the plotter when the Orthophot unit is disconnected at the drawing table after final closure of the cassette shutter, at which stage the plotter derives may be converted to conventional plotting mode. The identification of contour bands with elevation values was achieved after cassette closure, and before Orthophot disconnection, by moving slightly to the right of the last profile by a few Δx increments. With the cassette shutter microswitch short-circuited, a short scan length was then run with elevation raised through each band in turn, and the band limits were then labelled with model Z values and corresponding elevations as shown in plate 4.

In principle at this stage, guide contours and spot heights should be provided, as well as contours for missing details such as isolation contours between profile lines. In practice the complexity of contouring of model A, was such that it would have been very difficult for the operator to decide

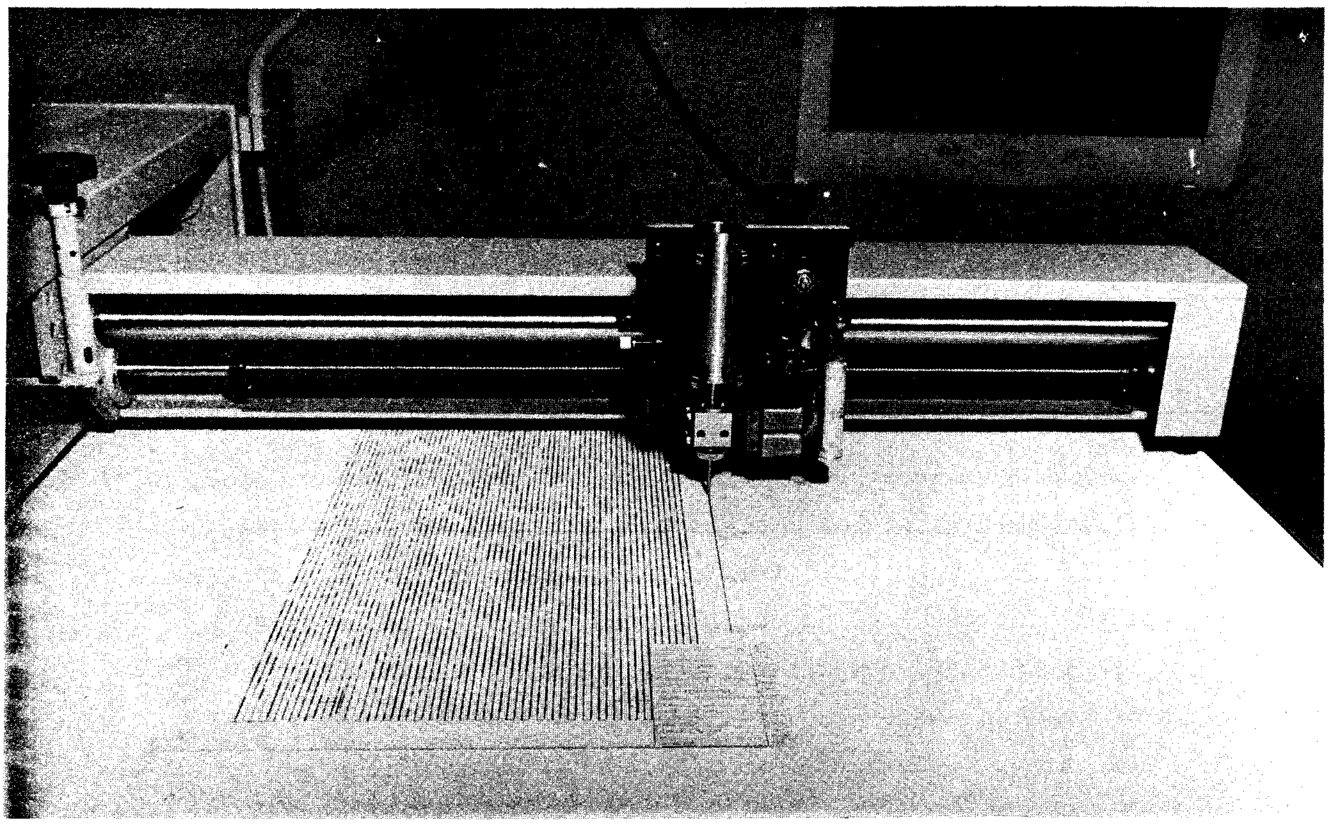

Production of drop-line charts by Orograph

PLATE 4

when to cease plotting in this conventional way. This procedure was therefore deliberately curtailed, and guide contours were provided only for one continuous contour along each fall line of the long sandstone ridge, and one isolation contour of the peak, both features referred to in 6.2.

The scan and completion times do not include the preparation period prior to scanning; comprising relative and absolute orientation, switching of the drive elements, test exposures, and insertion of the film and the cassette. The tests of model A were carried out over a period of 3 months, and the average of all preparation periods was 2 hours. The inner orientation of the plates was never altered, but several relative and absolute orientations were carried out.

In every test the control data used for orientation was simply that of the 4 outer pass points with coordinates derived from the aerial triangulation results (5.8). Absolute orientation was carried out by measuring model coordinates of these points and computing the orientation parameters by HP9810A with ABSOR program (appendix A). After setting corrections, orientation was considered satisfactory to normal production standards, when residual Ω and Φ errors did not exceed ±1 c, and scalar error ±0.5 $^{o}/oo$.

Test model B in flat terrain, was executed only at was considered to be normal production slit widths and speed for such a case; namely a fixed speed of 4 mm/sec in the orthophoto (1.67 mm/sec at plate), and exposure slit widths of only 8mm and 16mm.

The film used throughout the tests was KODAK Commercial Film 4127, estar thick base, 0.18 mm thick. Developement was by ILFORD Bromophen, a phenidone - hydroquinone developer, with stock solution diluted by 3 parts water; and developement variable but on average 1½ minutes with continuous agitation in a dish. The film was then washed, and subsequently fixed with ILFORD Ilfofix, an acid hardening fixer diluted 1:1 and fixed for 10 minutes. Finally all films were left in running water for 3 hours, and then allowed to dry naturally suspended in the darkroom for 24 hours. Subsequently they were suspended in a frame, and allowed to stabilise for a minimum of 48 hours in the laboratory where the coordinatorgraph was housed, before any coordinate measurements were made.

All operational tests and processing procedures were carried out by the writer.

6.6 Calibration of Coordinatorgraph

6.6.i

Plan measurements on the orthophoto negatives were to be made to the snap marked check points, using a spotting microscope in the pencil holder of a Wild 1000 mm square coordinatorgraph, and mechanical counter drums with direct reading to 0.01 mm and estimation to 0.001 mm. The coordinatorgraph is normally connected as plotting table to a plotter, but was disconnected for the orthophoto measurements. The coordinatorgraph is of the type with a fixed rail for one axis, usually the Y axis, carrying a movable cantilevered rail driven by lead screw, normally the X axis. The cantilevered rail contains a second lead screw driving the pencil holder.

This type of coordinatorgraph is prone to small systematic errors of non-orthogonality of the movable axis, and adjustment screws are provided to rectify this situation. The adjustment is however rather insensitive, and it was singularly difficult to adjust within ±30 seconds of orthogonality. This error is trivial in conventional plotting, amounting to a displacement on one axis of ±0.07 mm at a distance of 500 mm from the fixed axis, but the error would have caused an apparent systematic displacement of coordinates in the y direction on one side of the measured orthophotographs.

6.6.ii

It was decided to calibrate the coordinatorgraph, and the method of calibration is depicted in plate 5, in which three Wild T2 theodolites were used to intersect a pricker point placed in the pencil holder. Intersections were observed simultaneously by three observers, at successive nominal XY coordinate locations at 100 mm spacing, at 40 points defining a coordinate grid 400 mm X by 700 mm Y. The observing target was driven to successive locations, and directions read by estimation to 0.1 seconds with two pointings on one face at each location. One complete set of observations on one face took about 2 hours, and in view of this time lapse the observations were repeated after changing face, and the second set treated as an independent calibration. Derivation of adjusted coordinates was obtained by treating the observations as a triangulation network, and adjusting by the parametric

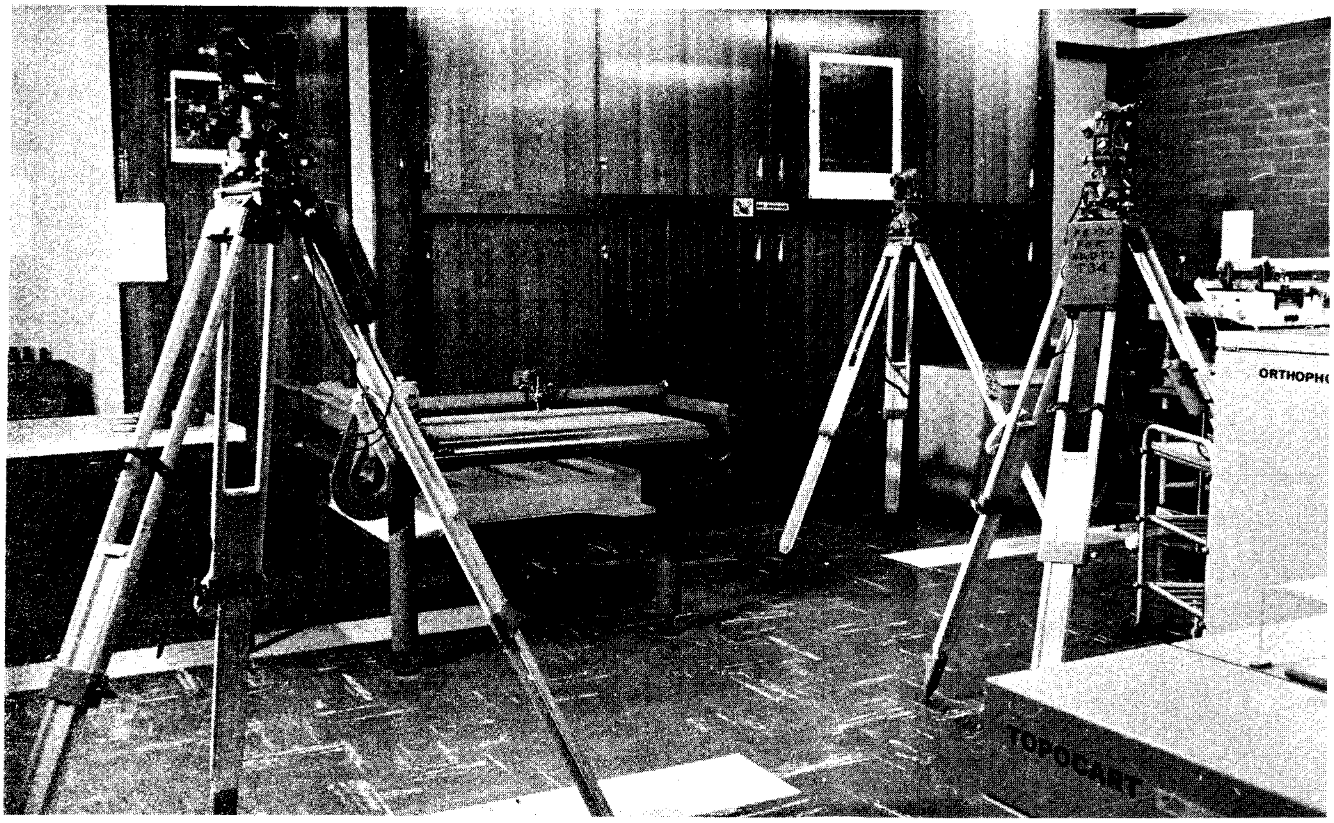

Calibration of Coordinatorgraph

PLATE 5

method holding only two stations of the network as fixed, namely the two stations at the greatest separation closest to the Y axis. The reliability of the calibration was judged by computing the standard deviation of the differences ΔX, ΔY between the coordinates derived from the two calibrations, the standard deviation (vector) being ±0.018 mm, maximum vector difference 0.032 mm. The differences V_X, V_Y between mean adjusted coordinates and nominal coordinates were analysed and found to be highly systematic. The standard deviation of V_X was ±0.017 mm with a mean of −0.025 and a maximum of −0.068 and of V_Y a standard deviation of ±0.036 mm with a mean of +0.053 mm and a maximum of +0.143 mm.

6.6.iii

Considering only the non-orthogonality α of the X axis, and assuming that the fixed axis is Y, the relationship between orthogonal coordinates X*Y* and non-orthogonal coordinates XY is given by:

$$X^* = X \cos \alpha$$

$$Y^* = Y + X \sin \alpha$$

Allowing also separate scalars λ_X and λ_Y for the X and Y axis, shifts of origin ΔX^* and ΔY^*, and a common rotation β, the relationship is:

$$X^* = \lambda_X.\cos\,(\alpha + \beta).X - \lambda_Y.\sin\,\beta.Y + \Delta X^*$$

$$Y^* = \lambda_X.\sin\,(\alpha + \beta).X + \lambda_Y.\cos\,\beta.Y + \Delta Y^*$$

The equations can be considered to take the general form of an affine transformation:

$$X^* = A1 + A2X + A3Y \qquad (6.i)$$

$$Y^* = B1 + B2X + B3Y \qquad (6.ii)$$

This formulation was used to transform nominal coordinates XY to adjusted coordinates X*Y* by a least squares solution for the 40 points, using the writer's program AFFTRAN, for HP9810A desk calculator. The transformed coordinates were then compared with the adjusted coordinates, and from the residual differences V_X V_Y the suitability of the transformation was judged as a model of the coordinatorgraph errors, compared to the figures given in 6.6.ii. The standard deviation of V_X was now ±0.015 mm, with a mean of zero and maximum of +0.030 mm; and the standard deviation of V_Y was now ±0.013 mm with a mean of zero and maximum of -0.033 mm. The systematic effects had been entirely removed.

6.7 Measurements of Planimetric Errors

The orthophoto negatives, after being allowed to stabilise in the laboratory environment, which is controlled for temperature and humidity, were measured over the illuminated glass table of the coordinatorgraph, using a spotting microscope and measuring to the snap marked images of the check points. The coordinate errors at the check points were obtained by processing through HP9810A desk calculator according to two procedures.

In the first procedure, aimed at deriving the internal errors (V_X, V_Y) due to the orthophotographic process, the measured coordinates were subjected to a linear similarity transformation using the most reliable control information, namely the 14 ground controls of model A and the 13 of model B. All measured coordinates were however first adjusted by affine transformation, using transformation elements derived from the calibration of the coordinatorgraph. The computation was carried out in one operation at the desk calculator, using program SIMTRAN (appendix A), which included an affine option for specified transformation elements. All check measurements were transformed, stored on magnetic card, and subsequently processed through program RESIDUALS. In this program the transformed coordinates were compared with stored correct coordinates for all of the check points; and the errors V_X, V_Y, and the plan vector errors V_P extracted and printed.

In the second procedure, the measured coordinates were teated in a similar manner except that the controls used for transformation were solely the aerial triangulation values of the four corner pass points in each model. The resulting errors V'_X, V'_Y, V'_P, were considered to be the external errors due to the influence of the aerial triangulation.

It would have been possible to transform the measured coordinates directly to check coordinates through the affine transformation AFFTRAN, but it was thought that this procedure would have tended to obscure the existence of possible affine effects from the orthophotographic production, and in any case the transformation would have been poorly determined in the case of the external errors with only four controls.

6.8 Measurement of Elevation Errors

The measurement of elevation errors on photogrammetric plans of any type, is beset by peculiar difficulties. The preferred method must be by actual checking in the field, but the time required in this case would have been prohibitive as nearly 800 checks were made. The graphical information, whether in the form of a profile limit-signal, or in the form of a derived contour, will rarely-coincide with a check control; so that some form of interpolation is necessary in order to derive values at the check controls. SCHMIDT-FALKENBERG (197[illegible]), has investigated the position errors which occur in interpolation procedures, and it is clear that unless the check-point falls by coincidence on the fall-line perpendicular to two parallel contours, that serious errors may occur in the estimation. In the case of profile signal limits, particularly if the profile separation is large, interpolation would hardly be possible. In the case of interpolation between contours, the precision is rather uncertain in the case of broken terrain.

For these reasons a more direct method of measurement was sought, and this was possible because of the availability of larger scale photography covering the orthophotograph test models. The drop line charts were measured directly in six parts each, each part being covered by a 1:10 000 model in Wild A.8 plotter from photography at picture scale 1:25 000, the model being reduced at the drawing table to the plot scale 1:25 000, as depicted in plate 6. A magnifying desk lamp was installed on the drawing table as a profiloscope, using a [illegible] needle as pointer in the pencil holder. The individual models were absolutely oriented using the correct ground control values of the four controls in each 1:10 000 model. In the case of measurements of profile signal accuracy, three elevation readings were then taken to the profile limit signal closest to a check point; and in the case of contour measurements to the closest contour point. As the models were set up on correct control, the discrepancy between a mean observed measurement and the corresponding indicated elevation was the external error V_Z. The observed measurements were however first subjected to an analytical correction for the small absolute orientation errors of the 1:10 000 models, through program ABSOR.

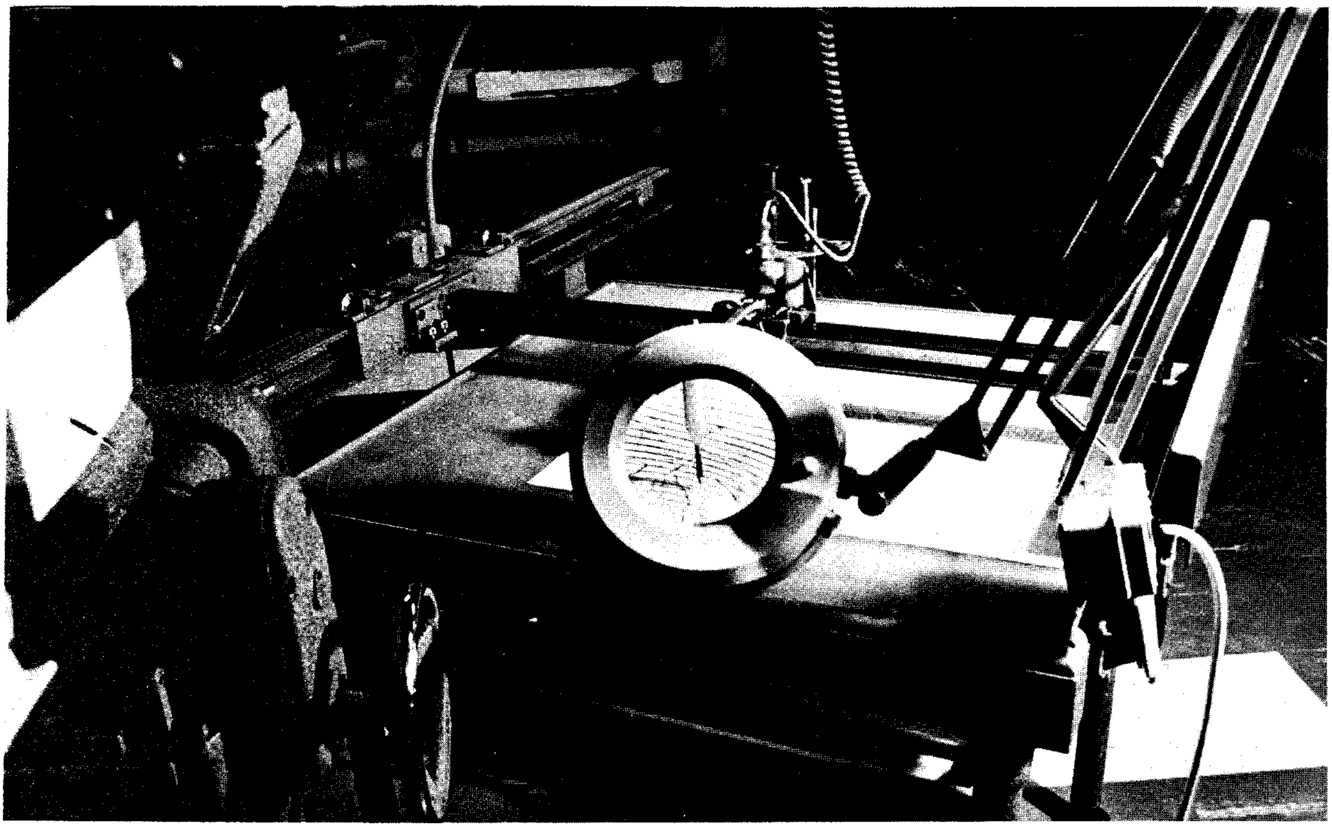

Direct Measurement of Elevation Errors

PLATE 6

The internal errors V_z were obtained by adjusting the external errors V'_z according to the calculated absolute orientation errors of the aerial triangulation coordinates of the ground controls of models A and B, derived from the analysis of errors given in 5.9.

6.9 Cartographic Treatment of Drop Line Charts

6.9.i

In principle, contours are derived from profile signals by joining corresponding signal band changes in successive profiles. If the charts are produced by the on-line process in an instrument such as the Topocart-Orthophot combination, then usually a few guide contours will have been added by conventional plotting, and it is a particular advantage of this instrument that conversion to conventional plotting is quick and convenient. It is generally recommended that a stereoscopic overlap of the model should be viewed in an ordinary mirror stereoscope, in order to correlate the signals with landforms.

In practice there are many difficulties, but the major problems can be attributed to two causes:

(a) irregularities in corresponding signal changes between successive profiles which may be due either to signal errors, or to topographic features,

(b) anomalies in neighbouring profiles [illegible] by topography, choice of signal frequen[illegible] and profile interval.

6.9.ii

In the former case of irregular signal changes in successive profiles, there is evidence that signal irregularities are not confined to a particular system, but appear to be a characteristic of profiling procedures. Both SCHMIDT-FALKENBERG *(1970)* and SCHNEIDER *(1970)* have investigated the causes and effects of signal irregularities in the GZ1 system, and very similar effects are produced by the Orograph system. Examination of the drop line charts in annexure 1, particularly in relatively flat areas, reveals several cases of irregular changes in successive profiles which cannot be attributed to topography, producing a characteristic 'broken comb' pattern along the supposed line of a contour. Some of these irregularities are certainly the result of profiling errors on the part of the observer, the scanning errors of 2.4, but these should be small, and non-systematic. An error ΔZ in scanning causes a corresponding position displacement of the profile signal change of $\Delta Z \cot \beta$, where β is the terrain slope in the direction of scan. It follows that a small profiling error produces a marked displacement in rather flat terrain. There are however very systematic irregularities extending over several profile lines which obviously cannot be attributed to scanning error.

Several experiments were carried out in an attempt to rationalise the causes of the irregularities. The principal experiment was one in which a model was created of terrain of completely uniform slope. Two identical diapositives were used, one of which was cut in half and viewed with the corresponding identical images of the other, the pictures themselves being devoid of X parallaxes except when these were artificially introduced. This was done by rotating the 'model' through variations of absolute tilt Ω, and scanning at several speeds and profile intervals. The experiments were inconclusive, in the sense that it was not possible to identify the precise causes of irregularities; nor was it possible to completely rationalise the behaviour at different variable parameters. The following rather tentative conclusions were made:

(a) the irregularities are not related to speed of scan,

(b) the irregularities do include a constant component traced to backlash in the Z counter gear wheels and the Z transmission,

(c) there appeared to be a tendency to produce displacements in opposite directions in alternate scans, as though scans were alternately high and low, and this was additional to the amount due to backlash from (b),

(d) the irregularities become less marked with increasing profile separation, on identical slopes,

(e) the irregularities were insignificant on slopes greater than 1½ g.

The backlash component (b) amounted to 0.02 mm ΔZ in the model, in the instrument used; which represents 10% of the length of profile signal (ΔZ = 0.2 mm) used in the majority of tests. It should be possible to compensate this effect by appropriate delays in the Orograph circuit, according to the direction of change of Z. However this effect, and also the deficiencies noted at (c) and (d) may well be due to some defect in this machine only. The conclusions are however very similar to those reached by SCHNEIDER, except that he concluded that direction of scan was not significant. On the question of how to deal with irregularities during the contouring process, the only possible conclusion is that of SCHNEIDER, namely that a mean line should be taken through irregular signal changes unless there is topographic evidence in support of an irregular course. It should be noted that an interpolation system such as that available with GZ1, tends to obscure the presence of these irregularities in the actual scanned profiles.

6.9.iii

Irregularities may also of course be attributed to genuine topographic features, particularly in broken terrain such as occurs in parts of model A. An additional problem due to topography, is that anomalies result in signals between successive profiles when the fall line for long features is perpendicular to the profile direction, such as occurs with the long ridge in the extreme south of model A (see annexures 1.3 and 1.4).

Profile scan intervals which are unsuitably wide result in loss of features narrower than the profile interval, and in loss of most small isolation contours. Examples may be noted in annexure 1.4 in the treatment of the peak in the extreme north of the chart, in the loss of the two small hills immediately south of the peak, and in the missing upper isolation contours of the long ridge in the extreme south. A particular difficulty in areas of complex broken terrain, is the treatment of contours in the area of watersheds.

Several rather abortive attempts were made with the interpretation of charts, before a satisfactory method of overcoming some of these problems was evolved. The key to an interpretation which is topographically correct, and which gives the derived contours some semblance of geomorphological meaning, is to combine a line drawing of the drainage pattern with the drop line signals before attempting to derive contours. The principle of the technique is illustrated in plate 7. The chart has been combined with a drainage drawing, and a single contour called the 'principal contour' has been identified throughout its course. The principal contour is defined as on at about the mean elevation of the chart which is at the same time easily identifiable on account of signal change, in this case the top end of the thickest signal at the 230 m (9.1 mm) level.

The drainage trace is quite easily obtained from the corresponding orthophoto negative over a light table using also for detailed reference a mirror stereoscope with the relevant diapositives. The drainage trace for model A

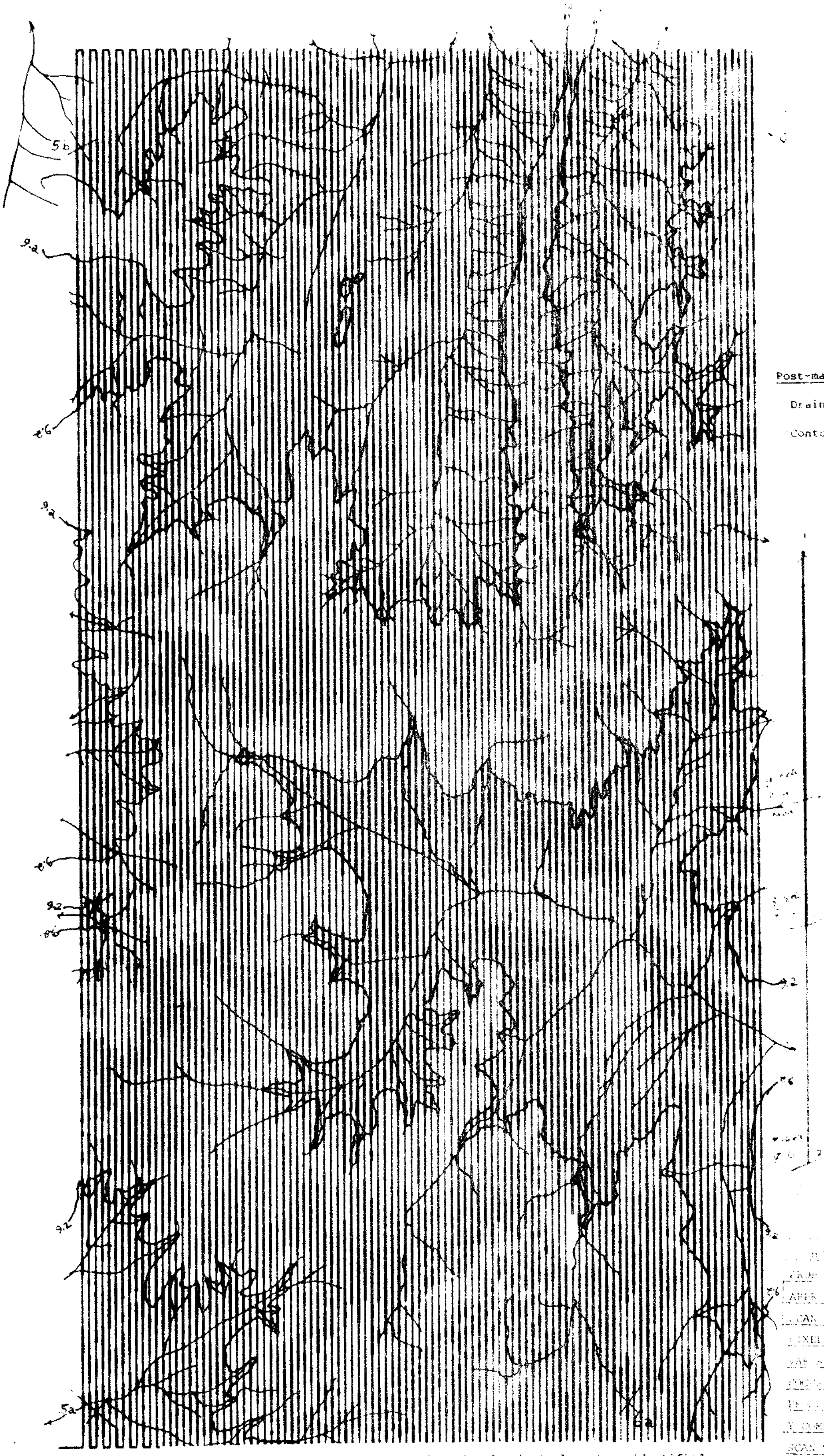

Post-machine times to this stage.

Drainage interpretation: 2 hrs.

Contour interpretation: 5 hrs.

Total: 7 hrs.

[illegible] SCALE	[illegible]
DROP LINE SCALE	[illegible]
APERTURE PICTURE [illegible]	[illegible]
SCAN SPEED	[illegible]
FIXED SPEED CONTROL	3
MAP [illegible] SPEED (IF FIXED)	2
[illegible]	[illegible]
[illegible]	
[illegible] COMPENSATION	
SCAN TIME	
[illegible] TIME	
DATE	23 [illegible]
OPERATOR	[illegible]

Drop Line Plot with drainage transferred and principal contour identified.

Principal contour: 9.20mm (230m).

PLATE 7

was completed in 2 hours, but this time excludes the time taken to transfer to the drop line chart. The reason for this is that in these experiments the transfer was somewhat crudely effected by means of ordinary carbon paper, and this was rather slow. In practice with the sophisticated facilities of a mapping organisation, more satisfactory and rapid means are available. It is thought that the most satisfactory interpretation medium would be a non-actinic blue base, on white plastic, produced photomechanically from a combined negative of drainage trace and drop line chart. It should be possible to carry out the interpretation first in pencil, and subsequently to ink as a fair-drawing.

After the initial phase of identification of the principal contour, it is relatively easy to identify the remaining contours upwards and downwards. The drainage key is a particularly valuable guide in peak areas, along profiles perpendicular to fall lines, and in areas of broken terrain. It is thought that the technique is of general applicability, for example also with contour segments, in areas of difficult terrain.

6.9.iv

The same general principle of combining a drainage trace with the drop lines was followed in the flat terrain of model B, except that here it was not necessary to identify a principal contour. The rather simple drainage pattern was traced from the orthophoto in 20 minutes. The complete treatment of test B/16/1 is shown in plate 8. Systematic irregularities of signal changes may be noted in particular along the course of the 145 m contour. Even in this rather simple case, the drainage pattern proved useful in drawing the contours through the floodplain area. The total drawing time for test B/16/1, including drainage interpretation, was 2 hours. Times for model A are given in 7.6.

It should be noted that all of the drop line chart examples are mirror-reversals. This occurs because the corresponding orthophotograph negatives were produced for correct reading emulsion to emulsion contact positive reproduction. Under these circumstances the gear switching possibilities to the drawing table produce a mirror-reversed positive.

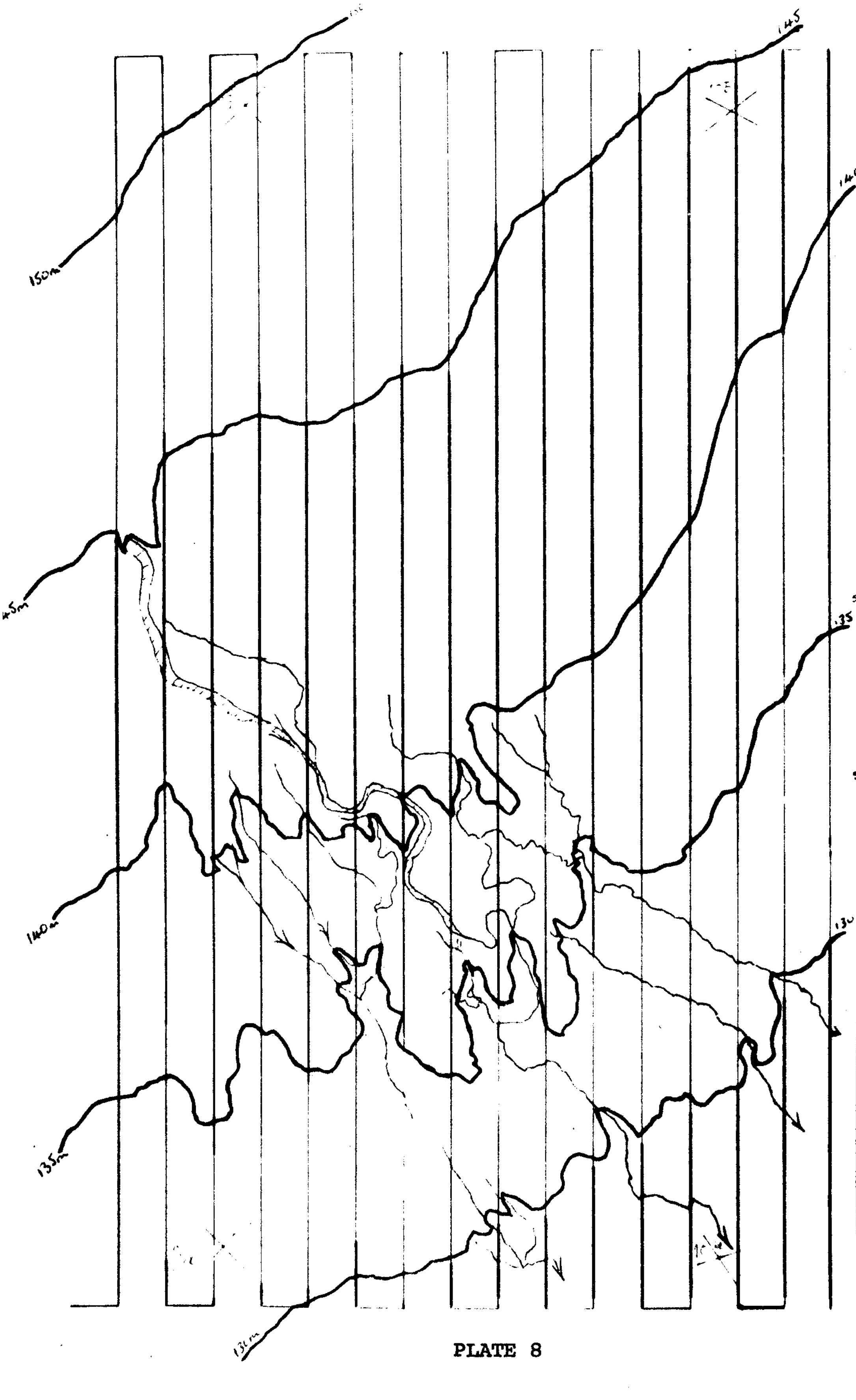

TEST NO.	B/16/1
MODEL	Ø91Ø
MODEL SCALE	1:25 000
ORTHOPHOTO SCALE	1:25 000
DROP LINE SCALE	1:25 000
APPROX. PICTURE SCALE	1:60 000
SCAN SPEED	4mm/sec
FIXED SPEED CONTROL	30 div
VARIABLE SPEED (IF FIXED)	[illegible]
FOCUS	[illegible]
PROJECTION LAMP	3
Y COMPENSATION	[illegible]
SCAN TIME incl 15 changes [illegible]	[illegible] min
COMPLETION TIME	[illegible] min
DATE	15 5 73
OPERATOR	[illegible]

PLATE 8

7. TEST RESULTS AND CONCLUSIONS

7.1 Internal Errors in Planimetry

7.1.i

Internal errors Vx, Vy, Vp, were derived for all orthophoto test models in both test areas, at all combinations of speeds and slit widths, by the measurement and computational procedures described in 6.7. From the residual errors, the mean and mean square errors were computed, and a twenty-cell histogram distribution diagram generated by HP9810A desk calculator (appendix A). In the case of test models A scanned at speeds in the orthophoto (Vd) of 4 mm/sec, which were also analysed for external errors, vector diagrams of the direction and magnitude of the errors were also produced, by HP9810A desk calculator and plotter. Similar diagrams were produced for the two tests carried out in test Model B. The vector diagrams and histograms are shown as figures 7.1 to 7.10 inclusive, and may be identified according to scan speed and slit width by reference to the table of test labels Table 4.I.

Mean square errors were computed in every case according to the formula:

$$m = \sqrt{\frac{VV}{n}} \qquad (7.i)$$

Table 7.I gives results for Model A of mx, my, mp in terms of micrometers at 1:25 000 orthophoto scale: µm(d), and also in terms of micrometers at 1:60 000 picture scale: µ m(b). Table 7.II gives the corresponding maximum coordinate errors ΔX, ΔY, ΔP in the same terms.

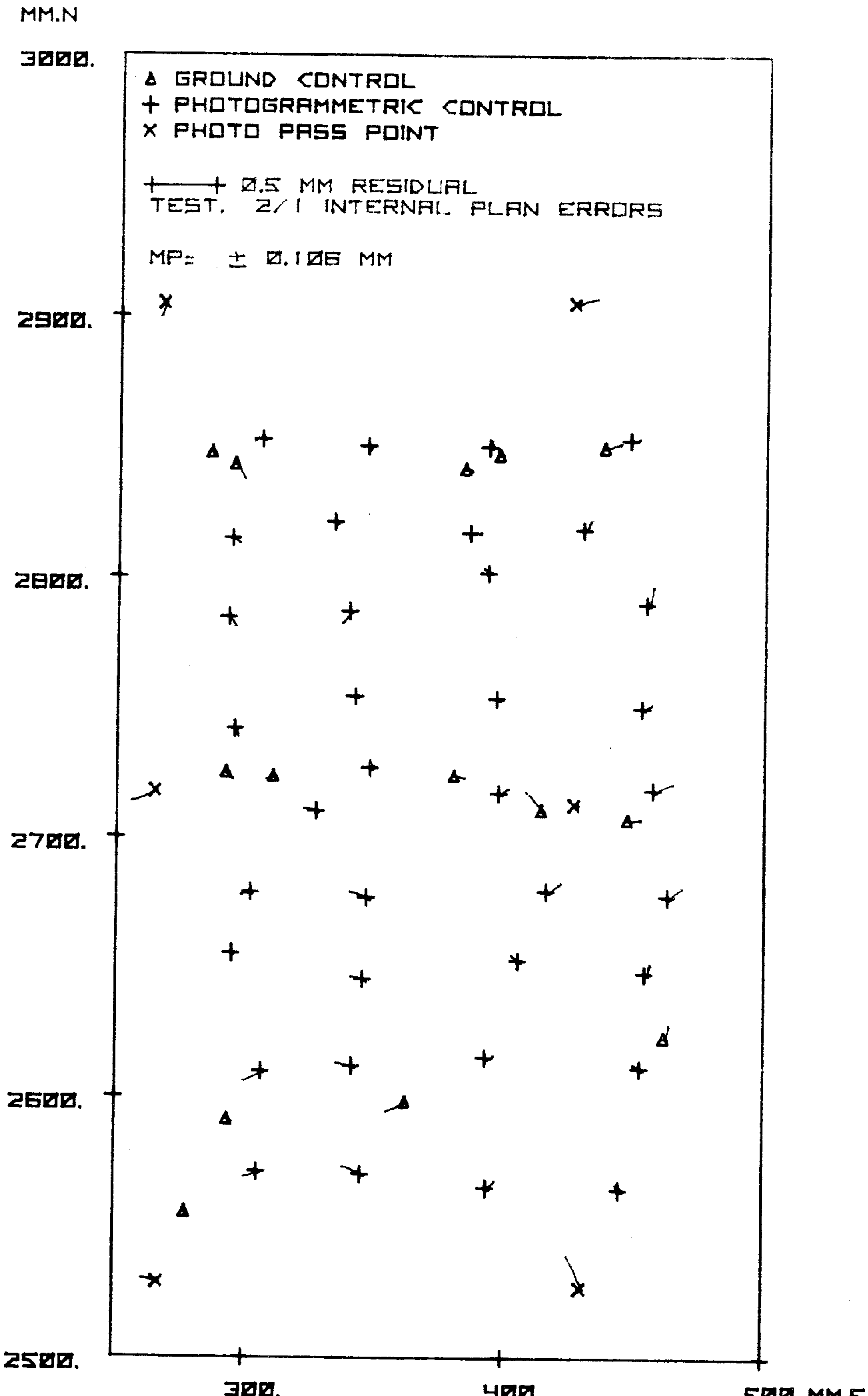

MODEL 0506 RESIDUAL ERRORS

FIG 7/1

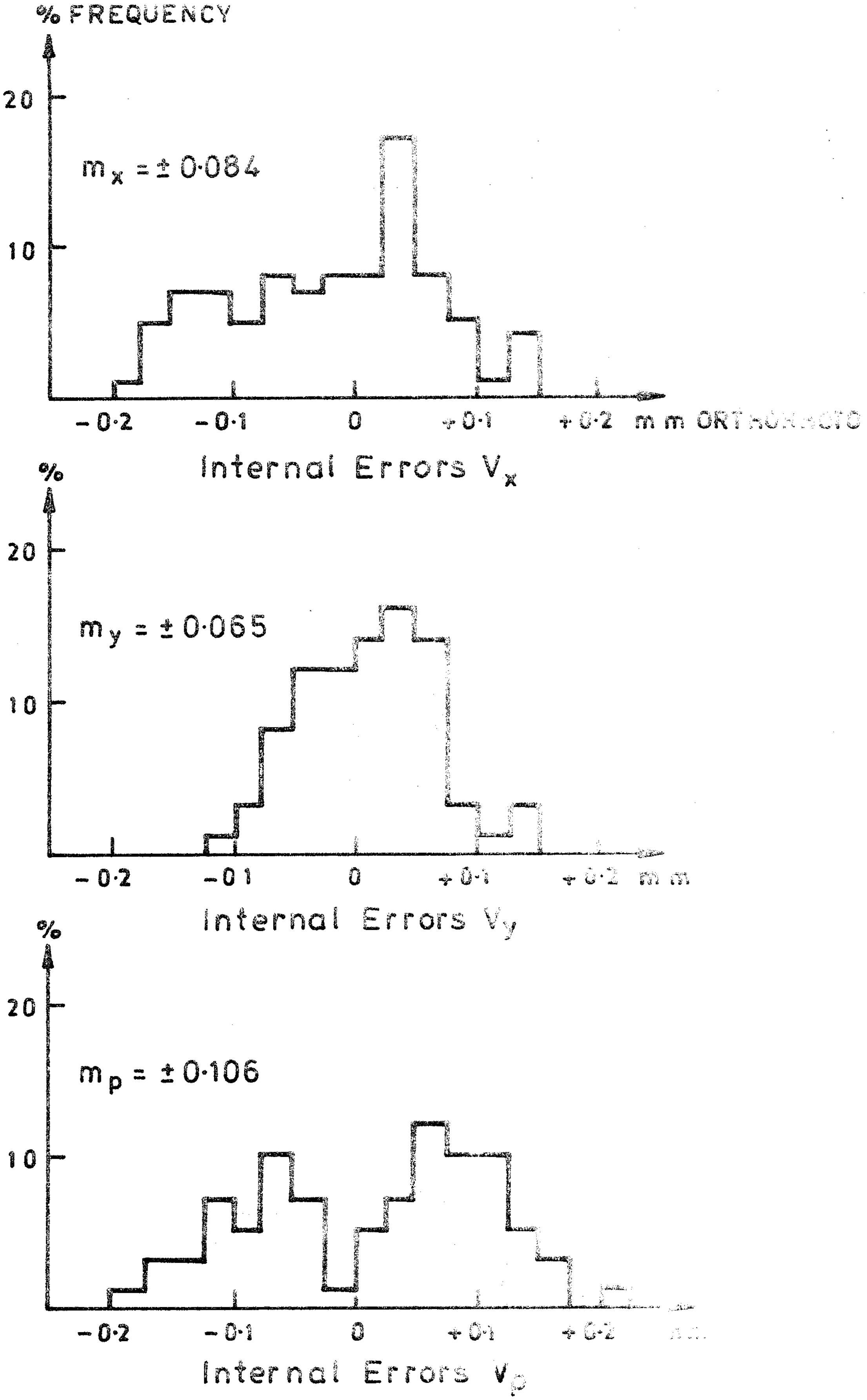

FIG. 7·2. DISTRIBUTION OF EXTERNAL ERRORS TEST 3/1

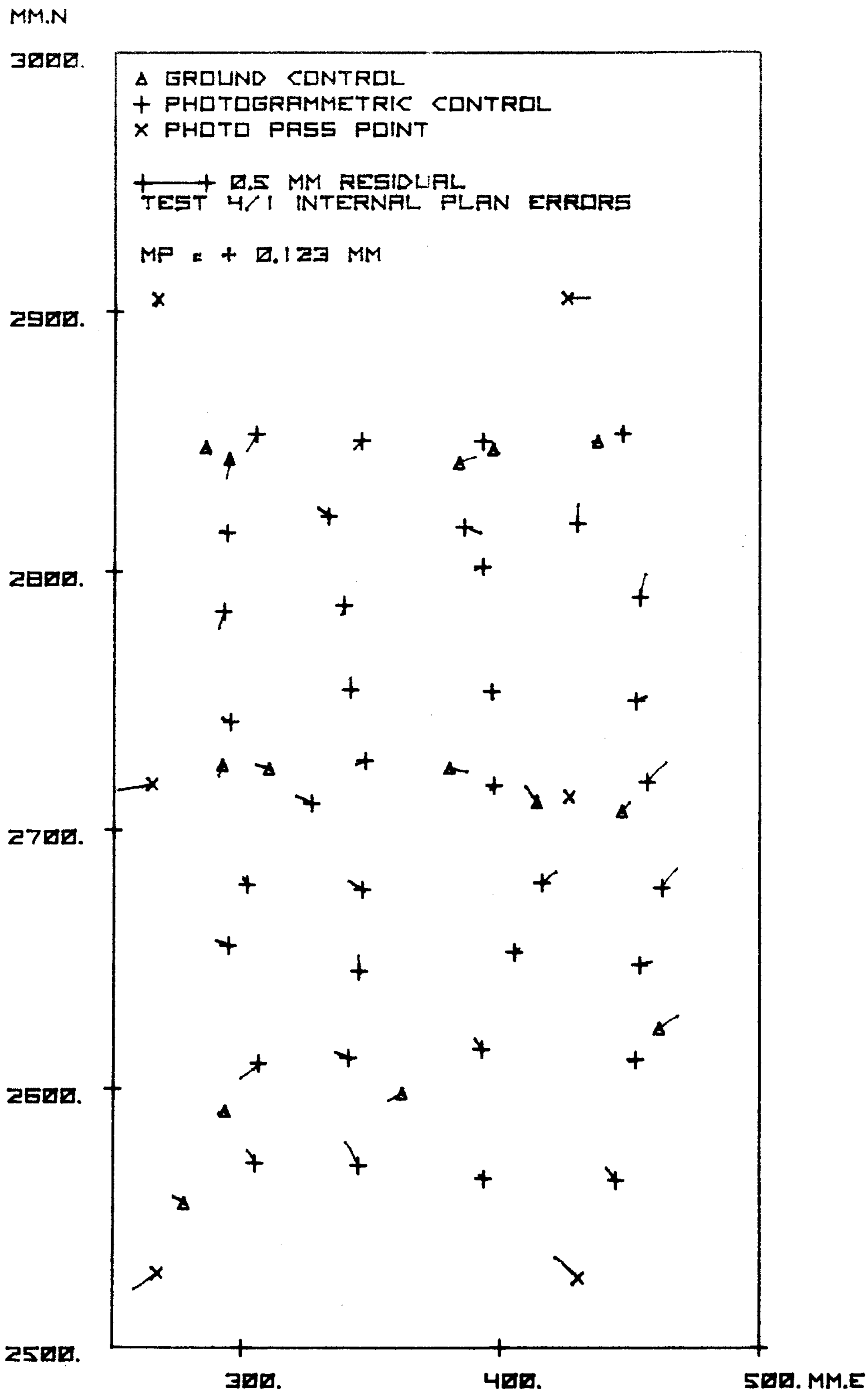

MODEL 0506 RESIDUAL ERRORS

FIG 7/3

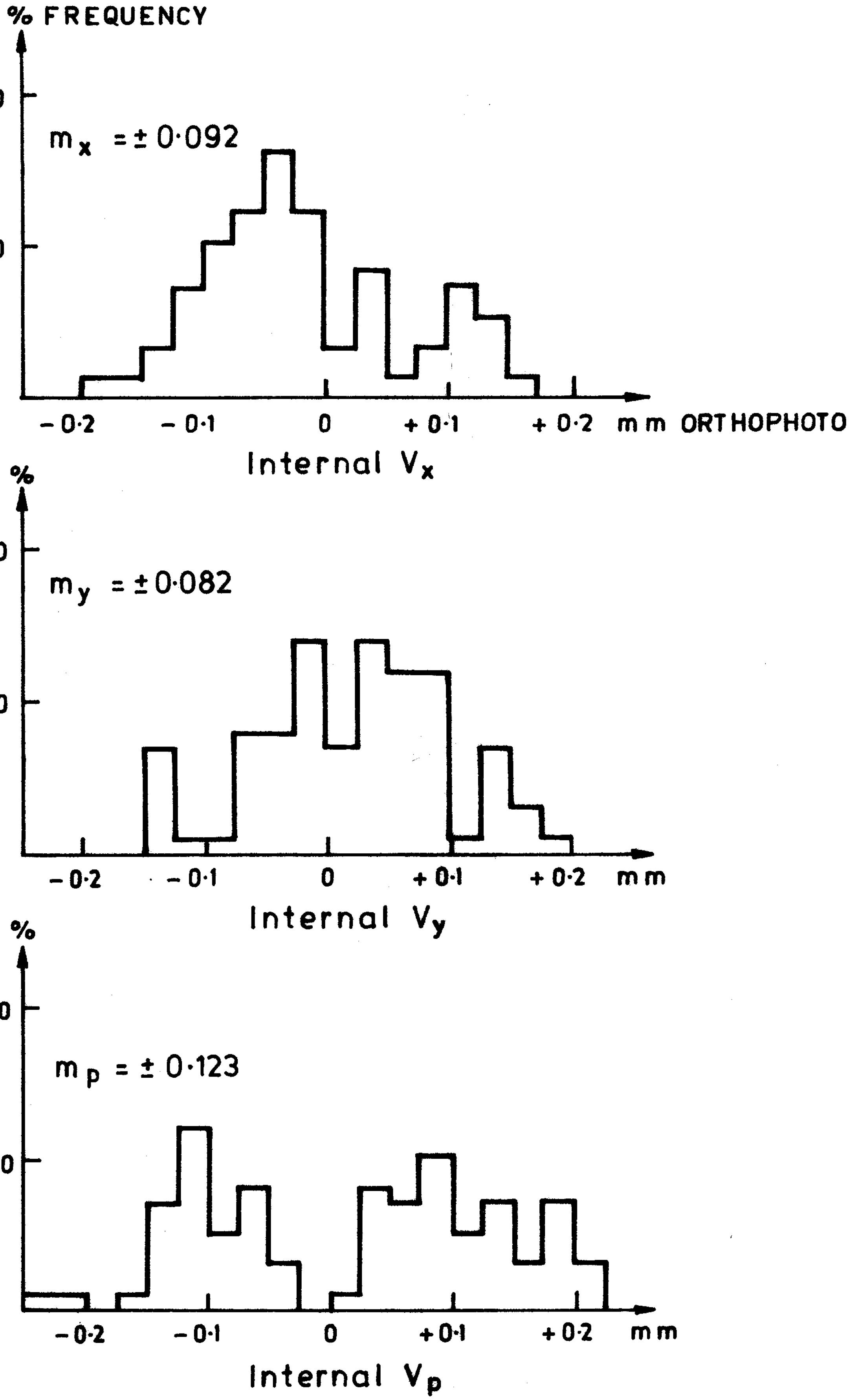

FIG 7·4. DISTRIBUTION OF INTERNAL ERRORS TEST 4/1

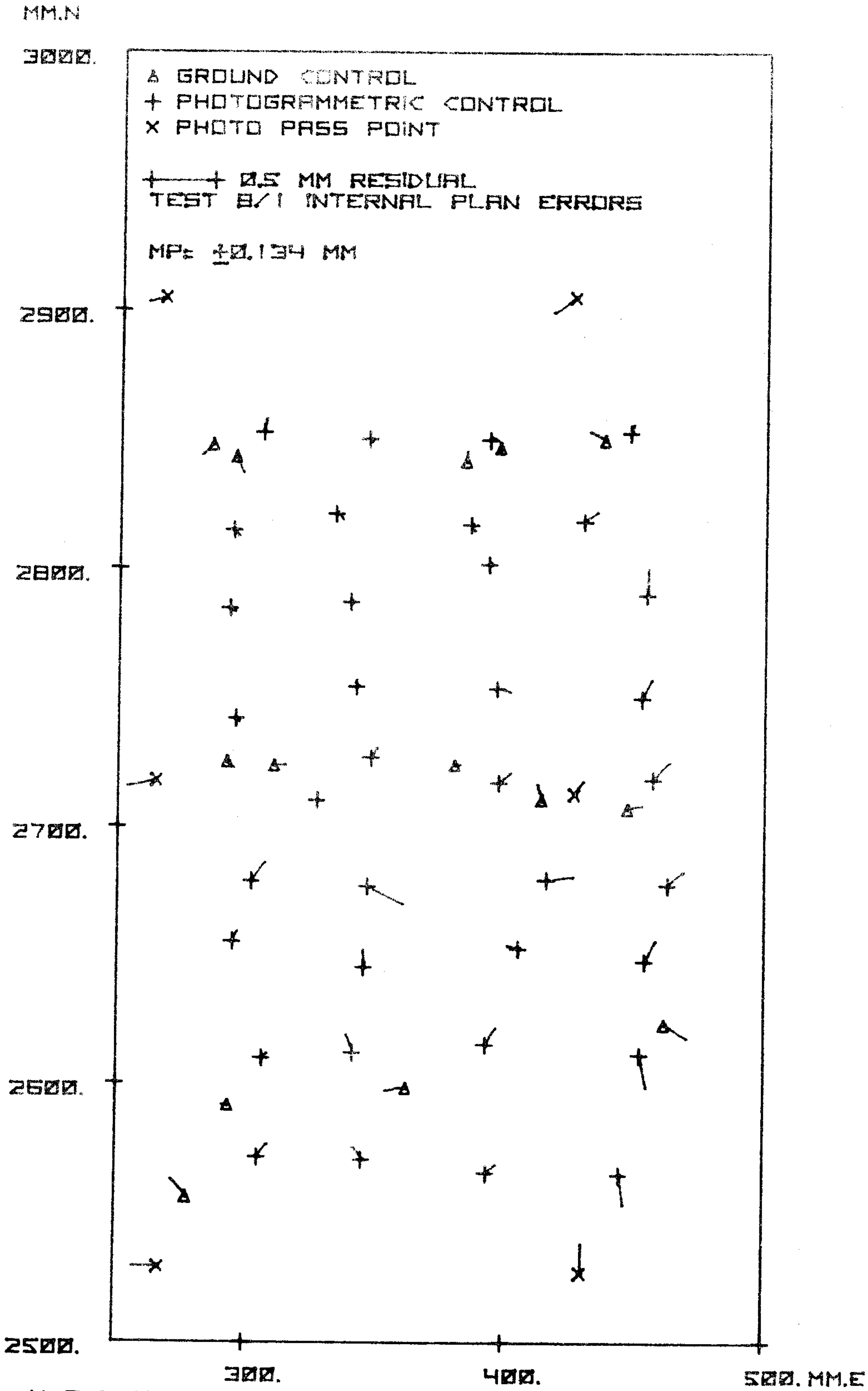

MODEL 0506 RESIDUAL ERRORS

FIG 7/5

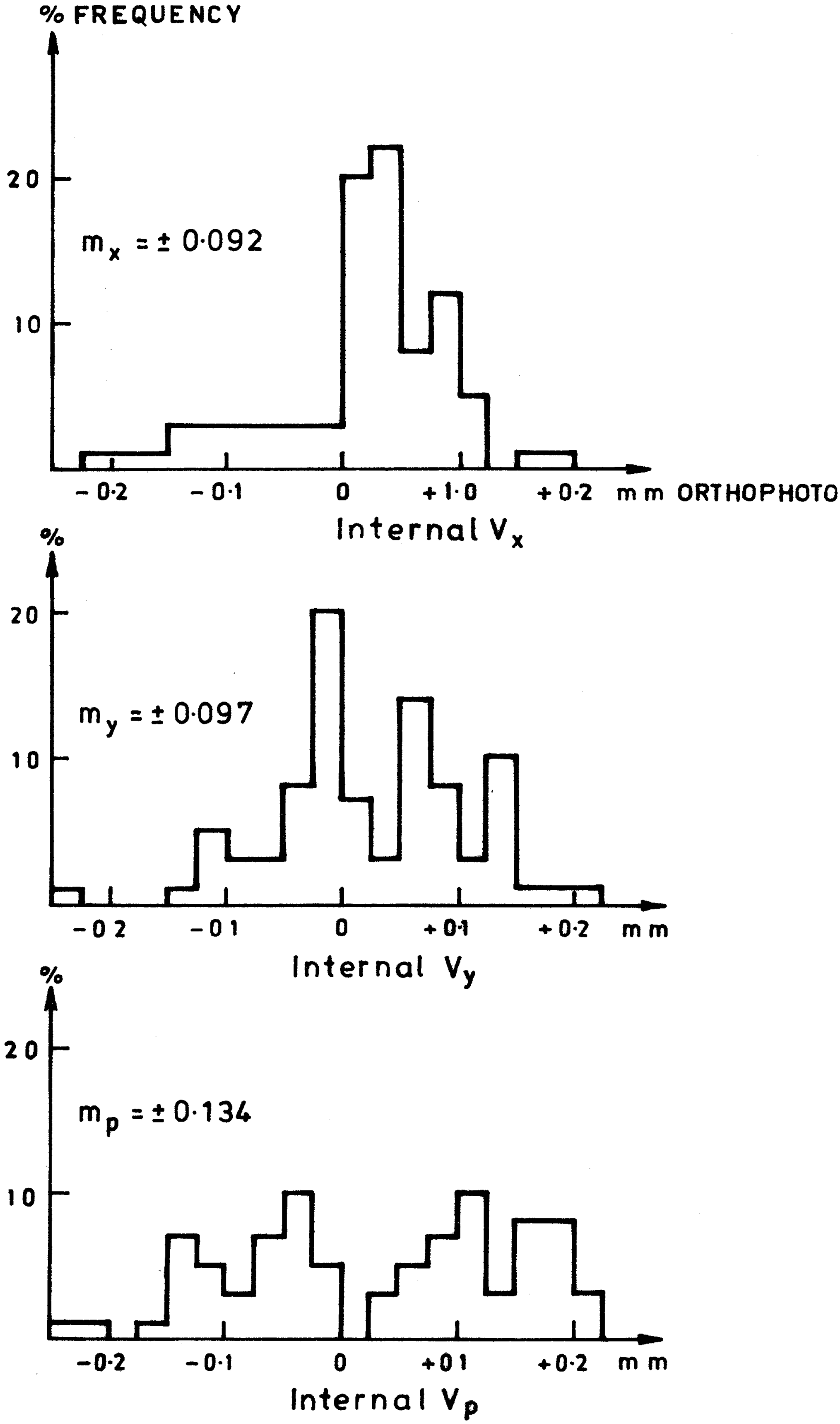

FIG. 7·6. DISTRIBUTION OF INTERNAL ERRORS TEST 8/1

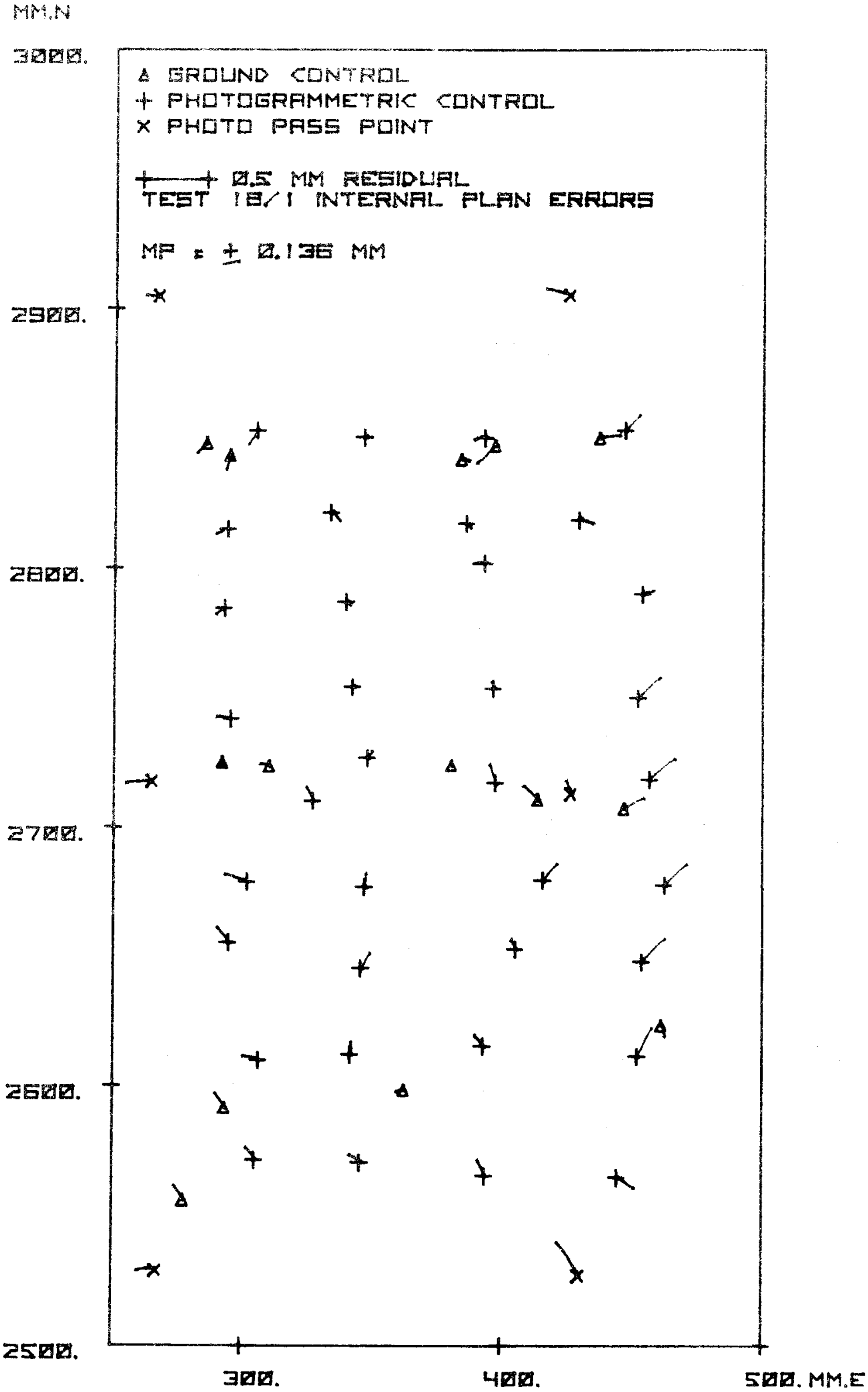

M O D E L 0 5 0 6 R E S I D U A L E R R O R S

FIG 7/7

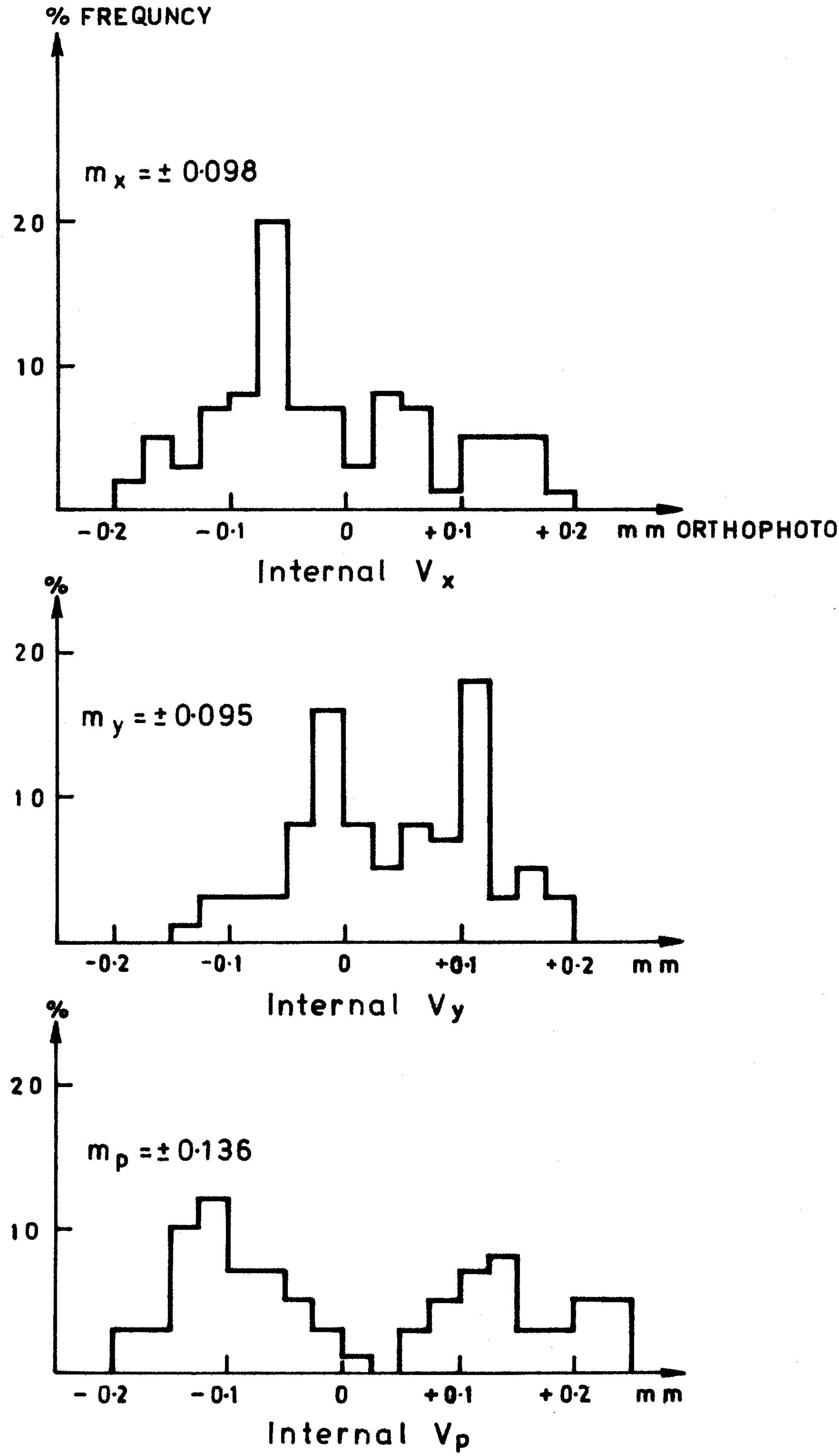

FIG. 7·8. DISTRIBUTION OF INTERNAL ERRORS TEST 16/1

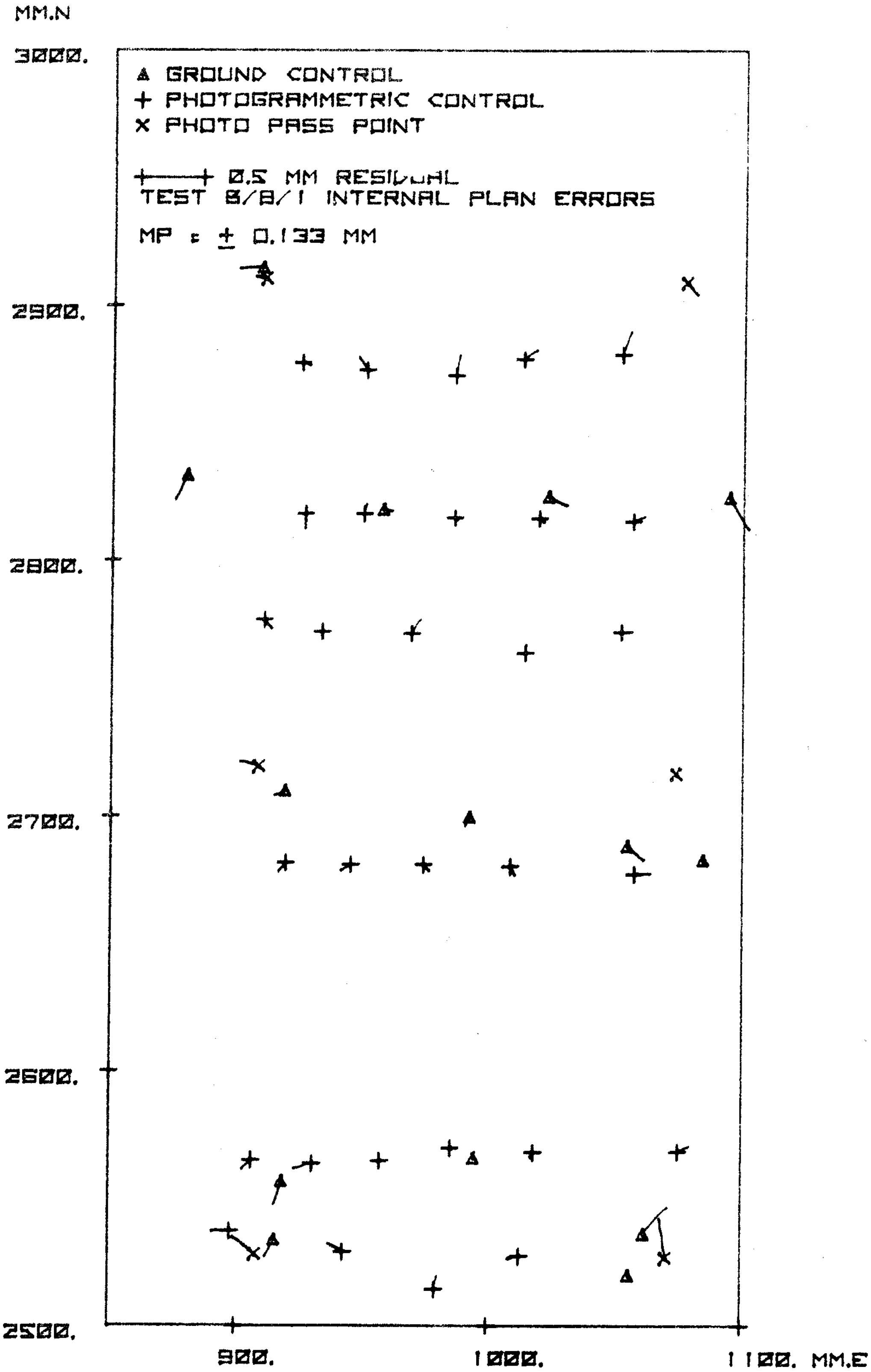

M O D E L 0910 R E S I D U A L E R R O R S

FIG 7/9

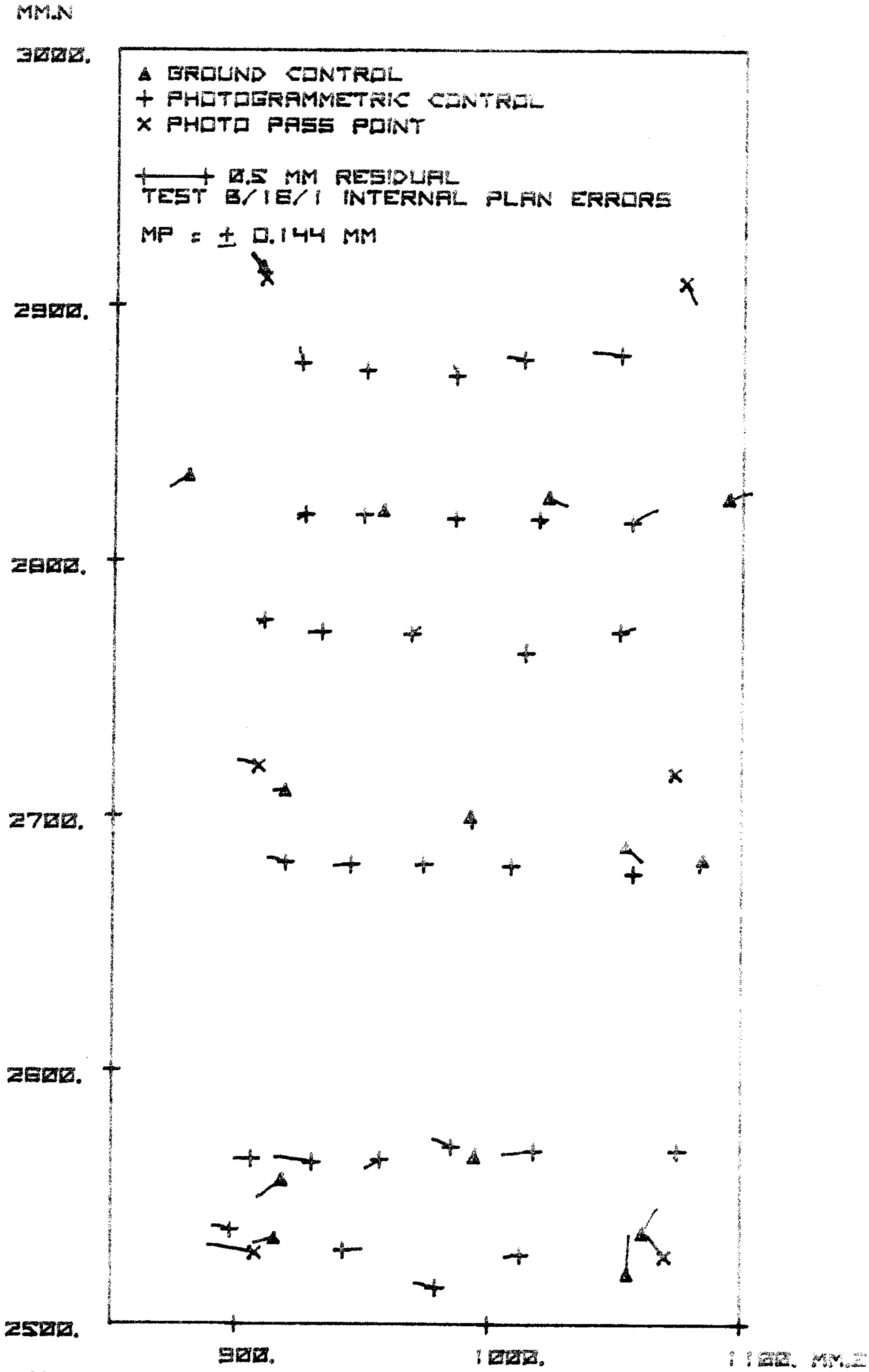

M O D E L 0910 R E S I D U A L E R R O R S

FIG 7/10

Scan Speed	Vd	2			Variable average 2.6			4			6			8		
mm/sec	V_b	0.83			average 1.08			1.67			2.5			3.34		
b = 2 mm	$\mu m_{(d)}$	104	91	138	98	87	131	84	65	106	78	70	105	96	71	119
	$\mu m_{(b)}$	43	38	58	41	36	55	35	27	44	33	29	44	40	30	50
b = 4 mm	$\mu m_{(d)}$	107	91	140	105	87	136	92	82	123	100	93	136	92	98	134
	$\mu m_{(b)}$	45	38	58	44	36	57	38	34	51	42	39	57	38	41	56
b = 8 mm	$\mu m_{(d)}$	95	102	139	103	95	140	92	97	134	89	99	133	108	70	129
	$\mu m_{(b)}$	40	43	58	43	40	58	38	40	56	37	41	55	45	29	54
b = 16 mm	$\mu m_{(d)}$	98	112	149*	101	115	153*	98	95	136*	115	107	157*	96	132	163*
	$\mu m_{(b)}$	41	47	62	42	48	64	41	40	57	48	45	65	40	55	68
		mx	my	mp	mx	my	mp	mx	my	mp	mx	my	mp	mx	my	mp

* maximum value of mp for a given speed of scan.

105 minimum value of mp for a given slit width b.

INTERNAL MEAN SQUARE ERRORS (PLANIMETRY) MODEL A

TABLE 7.J

Scan Speed	V_d	2			Variable average 2.6			4			6			8		
mm/sec	V_b	0.83			average 1.08			1.67			2.5			3.34		
	$\mu m_{(d)}$	224	265	305	222	383	-430	-197	255	281	219	-173	-235	229	284	-341
b = 2 mm	$\mu m_{(b)}$	93	111	127	93	160	-179	-82	106	117	91	72	98	95	118	-142
	$\mu m_{(d)}$	238	244	286	261	255	279	260	179	227	314	377	-348	-239	308	-310
b = 4 mm	$\mu m_{(b)}$	99	102	119	109	106	116	108	75	95	131	157	-145	-100	128	-129
	$\mu m_{(d)}$	-263	225	273	257	245	306	269	-253	-300*	-214	-286	-292	-254	158	256
b = 8 mm	$\mu m_{(b)}$	-110	94	114	107	102	178	112	-106	-125	-89	-119	-122	-106	66	107
	$\mu m_{(d)}$	-268	275	309*	-286	-429	-447*	-198	243	-291	289	299	378*	365	461	509*
b = 16 mm	$\mu m_{(b)}$	-112	115	129	-119	-179	-186	-83	101	-121	121	125	158	152	192	212
		ΔX	ΔY	ΔP	ΔX	ΔY	ΔP	ΔX	ΔY	ΔP	ΔX	ΔY	ΔP	ΔX	ΔY	ΔP

* maximum vector error for a given scan speed

227 minimum vector error for a given slit width

MAXIMUM INTERNAL PLANIMETRIC COORDINATE ERRORS MODEL A

TABLE 7.II

In each Table, the maximum vector error for the four tests with different exposure slits at the same scan speed is identified by means of an asterisk. Also identified by means of underlining is the minimum vector error in the five tests using the same exposure slit at different speeds.

7.1.ii

Some rather general conclusions may be inferred from the results presented in Tables 7.I and 7.II:

(a) the influence of system errors is apparent insofar as the largest m.s.e. vector error occurs for any given speed with the greatest exposure slit width of 16 mm;

(b) similarly the maximum vector error occurs in every case except one, with the 16 mm slit, and in the exception with the 8 mm slit;

(c) the influence of speed of scan upon errors is not as marked as might be expected, the minimum errors in every case for a certain exposure slit occurring at the faster scan speeds, rather than the slowest speed or the observers choice of variable speed;

(d) there is little evidence of differences of an affine nature between the errors in X and those in Y, as in the case of the mean square errors there are 13 examples from 20 in which m_x exceeds m_y, but in only 7 does the difference exceed 10 μm at orthophoto scale; and in the case of the maximum coordinate errors there are 13 examples in which ΔY exceeds ΔX, but in only 10 of these does the difference exceed 10 μm at orthophoto scale.

With respect to 7.1.ii(a), the influence of system errors is further confirmed because in every case the smallest m.s.e. vector error m_p occurs with the smallest exposure slit width, but on the other hand the influence is perhaps not as great as might be expected, since the range of results from minimum m_p to maximum m_p is quite small:

V_d		m_{pd}		
2 mm/sec	:	± 138	-	± 149 µm
variable	:	± 131	-	± 153 µm
4 mm/sec	:	± 106	-	± 136 µm
6 mm/sec	:	± 105	-	± 157 µm
8 mm/sec	:	± 119	-	± 163 µm

The total range of m_{pd} of ± 105 - ±163 µm may be compared with the range for the planimetric tests summarised at 4.4.1 of ± 120 - ± 460 µm, corresponding to ± 44 - ± 68 µm in the original picture scale compared to ± 42 - ± 123 µm. From the test results of Model A, we may therefore conclude that the Orthophot-Topocart combination is capable of accuracies which match those of restitution-differential rectification combinations based on restitution instruments of higher order classification. The arithmetic mean of the 20 m.s.e. vector errors is ± 135 µm, equivalent to 56 µm at plate. The contribution of differential rectification to the internal errors of mapping, for this type of broken terrain, is therefore exceedingly small compared to normal mapping accuracies. As a criterion, the National Mapping Council of

Australia Standards of Map Accuracy of February 1953 may be cited; which states: "for maps published at scales of 1:20 000 or smaller, not more than 10 per cent of points tested shall be in error by more than 1/50th of an inch (0.51 mm) measured on the publication scale." The criterion is therefore equivalent to a standard deviation at publication scale of ± 306 µm, compared to the arithmetic mean m.s.e. of ± 135 µm. Of the 1120 points tested in the 20 tests, only one point (0.1%) exceeded the 0.5 mm criterion, and only 15 points (1.3%) exceeded 0.3 mm, of which 8 points occurred in the tests with 16 mm exposure slit. It is interesting to note that the Australian Standards qualify the accuracy statement by limiting the application only to "well defined" points, classifying such points as those which are easily visible or recoverable on the ground. From this point of view it may be argued that any properly focussed point image on an orthophoto is well defined, and that since the total information content of the orthophoto is obviously much greater than that of the conventional line photogrammetric plot, one may speculate that the orthophoto is intrinsically *of greater accuracy than a conventional photogrammetric plot.*

7.1.iii

With respect to 7.1.ii(c), the results of tests of errors for dependency upon speed of scan are somewhat unexpected, particularly in so far as the best results judged by minimum m_p were not obtained at the variable speed, when the operator had complete control over the scan speed of the moving floating mark. The best results were obtained at speeds in the orthophoto of 4 mm/sec (m_p ± 106 - 136 μm), equivalent to 1.67 mm/sec in the plate. This figure corresponds almost precisely with the figure given by MEIER *(1966, 83)* of 1.7 mm/sec for the scan speed best suited to the case of medium relief. It seems therefore the the operator is not the best judge of his own scanning ability, but that it pays to put him under a slight stress in order to keep him alert.

However in order to test dependency upon speed, the test results of the series from 2 mm slit were subjected to testing by linear correlation using program LINEFIT (appendix A). The 2 mm series was selected since the influence of system errors should be negligible in this series, and the linear correlation tested by comparing the corresponding errors v_x between the slowest speed test (v_d = 2 mm/sec) and each of the faster speed tests in turn. The v_x errors were tested rather than the v_p errors, because in the latter case the sign of v_p was given somewhat arbitrarily, with vectors in the 1st and 3rd quadrants positive, and in the remaining quadrants negative. Program LINEFIT calculates the equation of the straight line of best fit of a set of data points, giving the factors m (slope), and b (constant), of the equation:

$$Y = m.X+b \qquad (7.ii)$$

The program also gives the correlation coefficient r *(Freund, 1962)*, where:

$$r = \frac{\sum_{i=1}^{n} (X_i - \overline{X})(Y_i - \overline{Y})}{\sqrt{\sum_{i=1}^{n} (X_i - \overline{X})^2 \sum (Y_i - \overline{Y})^2}} \qquad (7.iii)$$

and $-1 \leq r \leq +1$ where the sign corresponds to the slope m.

The correlation tests were therefore carried out by setting up equations for each case of the form:

$$v_{x_{2/i}} = m.v_{x_{2/0}} + b \qquad (7.iv)$$

and the results are given in Table 7.III, where the constant term b is in µm at the orthophoto scale:

TABLE 7.III

Correlation between X errors in the 2 mm exposure slit tests

Test	m	b	r
2/4-2/0	0.83	-23	0.87
2/1-2/0	0.57	-29	0.73
2/2-2/0	0.46	5	0.70
2/3-2/0	0.64	-14	0.74

The results show that the linear correlation is high between the various test, but that there is certainly no clear relationship based on speed of scan, since the slope of the lines does not increase with increased speed, but on the contrary decreases until the speed of 6 mm/sec in the orthophoto. The high correlation must occur on account of the common errors of identification and snap-marking and control accuracy of the tested points, since the system errors are minimal in this series of tests. This general conclusion is in agreement with that of VISSER given at 4.2.v.

7.1.iv

A number of cases of double or missing images were noted in the test measurements, and dependency upon system errors is quite marked, as shown in Table 7.IV:

TABLE 7.IV

Double or Missing Images in tests of Model A

Slit Width	Total Points	Double or Missing Points	%
2 mm	280	0	0
4 mm	280	7	2.5
8 mm	280	10	3.6
16 mm	280	11	3.9

7.1.v

Scale errors of each of the measured orthophotographs were derived from the transformation computations, and are given in parts pro mille in Table 7.V:

TABLE 7.V

Scalar errors of orthophoto negatives in Model A

Parts pro mille

Slit Width	V_d=2mm/sec	2.6mm/sec	4mm/sec	6mm/sec	8mm/sec
2	-0.3	-0.6	-0.7	-0.5	-0.8
4	-0.7	-0.6	-0.5	-0.2	-0.4
8	-0.5	-0.4	-0.6	-0.8	-0.2
16	-0.5	-0.6	-0.5	-0.4	-0.6

The mean square error of the scalars of the 20 tests is $0.53^{o}/_{oo}$, but it should be noted that scaling of the individual test models was considered satisfactory from a production viewpoint when correct within $\pm 0.5^{o}/_{oo}$ (see 6.5). It is not thought that the exclusively negative sign of the scalars is significant, because the b_x micrometer of the plotter was hardly changed throughout the series of tests. The b_x micrometer of the Topocart is somewhat insensitive to very small changes, and it is thought that a more precise scaling than $\pm 0.5^{o}/_{oo}$ could only be achieved by a very prolonged orientation testing procedure, which may hardly be justified in production.

The effect of a small scalar error is significant if several orthophoto film negatives are to be matched and joined to a control grid, as will be common in the case of medium scale mapping. If the figure of $\pm 0.53^{o}/_{oo}$ m.s.e. of scalar is representative, a corresponding planimetric error of ± 63 µm m.s.e. is obtained at each corner point of a 100 mm by 200 mm model at plate. The plate scale may therefore be enlarged twice without any great difficulty in fitting to a control grid, but for enlargements above this limit, scaling of the model in the restitution plotter is very critical, and the extra orientation time to achieve scaling of the order of say $\pm 0.2^{o}/_{oo}$, must be accepted as necessary.

7.1.vi

Test Model B was scanned with only 8 mm and 16 mm slits at the fixed speed of 4 mm/sec in the orthophoto, equivalent to 1.67 mm/sec at plate. The results of the tests are given in Table 7.VI.

TABLE 7.VI

Internal Planimetric Errors of Test Model B (flat terrain)

Slit Width		m_x	m_y	m_p	ΔX max.	ΔY max.	ΔP max.	Scale Error $^{o}/_{oo}$
8 mm	µm (d)	87	101	133	184	308	-311	+0.4
	µm (b)	36	42	55	77	128	-130	
16 mm	µm (d)	118	83	144	-321	294	-324	+0.4
	µm (b)	49	35	60	-134	123	-135	

(no missing or double points)

The results are very similar to the corresponding tests of Model A.

7.2 External Errors in Planimetry

7.2.i

All of the test models scanned at a speed of 4 mm/sec in the orthophoto were also analysed in order to derive external errors: v'_x, v'_y, v'_p, as defined in 4.4.i; by transformation of the measured coordinates through program SIMTRAN (applying the affine correction option); and using as control coordinates solely the four corner pass points with control coordinates derived from the aerial triangulation adjustment. The results are given, in terms of micrometers at orthophoto scale 1:25 000 at Table 7.VII, together with the corresponding internal errors in parenthesis.

TABLE 7.VII

External Planimetric Errors, Tests executed at 4 mm/sec Scan Speed V_d (μm at Orthophoto Scale 1:25 000)

Model A	m'_x	m'_y	m'_p	$\Delta X'$ max.	$\Delta Y'$ max.	$\Delta P'$ max.
b=2 mm	97(84)	79(65)	124(106)	212(-197)	281(255)	28[illegible] ([illegible])
b=4 mm	103(92)	131(82)	166(123)	250(260)	290(179)	326([illegible])
b=8 mm	173(92)	103(97)	202(134)	388(269)	-268(253)	-406 (-[illegible])
b=16 mm	181(98)	85(95)	200(136)	415(198)	217(243)	-4[illegible] (-[illegible])
Model B						
b=8 mm	111(87)	141(101)	179(133)	288(184)	-331(308)	-33[illegible] (-[illegible])
b=16 mm	135(118)	103(83)	170(144)	344(-321)	340(294)	427 (-3[illegible])

7.2.ii

Immediately apparent from Table 7.VII is the general degradation of accuracy due to the basis of aerial triangulation data. The arithmetic mean of the m.s.e. vector errors of Model A is degraded from ± 125 μm to ± 173 μm, and of Model B from ± 139 μm to ± 175 μm. The arithmetic mean of the absolute values of maximum coordinate errors is degraded from 275 μm in the case of Model A to 361 μm, and in the case of Model B from 318 μm to 383 μm. Coordinate vector errors greater than 300 μm totalled only 4 points from 324 tested points (1.2%) in both areas in the case of internal errors, but increased to 20 points (6.2%) in the case of external errors. The principal effect of transforming only to the pass points however, was to cause the residual errors to become strongly systematic in distribution, as may be seen from the vector diagrams and histograms 7/11 to 7/20 inclusive. It should be noted however, that the residual errors of both models are nevertheless acceptable in terms of the criterion of Australian National Mapping Standards of Map Accuracy (7.1.ii).

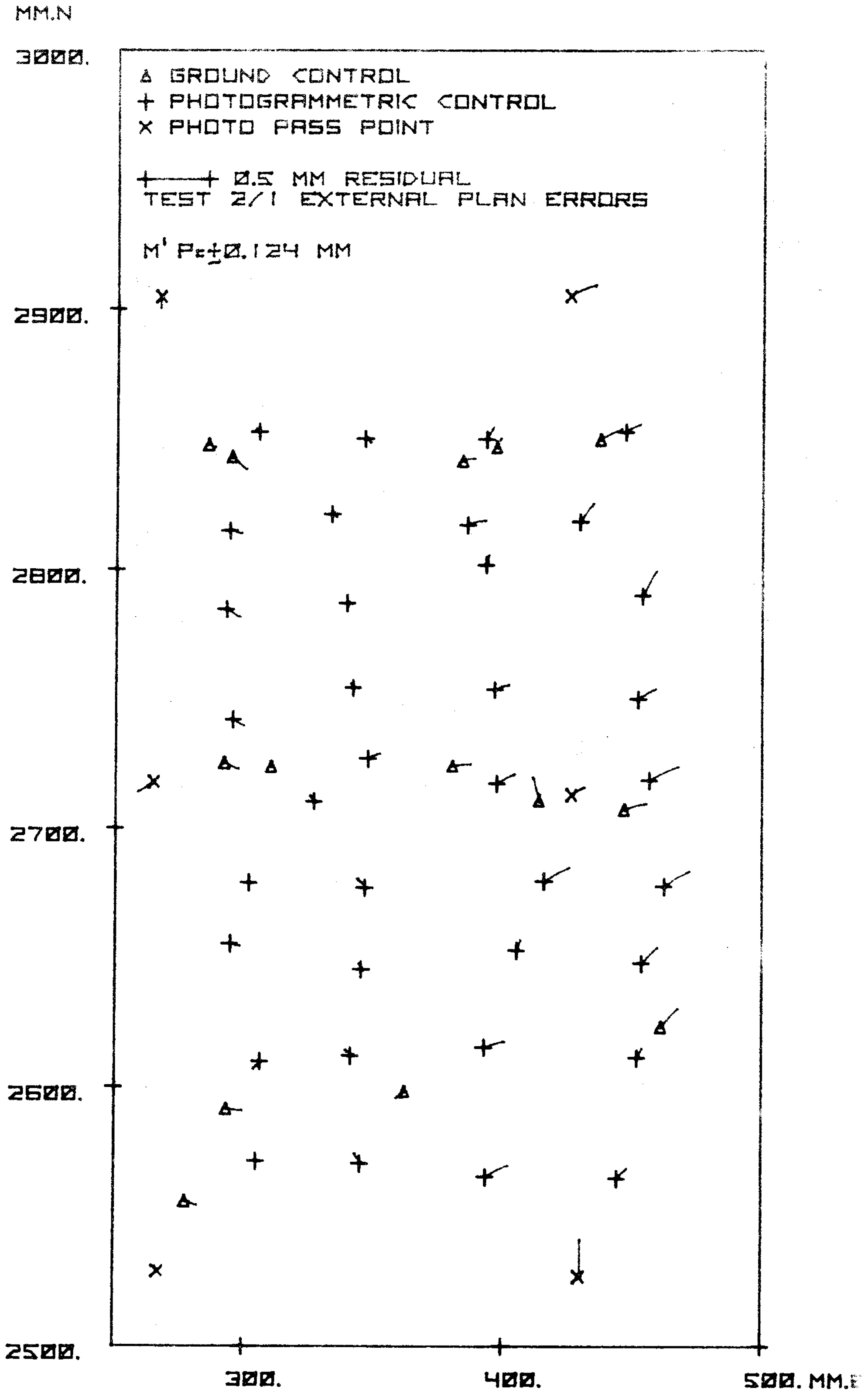

M O D E L 0 5 0 6 R E S I D U A L E R R O R S

FIG 7/11

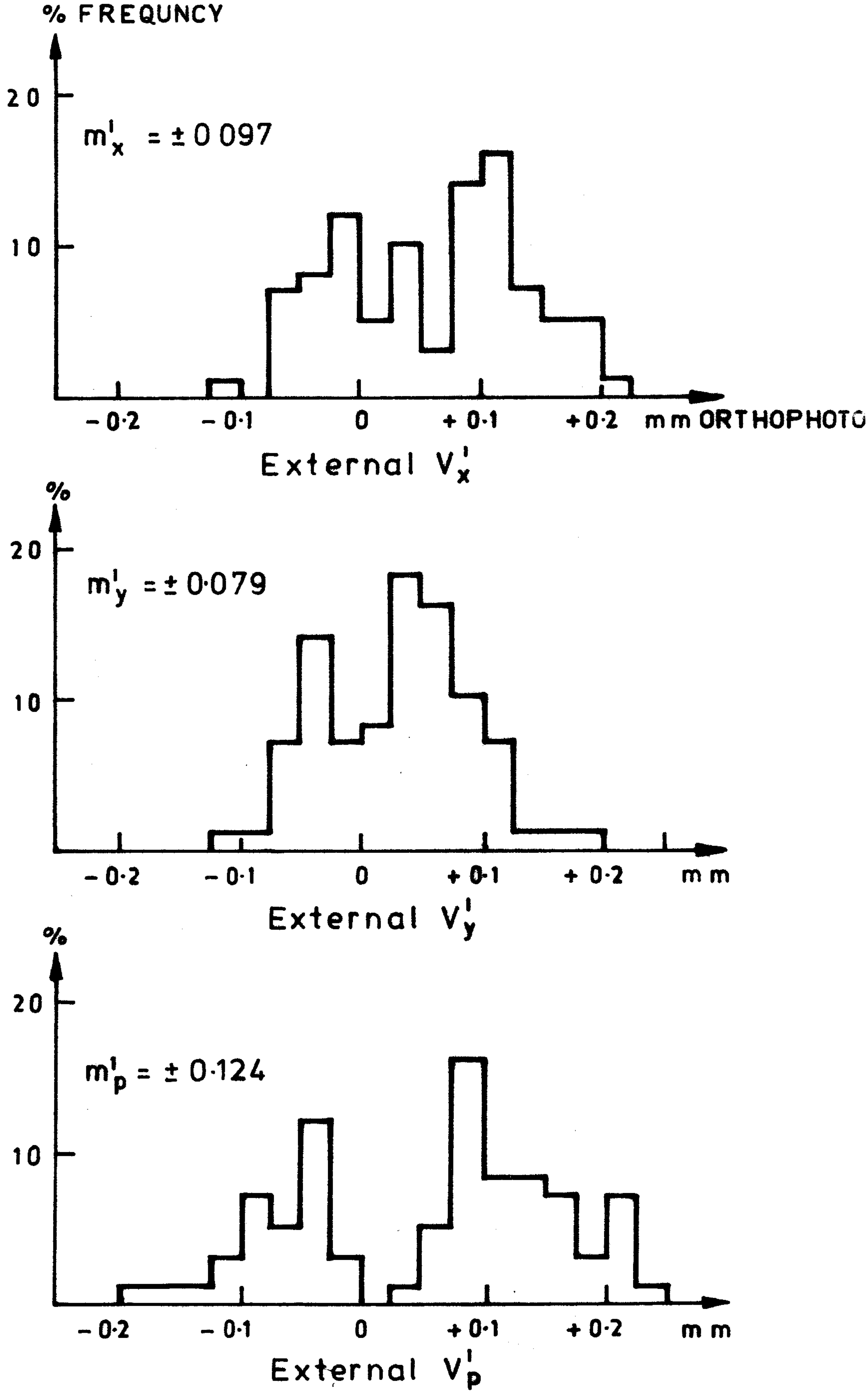

FIG. 7·12. DISTRIBUTION OF EXTERNAL ERRORS TEST 2/1

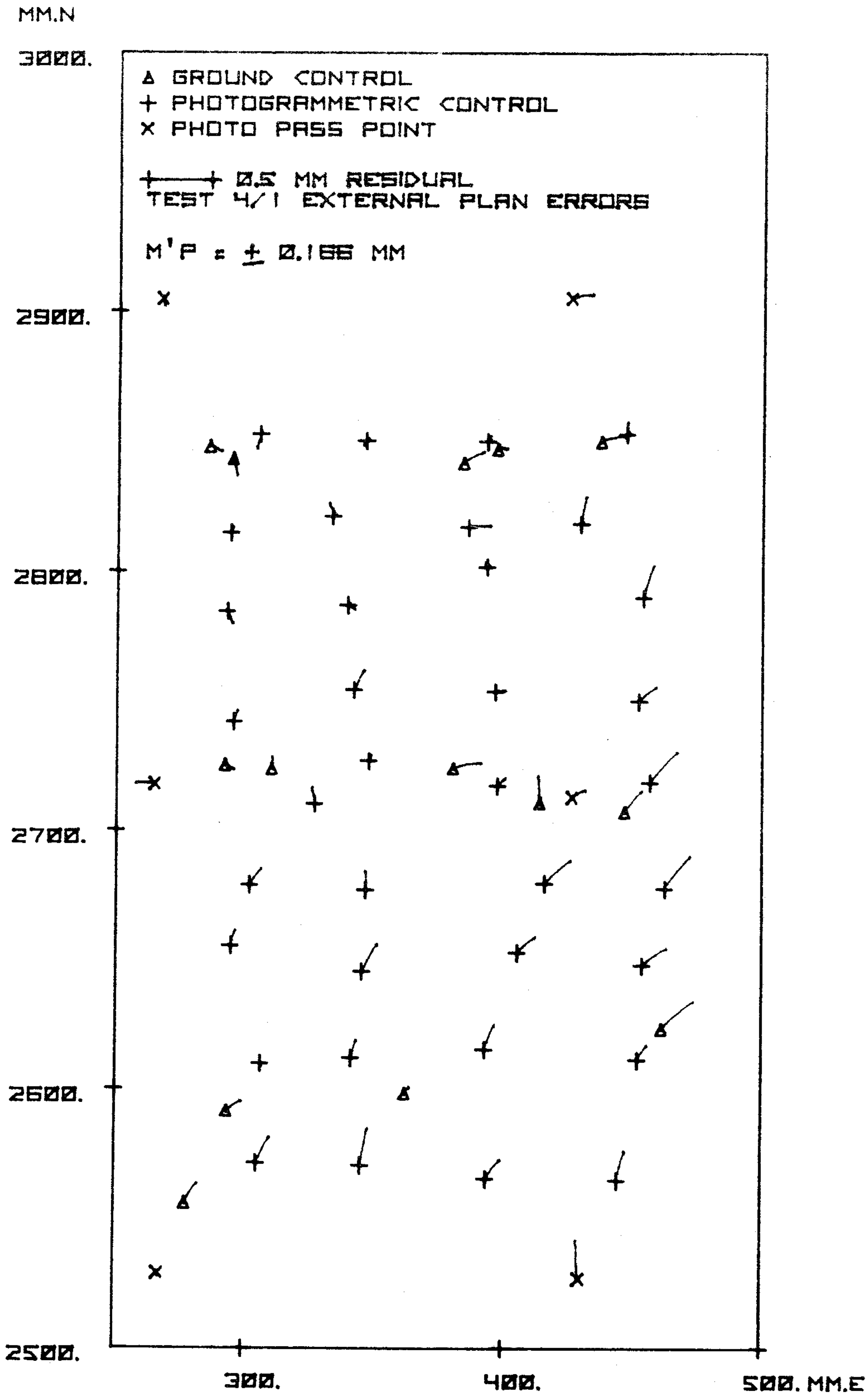

MODEL 0506 RESIDUAL ERRORS

FIG 7/13

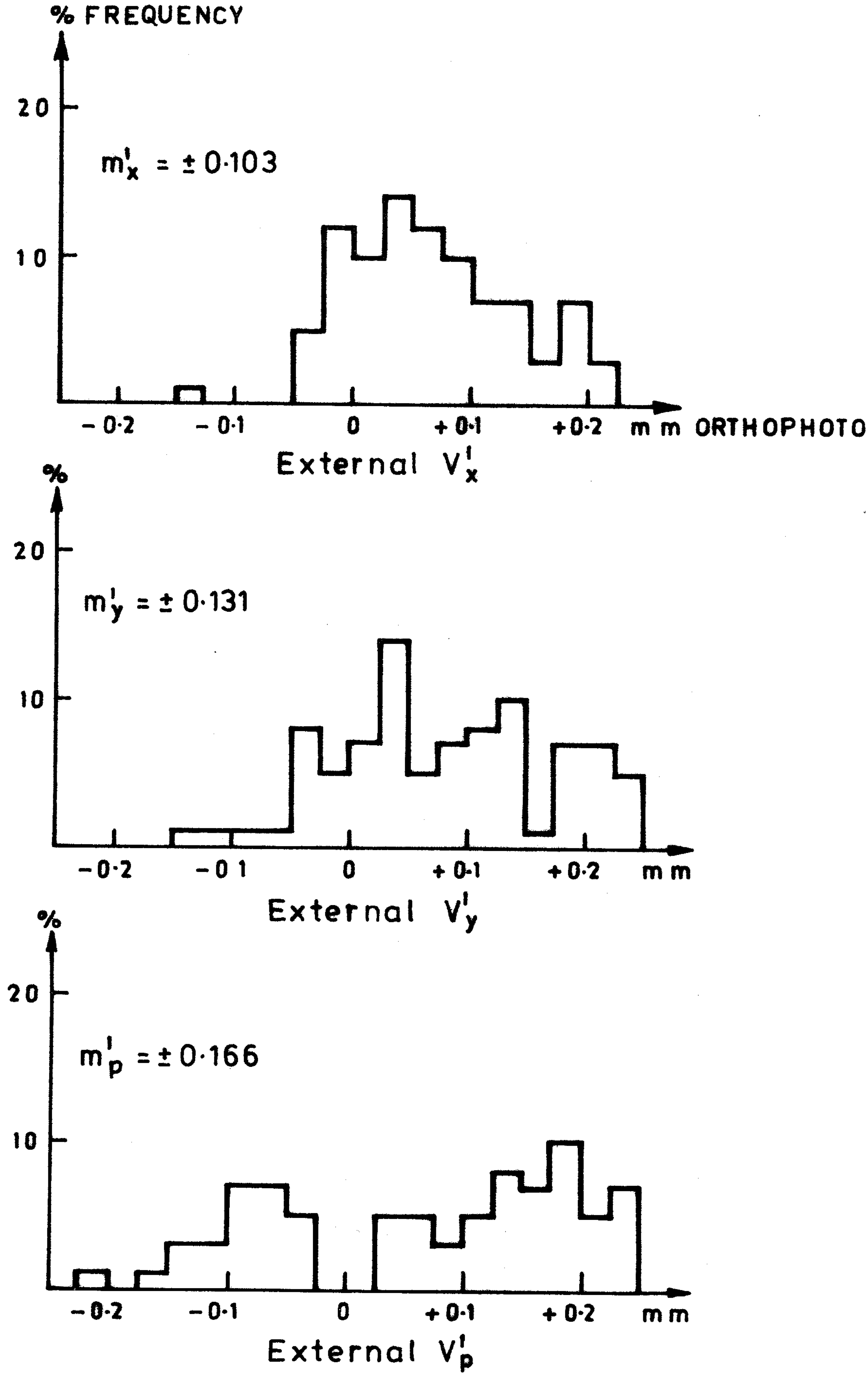

FIG. 7·14. DISTRIBUTION OF EXTERNAL ERRORS TEST 4/1

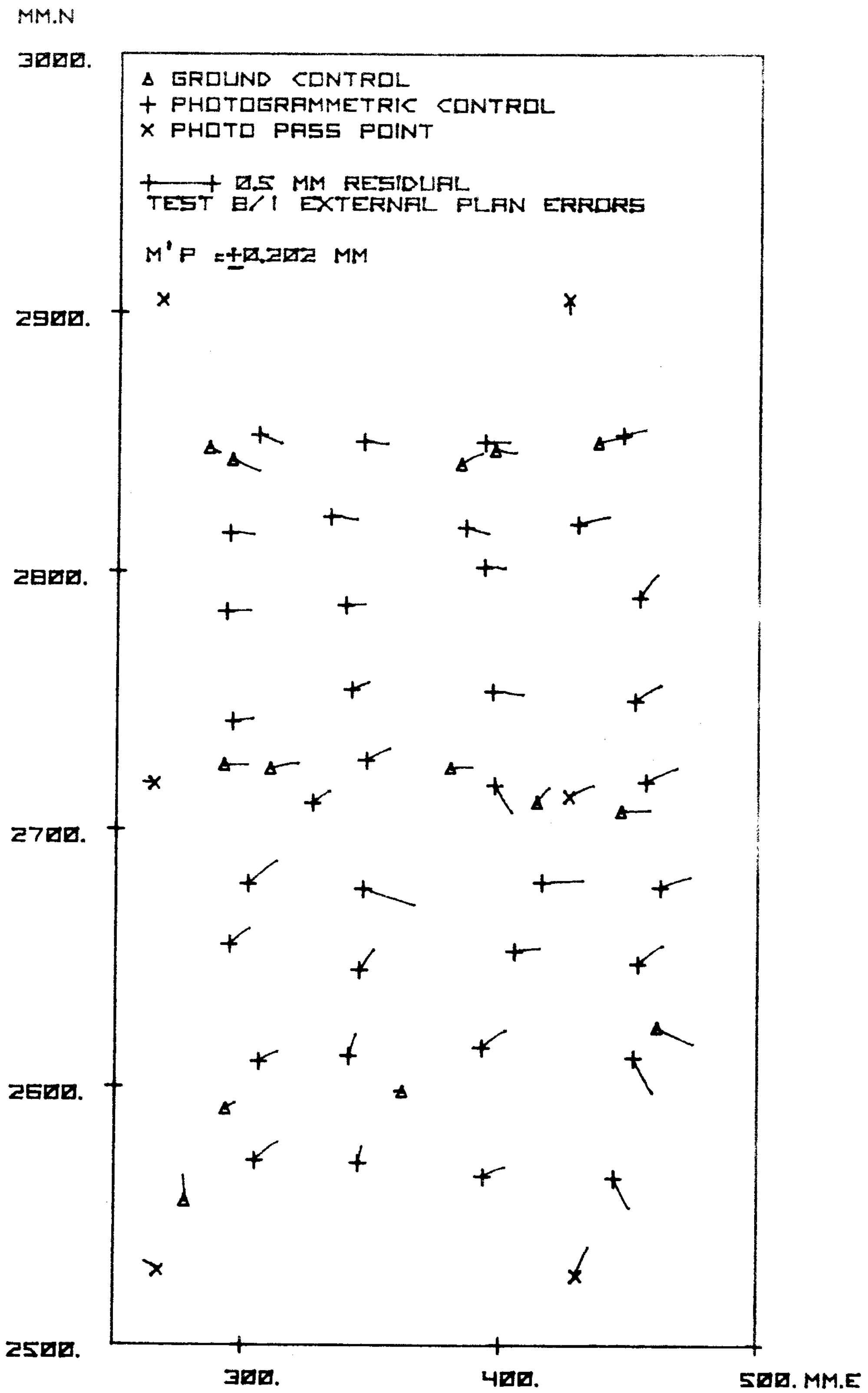

MODEL 0506 RESIDUAL ERRORS

FIG 7.15

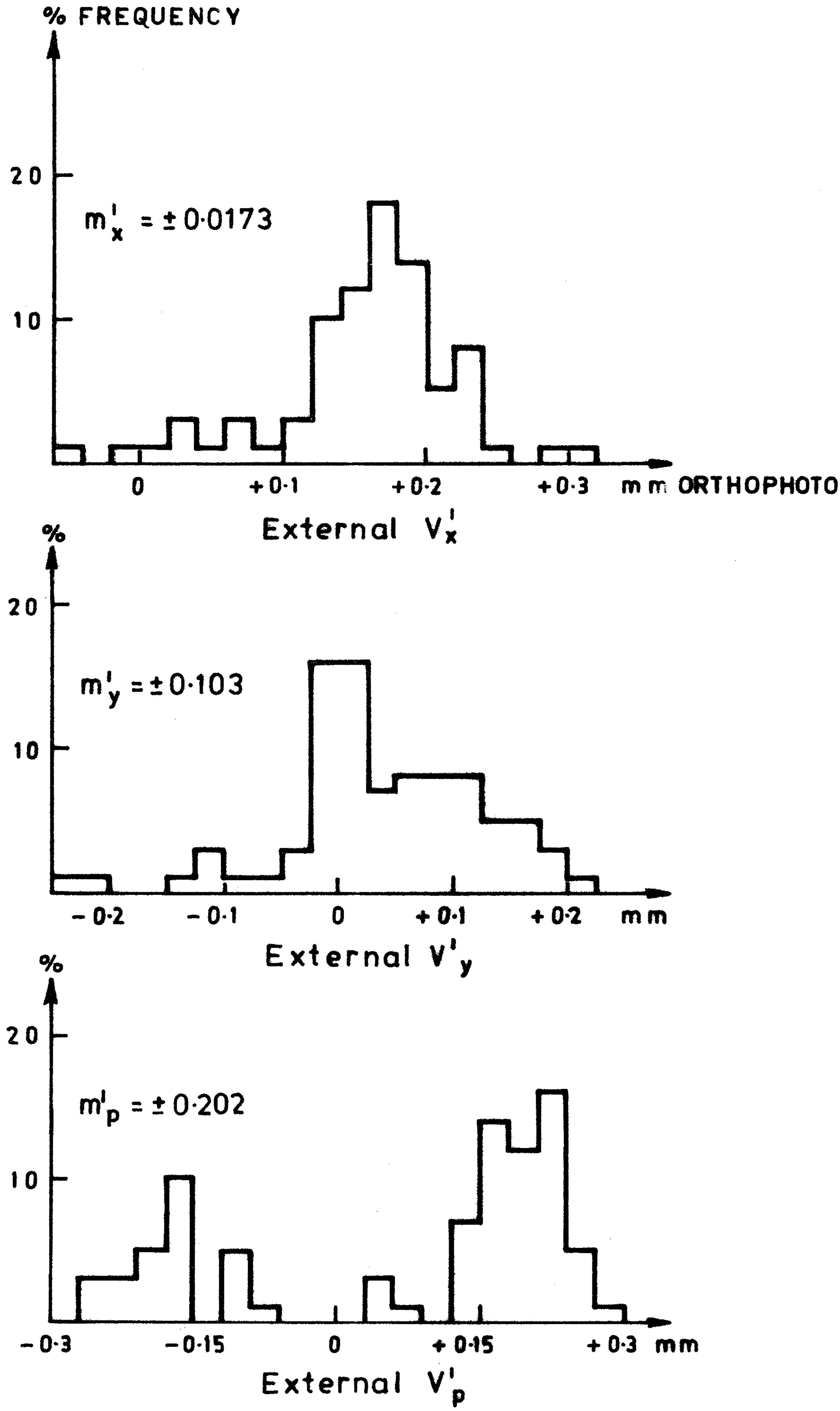

FIG. 7·16. DISTRIBUTION OF EXTERNAL ERRORS TEST 8/1

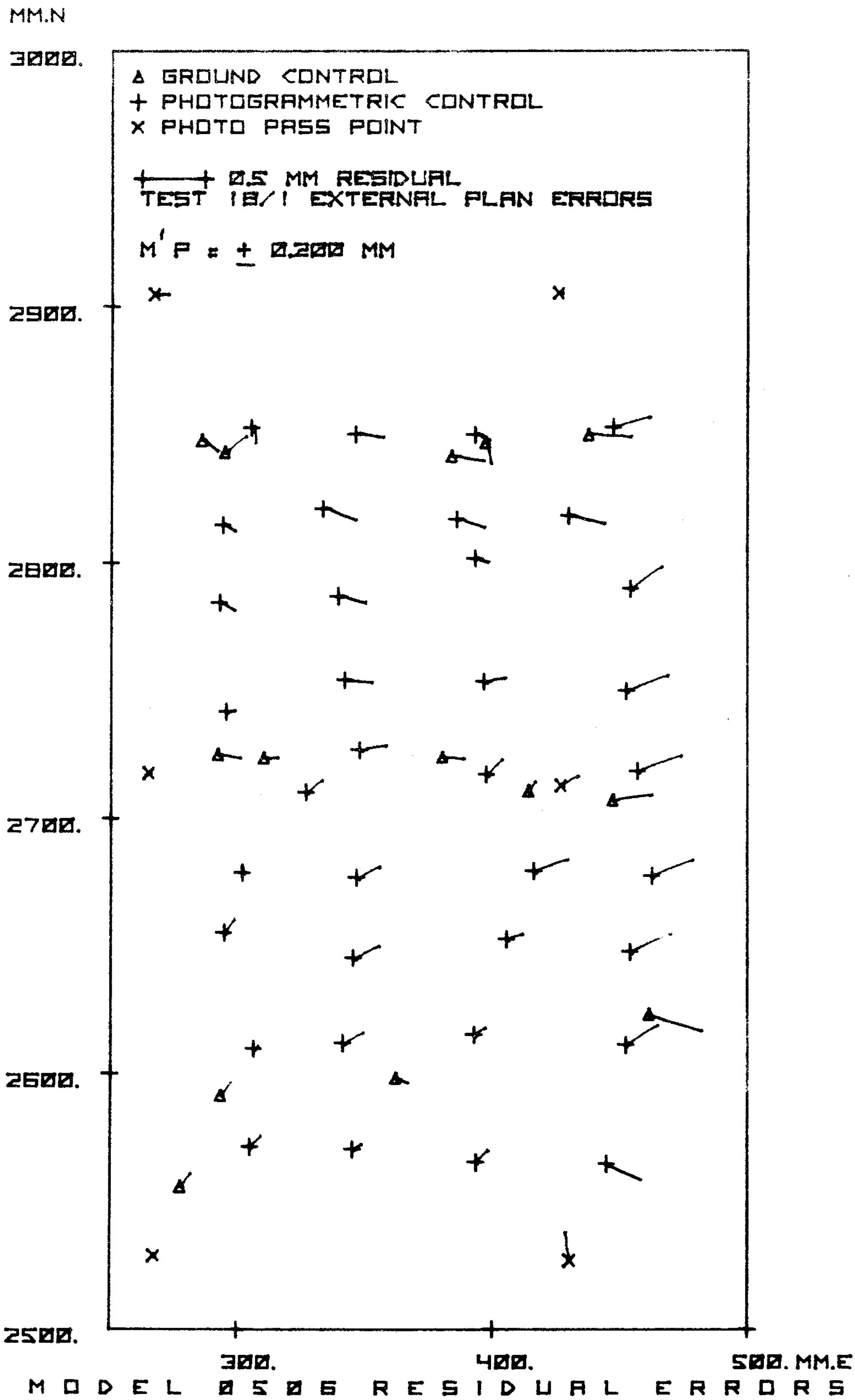
MM.N
3000.
2900.
2800.
2700.
2600.
2500.
300.
400.
500. MM.E
Δ GROUND CONTROL
+ PHOTOGRAMMETRIC CONTROL
× PHOTO PASS POINT
0.5 MM RESIDUAL
TEST 18/1 EXTERNAL PLAN ERRORS
M'P = ± 0.200 MM
MODEL 0506 RESIDUAL ERRORS

FIG 7/17

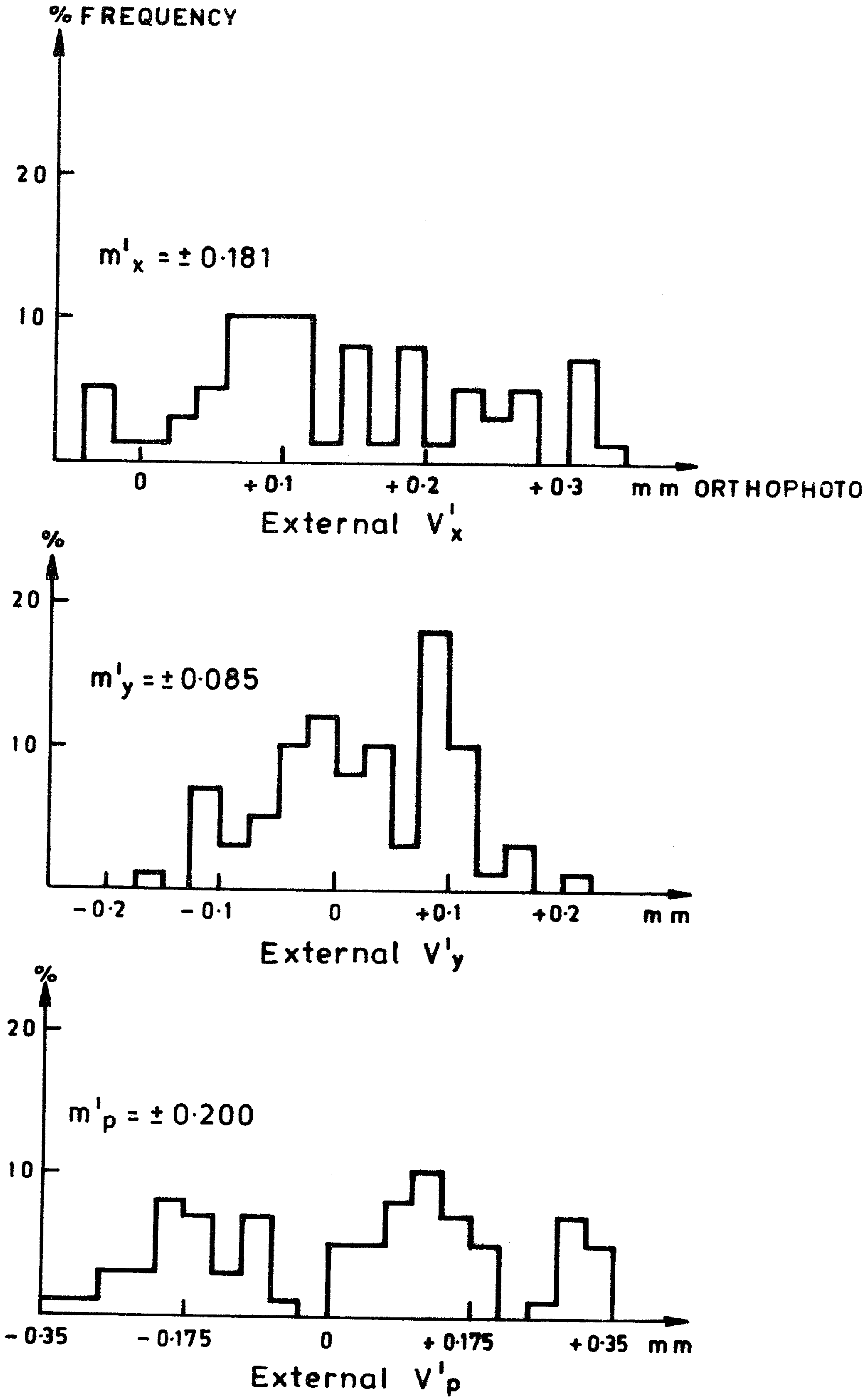

FIG. 7·18. DISTRIBUTION OF EXTERNAL ERRORS TEST 16/1

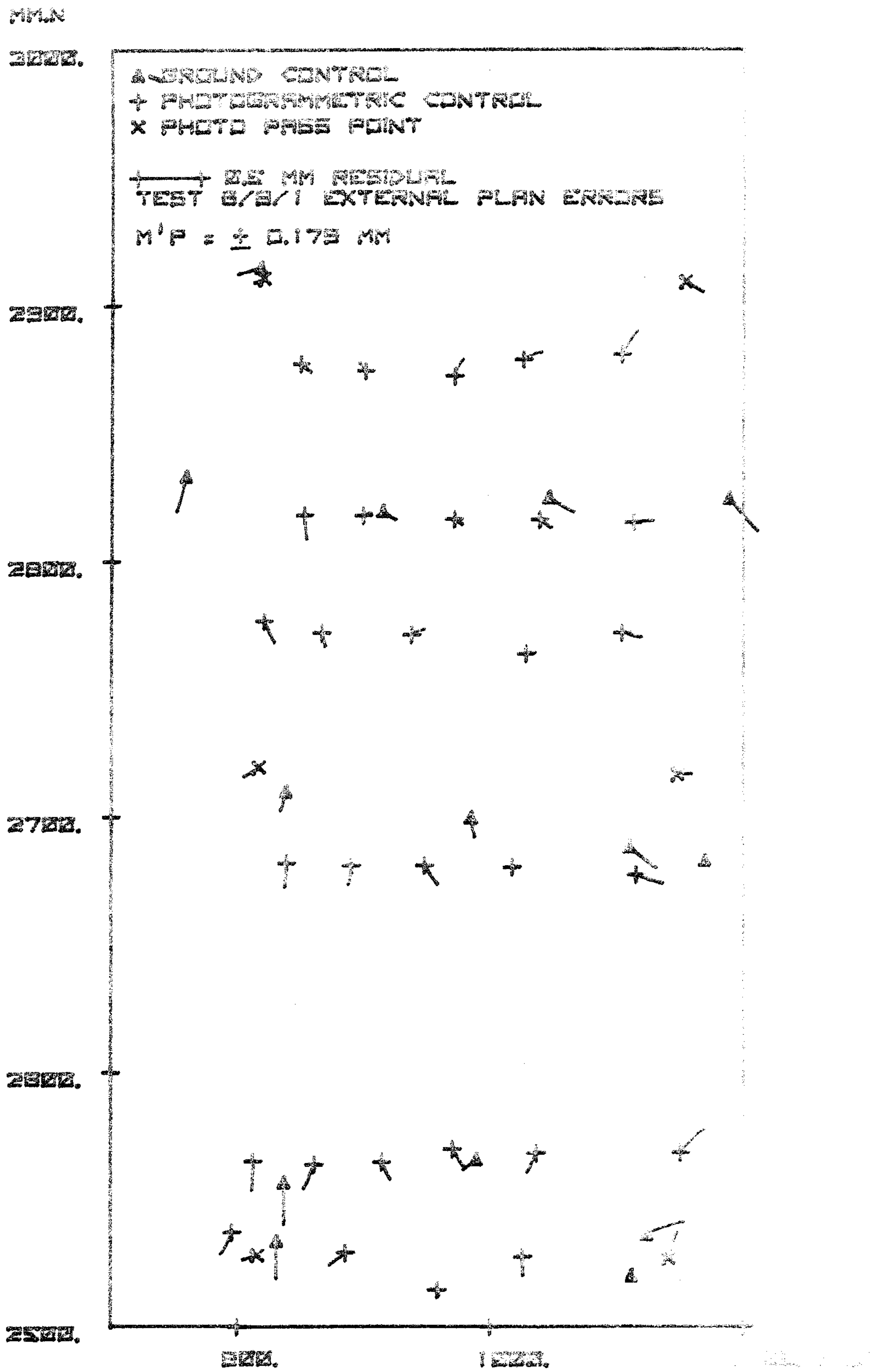

MODEL 2310 RESIDUAL ERRORS

FIG 7/19

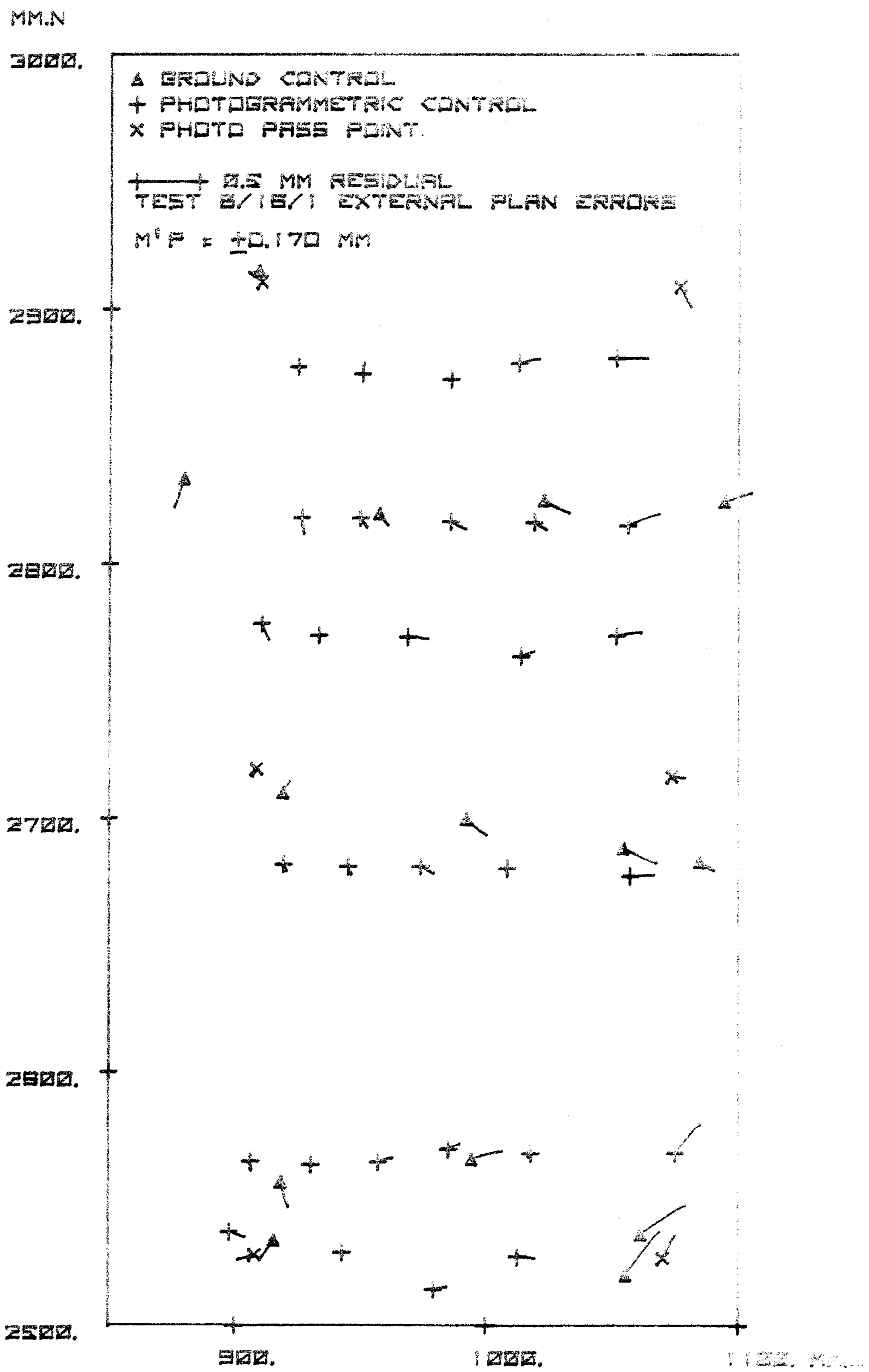

MODEL 0910 RESIDUAL ERRORS

FIG 7/20

7.3 Elevation Errors at Profile Signals

7.3.i

Elevation errors were measured directly on the profile signal change points, by the observational technique described in 6.8. Profile signal errors were tested throughout the scan speed range in the 2 mm exposure slit series of Model A, and also throughout the fixed speed series of 4 mm/sec scan speed (in the orthophoto) in Model A. As far as the accuracy of the signals is concerned, there is no theoretical dependency on the intervals of the profiles, which in principle can only effect the accuracy of the derived contours.

The accuracy of the profile signals is of particular interest because the results are considered to be of general application, i.e. not confined to the drop-line system alone. The signal change points, as tested by the direct observation technique, are equivalent to profile elevation signals of any type, including those of a purely digital nature, excepting only any electromechanical errors or delays caused because the signals have been converted to a graphical form.

Mean square errors and maximum errors are given in Tables 7.VIII and 7.IX; in terms of parts pro mille Z. The mean square errors have also been used to deduce nominal C numbers using the formula:

$$C = 1000/3.33(m_Z.{}^{\circ}/_{\circ\circ}Z) \qquad (7.V)$$

The formula assumes that contours could be produced from the profiles without further error degradations, and that the accuracy criterion for the contours should be that 90% of the points on the contours would be correct within one half the contour interval.

Tables 7.VIII and 7.IX are for the internal v_z, in so far as external influences due to the errors of aerial triangulation have been removed.

TABLE 7.VIII

Internal Profile Errors of Model A at Various Scan Speeds

Scan Speed (V_d) mm/sec (V_b)	2 0.83	Average 2.6 " 1.08	4 1.67	6 2.5	8 3.34
m_z $^o/_{oo}Z$	0.32	0.34	0.23	0.23	0.32
v_z max $^o/_{oo}Z$	1.08	1.01	1.07	0.62	1.04
C number	938	882	1304	1304	938

TABLE 7.IX

Internal Profile Errors of Model A at Speed V_d 4 mm/sec

Profile Interval	2 mm	4 mm	8 mm	16 mm
m_z $^o/_{oo}Z$	0.23	0.22	0.27	0.26
v_z max $^o/_{oo}Z$	1.07	0.63	0.53	0.70
C number	1304	1364	1111	1154

7.3.ii

Some general conclusions can be inferred from tables 7.VIII and 7.IX:

(a) As in the case of errors of planimetry (7.1.ii.c), the influence of speed scan is not what might be expected. Again the smallest mean square errors are achieved at the relatively fast scan speeds of 4 and 6 mm/sec in the orthophoto. The largest mean square error occurs at the variable speed, when the operator has complete control over the movement of the measuring mark. Once again it might be inferred that the operator is not the best judge of his own scanning ability, but that it is better to keep him alert for optimum efficiency, by putting him under slight stress.

(b) The extremely consistent results of the four tests at fixed scan speed of 4 mm/sec in the orthophoto may be noted, with a spread of mean square errors of only 0.22 - 0.27 °/oo. These results, and the derived C numbers in the range 1111 - 1364 suggest that *profiling accuracy is intrinsically as accurate as conventional photogrammetric contouring, provided that the profile signals can be converted to contours without a significant degradation in accuracy.*

7.3.iii

Comparison of the test results with those of HAMPEL given at 4.3.ii, may be obtained in particular with the four tests of Table 7.IX, where the scan speed at the plate is 1.67 mm/sec; compared to 1.56 mm/sec in the HAMPEL profile tests. The range of results is ±0.22 to 0.27 $^{o}/_{oo}$Z, and the result of HAMPEL was ± 0.5 $^{o}/_{oo}$Z. The rather large discrepancy may be partially due to the method of testing, since HAMPEL's checks were against derived profile sections rather than on the actual signal change points; but more probably the discrepancy occurs because of the wider range of slopes of the HAMPEL test of the order of 0 - 190%, compared to 0 - 33% in Model A.

7.3.iv

A more satisfactory comparison is obtained with the profile tests of VISSER in the second test model of the REICHENBACH area, given at 4.3.iv:

	Slopes	Speed V_b mm/sec	m.s.e.
REICHENBACH	0 - 19%	0.74 - 2.94	± 0.12 to 0.32 $^{o}/_{oo}$Z
FOWLERS GAP	0 - 33%	0.83 - 3.34	± 0.22 to 0.34 $^{o}/_{oo}$Z

The two sets of results confirm that a standard of accuracy is obtained in profile signals, in moderate slopes, of an order rather similar to that of conventional photogrammetric contouring.

7.4 Elevation Errors on Contours

7.4.i.

The profiles of the series of tests of Model A carried out at scan speeds V_d of 4 mm/sec, were converted to contours by the procedure described in 6.9.iii, and errors derived on the contour lines close to the check points by the measurement technique of 6.8. The internal errors are given in Table 7.X, corresponding to the profiling errors of Table 7.IX.

TABLE 7.X

Internal Contour Errors of Model A, Scan Speed V_d 4 mm/sec

Profile Separation:		2 mm	4 mm	8 mm	16 mm
m_z $^o/_{oo}Z$	:	0.24	0.24	0.36	0.46
V_z max $^o/_{oo}Z$	:	0.92	0.61	1.10	1.44
C number	:	1250	1250	833	652

Comparison between results from the profile signals and from the derived contours shows that there is a slight falling-off in accuracy of contours derived from the close profile separations of 2 and 4 mm, a rather more pronounced decline in the accuracy from the 8 mm profile separation, and a rather marked loss of accuracy with the 16 mm separation which is clearly unsuitable for the terrain type.

The relationship between the results was further investigated, by testing the linear correlation between the errors according to equations 7.ii and 7.iii, by forming equations of the type:

$$v_{zc} = m.v_z.p + b \qquad (7.vi)$$

where v_{zc} is the error on a contour nearest to a check point, and v_{zp} is the corresponding error on a signal change point nearest to a check point. The comparison is not strictly valid, since the errors do not refer to precisely the same points, but this small discrepancy was not thought to be very significant taking into account the relatively large number of points (56) in each test. The correlation coefficients found for each test were:

Profile separation	r
2 mm	0.86
4 mm	0.63
8 mm	0.37
16 mm	0.20

These results show that the intrinsic accuracy of the profile signals is retained after deriving contours, only by appropriate choice of profile separation interval. In the case of the first three tests, the mean interval of signal changes along the profiles amounted to 4 mm (6.1.ii), and for the 16 mm test the mean interval of signal change along the profile was 8 mm because the contour interval was doubled. It is apparent that in the first two tests with high correlation, that the profile separation is equal to or less than the signal interval along the profile. In the remaining tests, the profile separation is double the signal interval, and there is a marked decrease in correlation. *It may be concluded that a suitable choice of profile separation, is one in which the separation is equal to the mean signal plan interval along the profiles, so that on average contours are constructed from a square grid of discrete points.* Additionally of course, system errors must be considered, and the size and direction of topographic features taken into account.

7.4.ii

When the contour plots were being tested, the actual test locations on the contours were marked, and slope in the profile direction subsequently measured. It was then possible to test the correlation between elevation errors and ground slope β, by forming equations of the type:

$$v_{zc} = m.\tan\beta + b \qquad (7.vii)$$

The results, together with the correlation coefficient r, are given in Table 7.XI.

TABLE 7.XI

Internal Contour Errors as a Function of Slope

Test 2/1	$v_z = \pm(0.13 + 1.4 \tan\beta)\ ^o/_{oo}Z$	; r =	0.42
Test 4/1	$v_z = \pm(0.23 + 2.4 \tan\beta)\ ^o/_{oo}Z$	; r =	0.39
Test 8/1	$v_z = \pm(0.20 + 1.8 \tan\beta)\ ^o/_{oo}Z$	; r =	0.42
Test 16/1	$v_z = \pm(0.14 + 0.7 \tan\beta)\ ^o/_{oo}Z$	; r =	0.20

It should be noted that the linear correlation is rather weak, and in the case of 16 mm profile separation practically non-existent, so that not too much credence should be placed on the results as evidence of a KOPPE type law (4.3.vii). The critical value for r is 0.25 (for 54 degrees of freedom) at a level of significance $\alpha = 0.05$; i.e. a probability that there is no linear correlation of 5% *(Fisher and Yates, 1963)*. The first three tests therefore indicate that there is some statistical evidence, albeit rather weak, of correlation between elevation errors and ground slope. The mean result of the first three tests (the final test being excluded on acount of the very low correlation coefficient) is:

$$v_z = \pm(0.18 + 1.8 \tan \beta)\,^{\circ}/_{\circ\circ}Z \qquad (7.viii)$$

7.4.iii

The previous results were obtained after adjusting the direct measurements of elevation errors for the computed absolute orientation errors of the aerial triangulation, derived from the analysis of errors at 5.9. The unadjusted measurements are external errors (v'_z), and the results for contours of Test Model A are given in Table 7.XII, together with those of Test Model B, which was analysed only for external errors.

TABLE 7.XII

<u>External Contour Errors, Scan Speed V 4 mm sec</u>

Profile Separation:	2 mm	4 mm	8 mm	16mm	8 mm*	16mm*
m'_z $^o/_{oo}Z$:	0.27	0.23	0.39	0.53	0.27	0.31
v'_z max $^o/_{oo}Z$:	0.86	0.63	1.20	1.63	0.69	0.90
C number :	1111	1304	769	566	1111	566

* flat terrain models

Comparison with Table 7.X shows that the degradation of accuracy due to the aerial triangulation pass points, is not as marked as in the case of the planimetric errors, the range of mean square errors for Model A being ± 0.23 to 0.53 $^o/_{oo}Z$ compared to external accuracy of ± 0.24 to 0.46 $^o/_{oo}Z$. Indeed in one case (4 mm profile) the external accuracy is marginally better, due presumably to a slight error in levelling of the original model at its pass points. The results however are not unexpected since the computed levelling errors of Model A were very small (Table 5.IV.a), and during the test programme levelling of the models was carried out to ± 1c (6.5).

7.5 Contour Tests Assessed by Australian Map Accuracy Standards

7.5.1

The results of Table 7.XII may be assessed on the basis of Australian Map Accuracy Standards. The wording of the current (February 1953) standard is slightly ambiguous since it is not completely clear whether the standard is a straightforward statement of error tolerance, or whether the standard is of the KOPPE type (eqn. 4.1). The standard reads: "Vertical accuracy, as applied to contour maps on all publication scales, shall be such that not more than 10 per cent of the elevations tested shall be in error more than one-half the contour interval. In checking elevations taken from the map, the apparent vertical error may be decreased by assuming a horizontal displacement within the permissable horizontal error for a map of that scale". The standard may therefore be interpreted, where m_z is the mean square error of tested elevations, and VI is the contour interval as either:

$$m_z = \pm VI / 3.33 \qquad (7.ix)$$

$$\text{or,:} \quad m_z = \pm(VI / 3.33) + m_p.\tan \beta) \qquad (7.x)$$

7.5.ii

On the basis of equation 7.ix, for a 5 metre contour interval, $m_z = \pm 1.5$m; and on the basis of equation 7.x for a 1:25 000 publication scale map, $m_z = \pm (1.5 + 7.65 \tan \beta)$ m. The flight altitude (6875m), and mean square value of slopes at check points (5g) for Model A, give in terms of parts pro mille Z:

$m_z = \pm 0.22\ ^{o}/_{oo}Z$ or $\pm 0.31\ ^{o}/_{oo}Z$ for a 5 m contour interval

$m_z = \pm 0.44\ ^{o}/_{oo}Z$ or $\pm 0.53\ ^{o}/_{oo}Z$ for a 10 m contour interval

In the case of Model B, mean square value of slope 0.15 g:

$m_z = \pm 0.22\ ^{o}/_{oo}\ Z$

It follows that without taking into account horizontal displacement of the contours, none of the tests were within the permissable standard of accuracy, but that the test of Model A at 4 mm profile separation was very nearly so. Taking into account permissable horizontal error, the tests of Model A at 2 mm and 4 mm profile separation are within standard, together with the test at the reduced contour interval of 10 m with 16 mm separation. In the case of flat terrain, where the effect of ground slope on the standard is negligible, the two tests produce errors below standard. It may be remarked that had all the tests been carried out with 10 m contour interval, then all except the 16 mm profile separation in broken terrain would have been well within standard without taking account of horizontal displacement of contours. Such an interval ($m_Z = \pm 0.44\ ^{o}/_{oo}Z$) is equivalent to C number 685, and it may be concluded that a suitable choice for C for both broken terrain of moderate slopes, and for rather flat terrain, is of the order of 600 to 700, a result which confirms the conclusions of VISSER *(1968, 27)*.

7.5.iii

Diagrams of the elevation errors of the six models analysed for external contour errors are given as figures 7/21 to 7/26. A rather characteristic pattern of errors is evident in the figures for the tests of Model A, exemplified by a preponderance of larger errors in particular in the series of points on the eastern side of the model. Examination of the actual slopes in the vicinity of these check points, revealed that the points all occurred in areas of rather marked changes of slopes in the scan direction, rather than large absolute slopes.

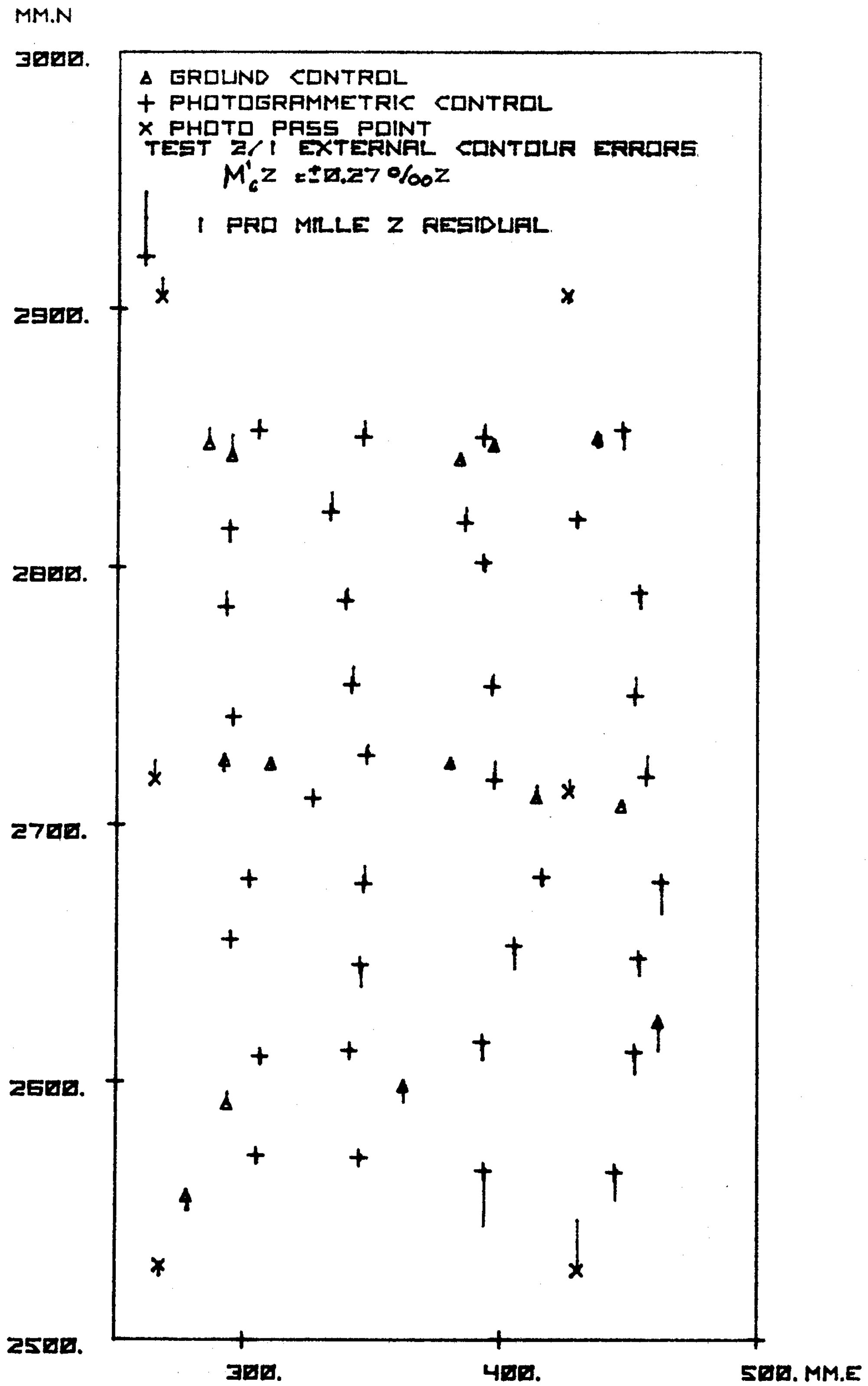

M O D E L 0 5 0 6 R E S I D U A L E R R O R S

FIG 7/21

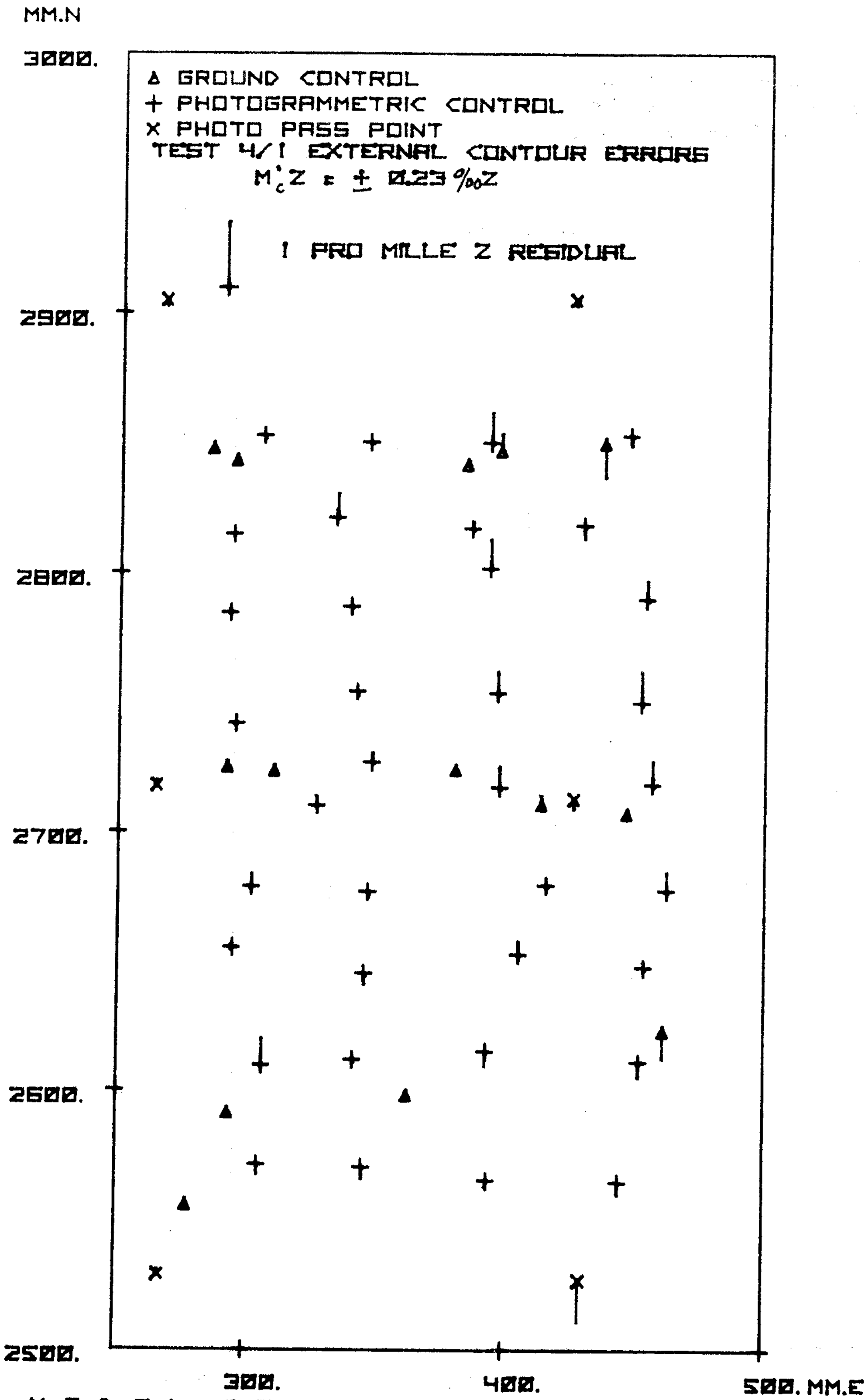

M O D E L 0 5 0 6 R E S I D U A L E R R O R S

FIG 7/22

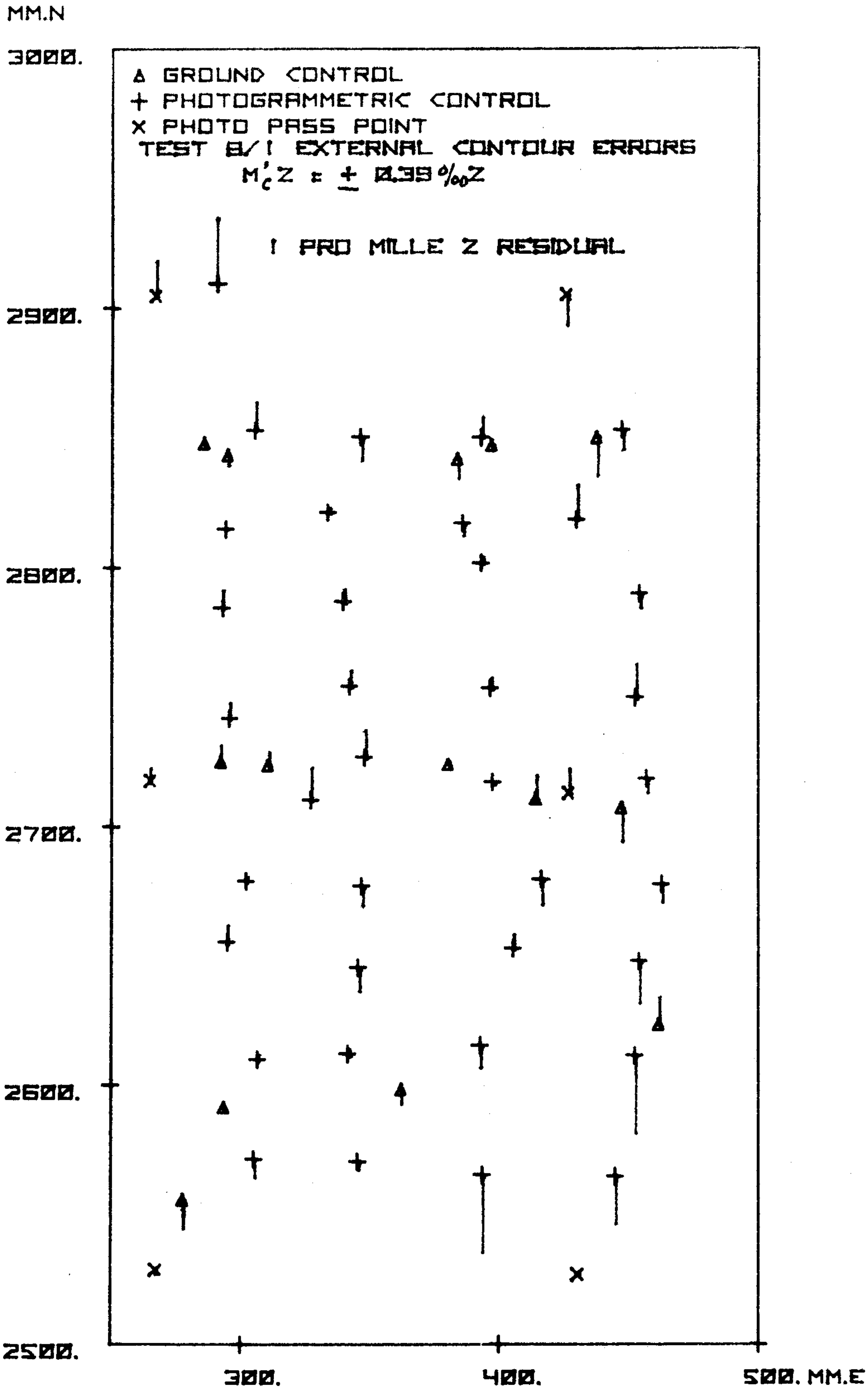

MODEL 0506 RESIDUAL ERRORS

FIG 7/23

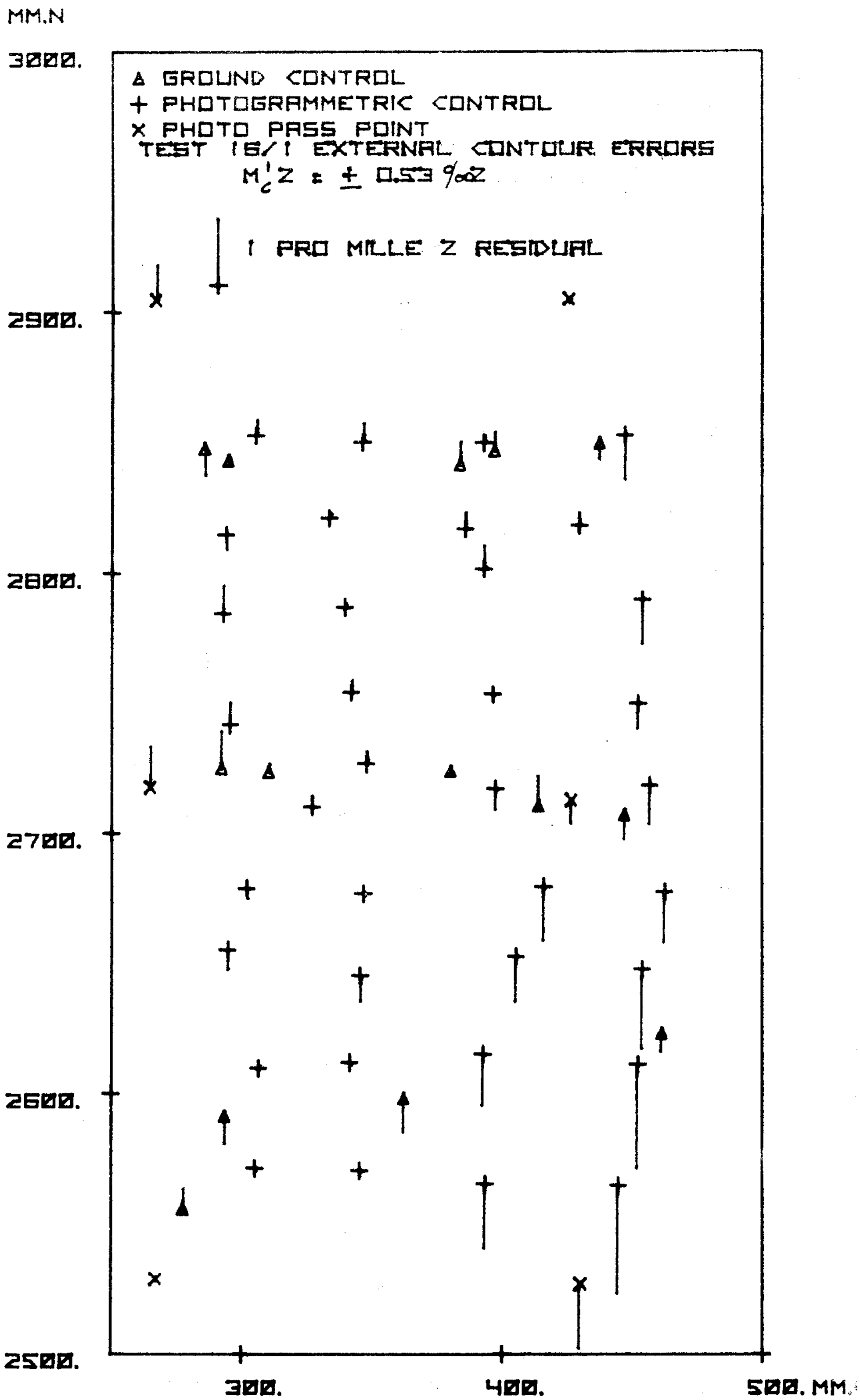

M O D E L 0 5 0 6 R E S I D U A L E R R O R

FIG 7/

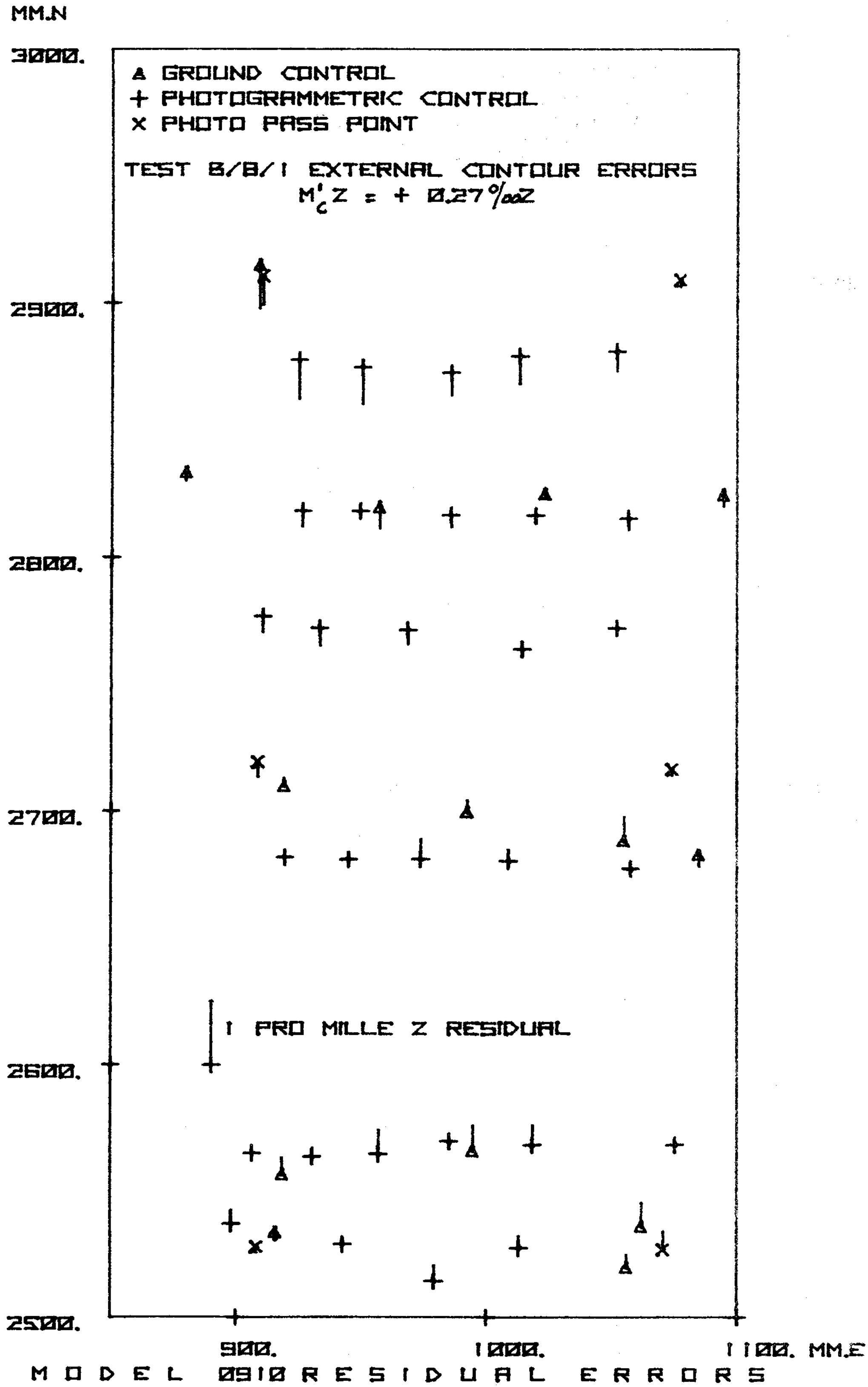
MM.N
3000.
2900.
2800.
2700.
2600.
2500.
900.
1000.
1100. MM.E
▲ GROUND CONTROL
+ PHOTOGRAMMETRIC CONTROL
x PHOTO PASS POINT
TEST B/B/1 EXTERNAL CONTOUR ERRORS
M'cZ = + 0.27 ‰Z
1 PRO MILLE Z RESIDUAL
MODEL 0910 RESIDUAL ERRORS

FIG 7/ 25

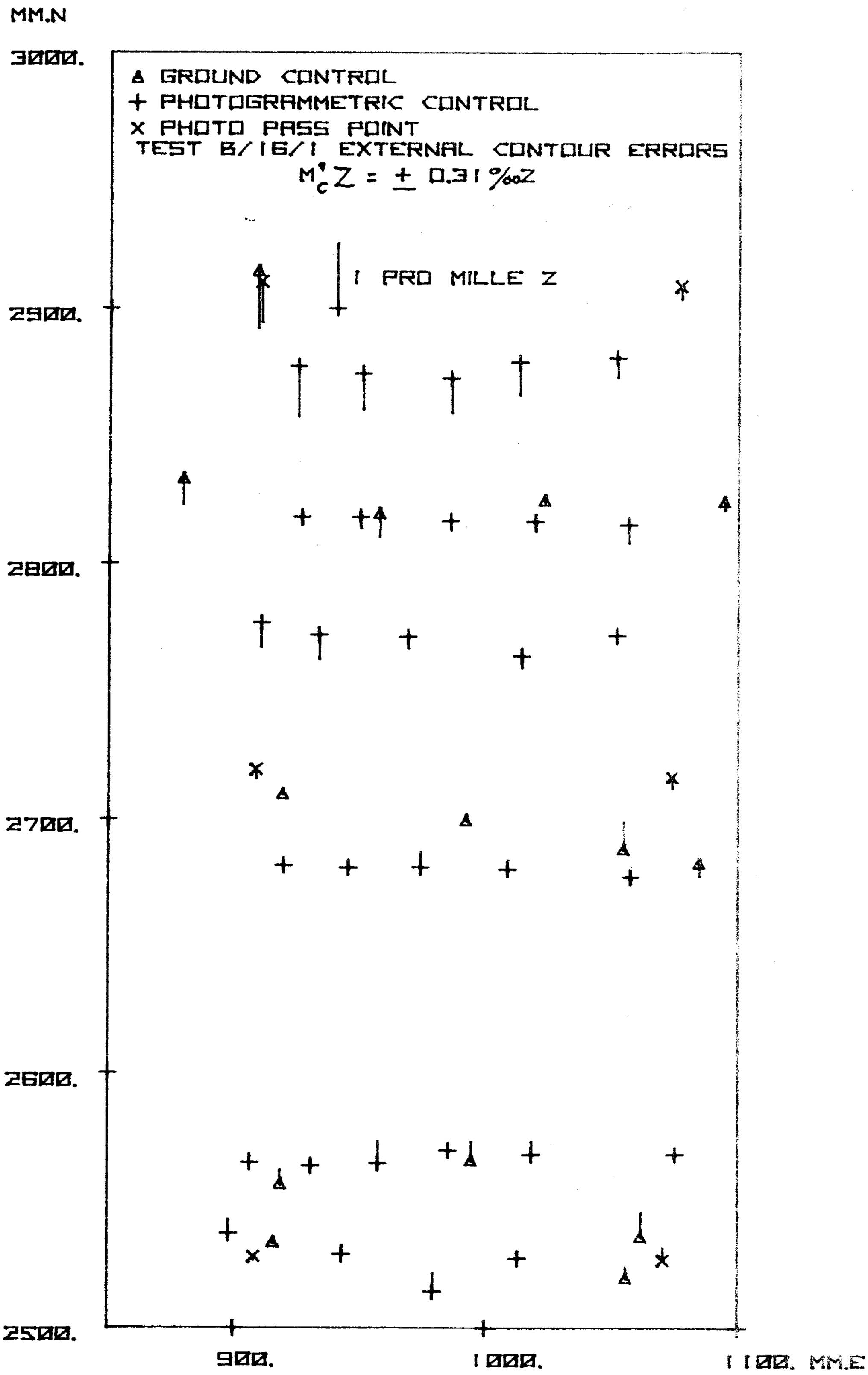

M O D E L 0910 R E S I D U A L E R R O R S

FIG 7/26

7.6 Production Times for Dropline Charts

7.6.i

Times for the conversion of the drop line charts to contour documents are given in Table 7.XIII, for an area in the chart of 400 mm by 200 mm.

TABLE 7.XIII

Contour Drawing by the Drainage Interpretation Technique

Area : 400 by 200 mm

Test	Mean HE (mm) *	Drainage	Principal Contour	Other Contours	Total hours	Points per minute
2/1	4	2	5	10	17	10
4/1	4	2	4	9	15	6
8/1	4	2	2.5	7.5	12	4
16/1	8	2	1.5	3.5	7	2
B/8/1	85	0.33	-	2.17	2.5	1
B/16/1	85	0.33	-	1.67	2	½

*Mean HE refers to the mean horizontal equivalent of signal changes occurring along a profile.

7.6.ii

The final column of Table 7.XIII relates to the approximate signal change points joined to form a continuous contour line in one minute, based on the mean density of points for the corresponding chart, and excluding the time taken to carry out the drainage interpretation and transfer. A relationship between the density of signal points and the time for conversion is rather evident, and based on these results figure 7/27 has been constructed. The figure represents contour conversion times per d_m^2, for areas of broken terrain, but again with the time spent on drainage interpretation excluded. It is clear that this element is rather variable, but it is thought that the time actually taken in these tests, equivalent to 15 minutes per d_m^2, represents an upper limit, due to the complexity of the drainage pattern.

It is clear that contour documents produced manually from dropline charts are by no means a free bonus of the orthophotographic process. On the contrary, considerable time and effort is necessary, together with an expertise which may only be achieved by proper training. One should also recognise that the document produced is not a fair-drawn trace, and that a considerable amount of extra cartographic time may be required for this purpose. However it should be possible, within the more sophisticated facilities of a production mapping agency, to overcome this disadvantage by use of a suitable drawing medium, such as is suggested in 6.9.iii.

In spite of the foregoing remarks, the production of contour overlays by drop-line techniques should not be condemned, or dismissed as merely a passing phase. It has been demonstrated in these tests that contours can be produced in terrain conditions of some complexity. It should be acknowledged that the data for the contours has not involved a photogrammetric operator in any considerable extra machine time over and above that required for the scanning operation.

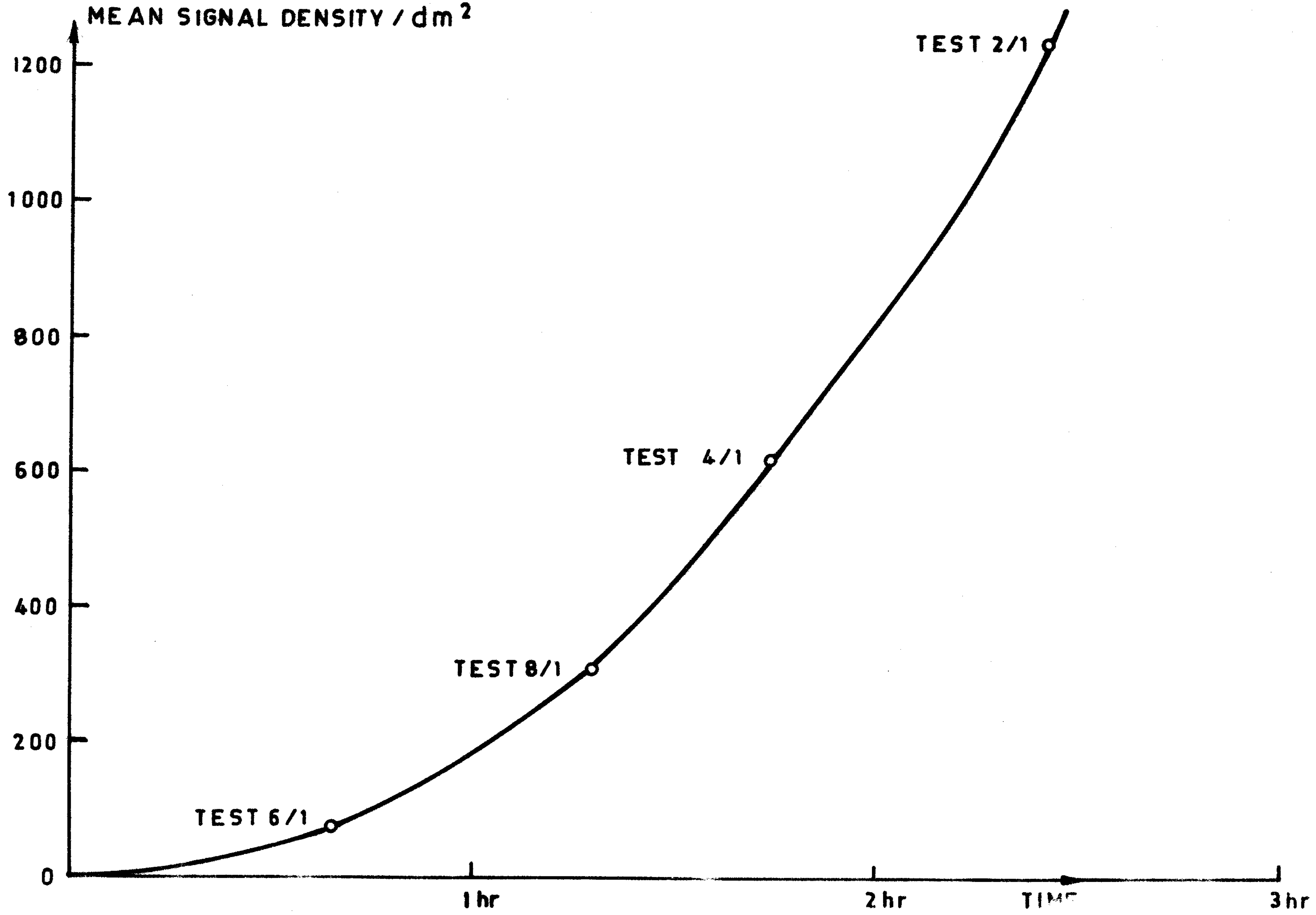

FIG. 7·27. DROP-LINE CONTOUR CONVERSION TIME BROKEN T. RRAIN

Furthermore there is no requirement for additional expensive equipment, such as would be the case if the scanned profiles were digitised. It is clear that the additional conversion work could be carried out by a junior cartographic technician after appropriate training. Whilst the results may lack the elegance, topographical exactitude, and geomorphological quality of a conventional photogrammetric plot, such contours could satisfy the requirement for elevation data rather rapidly in the context of the mapping of an underdeveloped territory, based on qualitative and quantitative criteria realistically lower than is normal with conventional mapping.

7.7 Conclusion

7.7.i

The various tests have been carried out under conditions which simulate a medium-scale mapping project of underdeveloped terrain, and in which the phases of production have been integrated from initial field-work onwards. The tests confirm:

(a) the high internal planimetric accuracy of orthophotographs,

(b) that good elevation results are achieved internally with profile signals during the scanning operation,

(c) that the influence of scanning speed is rather low both in respect of horizontal and vertical accuracy,

(d) that the influence of system errors is rather marked with unsuitable choice of slit width in broken terrain.

From (a) above, it follows that the usual standards achieved for example in Independent Model Triangulation, are sufficient to ensure that the final map product should meet established map accuracy standards. From (b) above, it would appear that results may be achieved from continuous digitising techniques, which are comparable to conventional photogrammetric contouring.

7.7.ii

Additionally it is shown that considerable effort is required to produce contours from drop-line charts, if the terrain structure is rather complex. A technique has been developed, based on interpretation by drainage pattern, which may have general applicability to the interpretation of pictorial elevation signals.

7.7.iii

In conclusion, Resolution 9 of 7th November 1970, framed by the Sixth United Nations Regional Cartographic Conference for Asia and the Far East *(U.N., 1970, 16)* is wholeheartedly endorsed:

The Conference

Noting the urgent need for maps at various scales and the importance of providing them for purposes of economic and social development in the countries of the region, *Drawing attention* to the wealth and completeness of the information presented by orthophot maps, especially for the planning and execution of natural resources development projects,

Noting further that in appropriate cases modern orthophoto-techniques can be used to economic advantage in the production and revision of maps,

Recommends that increased use should be made or orthophotos for map production and revision in order to save time, expense and highly skilled manpower, and that map users in general should be educated in the practical application or orthophotos and orthophoto maps;

Further recommends that assistance should be made available to the countries of the region by those countries which have already gained experience in the practical application and production or orthophoto maps and in map revision using orthophotos, and that close cooperation should be encouraged between the different disciplines using maps in the countries of the region in order to obtain the maximum benefit from orthophoto maps;

Urges all Governments to encourage the training of map users in the use of air photographs and orthophotos.

ACKNOWLEDGEMENTS

The author acknowledges with gratitude the active interest and encouragement of Professor P.V. Angus-Leppan, Head of the School of Surveying, University of New South Wales. He is very much indebted to his colleague and Supervisor Dr. J.C. Trinder, for advice, guidance, helpful criticism, and particularly for his assistance in the latter stages of this work.

In a University School as active as the School of Surveying it is rather invidious to single out some colleagues to the exclusion of others; because the author is very much aware that all staff, administrative as well as academic, cheerfully undertake extra burdens when a full-time staff member is engaged on research work. However a particular debt of gratitude is owed to Messrs. A.J. Robinson and A.P.H. Werner for their expert (and unpaid) participation in field work, and again to the latter for much help in translation work. The author has also been fortunate to find in Mr. L. Berlin a stimulating, willing collaborator, especially in the work associated with perspective centre calibrations. He is most grateful to Dr. S. Nasca for the painstaking and time-consuming task of plan measurements carried out on the orthophotograph test negatives.

BIBLIOGRAPHY

ACKERMANN, F. 1966 — "On the theoretical accuracy of planimetric block triangulation". *Photogrammetria*, 21.

ACKERMANN, F. 1969 — "Überprüfung einer grossmasstäbigen orthophotokarte". *Bildmessung und Luftbildwesen*, 37, 5/69.

AHREND, M. 1966 — "Analysis of Photogrammetric errors". *Zeiss-Mitteilungen*, 4, (1966), No. 2.

ALBERTZ, J. KREILING, W. 1972 — "Photogrammetric Guide". *Wichmann*, Karlsrube.

BEAN, R.K. 1968 — "The Orthophotoscope and its Development". *Canadian Surveyor*, Vol. XXII, No. 1.

BERLIN, L. HOLDEN, G.J.F. 1974 — "Programmable Desk Calculators and Independent Model Triangulation". (In Print) *Photogrammetric Engineering*,

BERVOETS, S.G. 1973 — "Aerotriangulation and Block Adjustment in Australia". *Proc. 16th Australian Survey Congress*, Canberra.

BLACHUT, T.J. 1968 — "Further Extension of the Orthophoto Technique". *Canadian Surveyor*, Vol. [illegible], No. 1.

BLACHUT, T.J. 1972 — "Orthophoto technique: basic instruments and Methods". *World Cartography*, Vol. XII, U.N., N.Y.

BORMANN, G. 1970 — "Orthophoto Attachment for the Wild [illegible] Autograph". *Proc. ASP-ACSM Convention*, Washington, D.C.

BROWN, M.S.
1968

"Refraction Measurements in an Arid Climate". *R.E.F.-E.D.M. Conference November 1968.* University of New South Wales.

BRUNNTHALER, F.J.
1972

"Orthophoto Mapping in Practice". *World Cartography,* Vol. XII, U.N., N.Y.

CIMERMAN, V.J.
TOMASEGOVIĆ
1970

"Atlas of Photogrammetric Instruments". *Elsevier,* Amsterdam.

EBNER, H.
WAGNER, W.
1972

"Aerotriangulation with Independent Models in the Zeiss Planimat". *Nachrichten aus dem Kasten und Vermessungswesen,* Series II, No. 27,

ECKHART, D.
1966

"The Anblock Method: Practical Results" *International Symposium on Aerial Triangulation,* Urbana, Illinois, A.S.P.

FERBER, R.
1928

"Gallus apparatus for photo-reconstruction". *International Civil Aeronautics Conference,* Washington, D.C.

FISHER, R.A.
YATES, F.
1963

"Statistical Tables for Biological, Agricultural and Medical Research". *6th edn., Oliver and Boyd,* Edinburgh.

FLEMING, E.A.
1973

"Accuracy and Image Quality of Production Orthophotographs". *Orthophoto Workshop II,* A.S.P.

FÖRSTNER, R.
1968

"Experience with GZ-1 Orthoprojector". *Canadian Surveyor,* Vol. XXII, No. 1.

FREUND, J.E.
1962

"Mathematical Statistics". *Prentice-Hall.*

HAMPEL, G.
1967

"Orthoprojektion und Grundkartenwerk 1:2 500 unter besonderer Berucksichtigung der Hohendarstellung". *Bildmessung und Luftbildwesen*, 35,

HASSETT, T.J.
1966

"Aerial Mosaics and Photomaps" *Manual of photogrammetry*, 3rd Edn., Vol. II, A.S.P.

HELAVA, U.V.
1968

"On Different Methods of Orthophotography" *Canadian Surveyor*, Vol. XXII, No. 1.

HOBBIE, D.
1969

"Gigas-Zeiss Orthoprojector equipment news". *Bildmessung und Luftbildwesen*, 37, 5/1969.

HÖHLE, J.
SCHNEIDER, H.
1973

"The Use of the Wild PPO-8 Orthophoto Equipment for the A-8 Autograph" *Orthophoto Workshop II*, A.S.P.

HOLDEN, G.J.F.
BERLIN, L.

"Programmable Desk Calculators and Independent Model Triangulation" (In Print) *Photogrammetric Engineering*.

JERIE, H.G.
1968

"Theoretical Height Accuracy of Strip and Block Triangulation with and without the use of Auxiliary Data". *Photogrammetria*, 23.1.

JERIE, H.G.
1972

"New concepts of topographic mapping in developing countries". *World Cartography*, Vol. XII, U.N., N.Y.

JOHANNSON, O.

"Orthophoto Maps as a Basis for the Economic Map of Sweden at the scale 1:10 000". *Canadian Surveyor*, Vol. XXII, No. 1.

KOPPE, C. 1902 — "Die neue topographische Laudeskarte des Herzogtums Boraunschweig im Masstab 1:10 000". *Zeitschrift für Vermessungswesen*, 14/1902. Stuttgart.

LACMANN, O. 1931 — "Entzimungsgerät für richt ebenes Gelände". *Bildmessung und Luftbildwesen.*

LAMBERT, B.P. 1971 — "Production of Small and Medium Scale Maps with the aid of Orthophotography" *Commonwealth Survey Officers Conference*, Paper Cl.

LAMBERT, B.P. 1973 — "Statement of Activities of the Division of National Mapping for the period 1st January 1972 to 31st December 1972" *Department of Minerals and Energy*, Canberra.

LIGTERINCK, G.H. 1970 — "Aerial Triangulation by Independent Models". *Photogrammetria*, 26/1970.

MEIER, H.K. 1966 — "Theory and practice of the Gigas-Zeiss Orthoprojector". *Zeiss-Mitteilungen*, 4 (1966) No. 2.

MEIER, H.K. 1966 (b) — "Art und Genauigkeit der Höhendarstellung in Orthoprojektor Gigas-Zeiss". *Bildmessung und Luftbildwesen*, 34, 1966.

MEIER, H.K. 1968 — "The Gigas-Zeiss Orthoprojector Design Features and Practical Results". *Canadian Surveyor*. Vol. XXII, No. 1.

NEUBAUER, H.G. 1964 — "Uber die Genauigkeit von Orthophotoplänen" *Institut für Angewandte Geodäsie*, Frankfurt.

NEUBAUER, H.G. 1969 — "Die Geländeneigungen und über Einfluss auf die Lagefehler der differentiellen Entzeming" *Bildmessung und Luftbildwesen*, 37, 4/1969.

OLSEN, R.W. 1973 — "Orthophotoquad Production in the Geological Survey". *Orthophoto Workshop II*, A.S.P.

PARENTI, G. 1968 — "Analytical Plotter with Orthoprinter". *Canadian Surveyor*. Vol. XXII, No. 1.

ROBINSON, A.J. 1972 — "Field Tests with the HP3800A Distance Meter". *Australian Surveyor*, Vol. 24, No. 3.

RYSER, H.A. 1973 — "A Multipurpose Mapping Program for the County of San Mateo". *Orthophoto Workshop II*, A.S.P.

SCHMIDT-FALKENBERG, H. 1970 — "Höhenlinien aus photogrammetrisch gemessen Geländeprofilen und über Brauchbarkeit fur den Kartenmasstab 1:5 000." *German Geodetic Comission*, Series C, No. 151.

SCHNEIDER, H. 1970 — "Untersuchungen am Orthoprojektor GZ1 über die Höhengenauigkeit der Profilschraffenmethode". *German Geodetic Commission*, Series C, No. 162.

SCHNEIDER, H. HÖHLE, J. 1973 — "The Use of the Wild PPO-8 Orthophoto Equipment for the A-8 Autograph". *Orthophoto Workshop II*, A.S.P.

SCHUT, G.H. 1967 — "Formation of Strips from Independent Models". *N.R.C. Canada Report AP-PR 36.*

SCHUT, G.H. 1968 — "A Fortran Program for the Adjustment of Strips and Blocks by Polynomial Transformations". *N.R.C. Canada Report AP-PR33.*

STEWARDSON, P.B.
1972
"The Determination of Projection Centre Coordinates". *International Archives of Photogrammetry,* XII Congress.

SZANGOLIES, K.
1972
"Method and accuracy of differential rectification with the Topocart-Orthophot-Orograph". *Jena Review,* 1972/2.

SZANGOLIES, K.
1973
"Economy and Accuracy in the production of Orthophoto Maps". *Orthophoto Workshop II,* A.S.P.

THOMPSON, E.H.
1959
"An Exact Linear Solution of the Problem of Absolute Orientation". *Photogrammetria 1958-59,* Vol. 15, No. 4.

TOMASEGOVIČ
CIMERMANN, V.J.
1970
"Atlas of Photogrammetric Instruments". *Elsevier,* Amsterdam.

TRINDER, J.C.
1971
"Some Remarks on Numerical Absolute Orientation". *Australian Surveyor,* Vol. 23, No. 6.

UNITED NATIONS
1970
"Report of the Sixth United Nations Regional Cartographic Conference for Asia and the Far East". *Document E/CONP/.57/2.,* U.N., New York.

URBAN, F.
1973
"Large Scale Mapping in New South Wales". *16th Australian Survey Congress,* Canberra.

VISSER, J.
1968
"Orthophotos at the I.T.C." *I.T.C. Publication* A41/42.

VOSS, F.
1968
"Die Herstellung von Orthophotokarten 1:5 000 in Nordrheim-Westphalen". *N.Ö.V. - Nachrichten aus dem öffentlichen Vermessungsdienst.* Nordrheim-Westfalen. 1/1968.

YATES, F. FISHER, R.A.	"Statistical Tables for Biological, Agricultural and Medical Research". *6th edn., Oliver and Boyd,* Edinburgh.
ZEISS-VEB Carl Zeiss JENA 1971	"Instruction Manual Topocart B". *Brochure 14* - G3686-2.
ZEISS-VEB Carl Zeiss JENA 1971	"Instruction Manual Orthophot". *Brochure 14* - G373-2

APPENDIX A

Notes on Computing Methods and Programs

1. Much of the experimental work described involved considerable calculation effort, the mathematical complexity of which was rather trivial, but the volume of which presented some problems. During the period in which the work was executed, turn-around times at the IBM 360 computer of the University of New South Wales were particularly slow during teaching sessions, amounting to 48 hours or more. Terminal facilities were not available to the computer from the photogrammetric laboratories, so that it was not possible for example to test model connections between successive models in Independent Model Triangulation without unacceptable delay. At a rather early stage in the work, the School of Surveying obtained a programmable desk calculator, HEWLETT-PACKARD Model 9810A, and virtually all computational work was carried out by this means; excepting only work requiring massive storage such as Block Adjustment. The calculator was operated almost as a mini computer, in a role practically on-line to photogrammetric plotters, except that there was no physical connection other than through the operator. It proved possible to devise programs which were subsequently combined into a 'photogrammetric package', handling all phases of Independent Model triangulation from perspective centre calibration to strip adjustment *(Berlin and Holden, 1974)*.

2. The HP9810A calculator is the basic unit of a 9800 system, for which there are numerous plug-in and peripheral devices, such for example as the Plotter used to draw the model error diagrams of Chapter 7.

The calculator may be manually operated, or program operated; the standard program memory storing up to 500 program steps, with standard data memory to 51 data numbers, the two memories being separate. Programming features include conditional and unconditional branching, direct and indirect data storage, data register arithmetic, relocatable programs, subroutines, program editing, and the ability to automatically load magnetic cards containing either programs or data. The calculator used in this work was extended so that the available program steps became 2036, and the data memory was extended to 111 registers. In addition two ROM's (read-only-memories) were available. The Mathematics ROM permits automatic keying of logarithms and exponential functions; trigonometrical functions in degrees, radians, or grads; coordinate transformation; vector arithmetic; manipulation of complex numbers; and the programming facility of iterative subroutines (do-loops). A Printer Alpha ROM was also installed together with a Printer, permitting the printing of alphanumeric characters and messages. The basic calculator includes a 3 line display, in which up to 10 digits and 2 exponent digits are displayed in either fixed point or floating point numbers. However, calculations are performed and data is stored, with two additional digits to maintain greater than 10 digit accuracy. The working range of calculation is from $(\pm)10^{-98}$ to $(\pm)9.99999999999 \times 10^{98}$.

3. The programs used most frequently were:

MSE/HISTOGRAM: Calculates the mean square error and mean of an unlimited series of numbers, and generates a twenty cell histogram, of distribution by frequency on the printer.

RESIDUALS: Extracts and prints the differences (V_X, V_Y) between corresponding sets of coordinates stored in data registers from magnetic cards, and calculates and prints the vector differences V_P.

PLOTMODEL: Plots vector diagrams such as those of chapter 7, from coordinates and residuals stored on magnetic card.

LINEFIT: Calculates the equation of the straight-line of best fit of a set of data points, by minimising the sum of the squares of the deviations of the points from the line, and calculates a correlation coefficient.

SIMTRAN: Calculates a similarity transformation, with a least squares solution, of the form:

$$X^* = AX + BY + C1$$
$$Y^* = AY - BX - C2$$

AFFTRAN: Calculates an affine transformation, with a least squares solution, of the form:

$$X^* = A1 + A2X + A3Y$$
$$Y^* = B1 + B2X + B3Y$$

ABSOR: Calculates an orthogonal three dimensional rotation, shift of origin, and scale change, between sets of three dimensional coordinates.

INDEMODFORM: Forms the individual sets of coordinates of Independent Models into a continuous strip, either in ground coordinates or in the coordinates of the first model.

The first four programs listed are trivial, and descriptions are given only of the remainder. An additional program used was PERCAL, for perspective center calibrations, devised by L. BERLIN, and described elsewhere *(Berlin and Holden, 197-)*.

4. SIMTRAN

4.1 The program computes a linear similarity transformation of the form:

$$X^* = AX + BY + C1$$
$$Y^* = AY - BX + C2$$

in which A, B, C1, C2 are functions of four unknowns:

$$A = \lambda.\cos\theta$$
$$B = \lambda.\sin\theta$$
$$C1 = \Delta X^*$$
$$C2 = \Delta Y^*$$

in which λ is a scale factor, θ a rotation, and ΔX^* and ΔY^* are shifts of origin of the system X, Y in units of system X*, Y*.

4.2 The least squares solution is direct, by calculating the following terms after all corresponding data is entered for (n) points:

$$I = [XX^*] + [YY^*]$$

$$II = [YX^*] - [XY^*]$$

$$III = [XX] + [YY]$$

$$IV = n.III - [X]^2 - [Y]^2$$

$$A = \frac{n.I - [X][X^*] - [Y][Y^*]}{IV}$$

$$B = \frac{n.II - [Y][X^*] + [X][Y^*]}{IV}$$

$$C1 = \frac{[X^*] - A[X] - B[Y]}{n}$$

$$C2 = \frac{[Y^*] + B[X] - A[Y]}{n}$$

$$\lambda = \sqrt{A^2+B^2}$$

$$\theta = \tan^{-1}. \frac{B}{A}$$

4.3 Both sets of coordinates are retained in storage in order to compute residuals $V_X V_Y$ between X^*Y^* and the transformed values of XY. A radius vector standard error is computed from the residuals in the form:

$$\sigma = \sqrt{\frac{V_X V_X + V_Y V_Y}{2n - 4}}$$

Because the corresponding pairs of coordinates are retained in store, the total number of corresponding pairs to compute the transformation is limited to 20, occupying 80 registers. After the calculation, as many other points may be transformed as desired.

4.4 The program includes an affine option, intended to be used with program stored functions A1, A2, A3, B1, B2, B3, in order to adjust coordinate XY as they are entered. This facility compensates for the known non-orthogonality of the measuring instrument (6.6). The complete SIMTRAN program has 1280 instructions with 100 data registers allocated. An example of the input/output print is given in Table A.I.

```
SIMILARITY
TRANSFORM
X*=AX+BY+C1
Y*=AY-BX+C2
WITH AFFINE
OPTION

G.J.F.HOLDEN
U.N.S.W.MAY 1972

SET FLAG IF
AFFINE OPTION
REQUIRED

ENTER N NUMBER
OF COMMON POINTS
FOR COMPUTATION
OF COEFFICIENTS
(2 TO 20)

AFFINE NOT USED

         9.00000*

ENTER N SETS XY
IN FINAL SYSTEM

        99.99540*
       200.02180*

       299.98110*
       200.05710*

       499.96490*
       200.09290*

        99.98490*
       399.99220*

       299.96320*
       400.05390*

       499.93210*
       400.08870*

        99.96280*
       599.99450*

       299.96970*
       600.05740*

       499.95150*
       600.06880*
```

```
ENTER N SETS XY
INITIAL SYSTEM

       100.00000*
       200.00000*

       300.00000*
       200.00000*

       500.00000*
       200.00000*

       100.00000*
       400.00000*

       300.00000*
       400.00000*

       500.00000*
       400.00000*

       100.00000*
       600.00000*

       300.00000*
       600.00000*

       500.00000*
       600.00000*
A
           0.99994
B
          -0.00012
C1
           0.03538
C2
           0.03435
SCALAR
           0.99994
ROTATION IN ARC
          -0.00012
```

```
RESIDUALS
           0.00897
           0.01288

           0.01113
           0.00252

           0.01519
          -0.00834

          -0.00547
           0.03034

           0.00409
          -0.00642

           0.02305
          -0.01628

          -0.00631
           0.01589

          -0.02735
          -0.02206

          -0.02129
          -0.00851

STANDARD ERROR
RADIUS VECTOR
           0.02553

ENTER XY OTHERS
SET FLAG IF
AFFINE OPTION
WAS USED
```

TABLE A.I

5. AFFTRAN

This program computes an affine transformation:

$$X^* = A1 + A2X + A3Y$$
$$Y^* = B1 + B2X + B3Y$$

The upper triangular terms of the normal equations from n corresponding points are similar for both A and B unknowns, and the A equations including the vector of constant terms are:

$$\begin{aligned} n.A1 + [X].A2 + [Y].A3 - [X^*] \\ [XX].A2 + [XY].A3 - [XX^*] \\ [YY].A3 - [YX^*] \end{aligned}$$

Solution of the normal equations is by Choleski decomposition. The program then computes residual errors $V_X V_Y$ for the transformed XY coordinates, and standard errors in the form:

$$\sigma_{V_X} = \sqrt{\frac{V_X V_X}{n-3}} \quad \text{and} \quad \sigma_{V_Y} = \sqrt{\frac{V_Y V_Y}{n-3}}$$

A specimen input/output of the 1032 instruction, 98 register program, in a version for a maximum of 20 corresponding points is given in Table A.II. Data entry 1 is the number n, data entry 2 is initial XY coordinates, and data entry 3 is the final X*Y* coordinates. The data is identical to that of Table A.I, and the improved residuals $V_X V_Y$ may be noted.

```
AFFINE
TRANSFORMATION

X* = A1+A2X+A3Y
Y* = B1+B2X+B3Y

G.J.F.HOLDEN
UNSW MAR 1972

DATA ENTRY 1

        9.00000

DATA ENTRY 2

      100.00000*
      200.00000*

      300.00000*
      200.00000*

      500.00000*
      200.00000*

      100.00000*
      400.00000*

      300.00000*
      400.00000*

      500.00000*
      400.00000*

      100.00000*
      600.00000*

      300.00000*
      600.00000*

      500.00000*
      600.00000*
```

```
DATA ENTRY 3

       99.99540*
      200.02180*

      299.98110*
      200.05710*

      499.96490*
      200.09290*

       99.98490*
      399.99220*

      299.96320*
      400.05390*

      499.93210*
      400.08870*

       99.96280*
      599.99450*

      299.96970*
      600.05740*

      499.95150*
      600.06880*
```

```
TRANSFORMATION
ELEMENTS

A1
       0.01007

A2
       0.99992

A3
      -0.00005

B1
       0.00404

B2
       0.00020

B3
       0.99996

RESIDUAL ERRORS
VX
VY
      -0.00278
      -0.00612

      -0.00424
      -0.00111

      -0.00381
       0.00341

      -0.00184
       0.01496

       0.00409
      -0.00642

       0.01942
      -0.00091

       0.01069
       0.00414

      -0.01198
      -0.01844

      -0.00954
       0.01048

SIGMA VX
      VY
       0.01145
       0.01143

ENTER XY OTHERS
```

TABLE A.II

6. ABSOR

6.1 The absolute orientation program is a spatial similarity transformation with over-determination, the formulation of which is similar to that given by ALBERTZ *(1972)*. The orthogonal transformation equation is rigorous but the solution for the 7 unknowns (1 scalar, 3 shifts, 3 rotations) is not a simultaneous solution of all. The shifts are determined as centre of gravity origin shifts for the two systems, the scalar as the mean scalar for all corresponding distances from the two origins. The 3 rotations are determined by a least squares procedure, in which the normal equations are solved for corrections to initial values of the rotations (usually zero) to provide updated values, which are then used in the transformation to compute new constant terms to reiterate the normal equations. The iterations terminate (usually after one or two with near vertical photography) when the corrections to all rotations are smaller than 10^{-5} radians. The solution of the normals is by Cholesky decomposition using only the upper triangular elements and the vector of constant terms.

6.2 The program calculates in the following sequence after data is entered for (n) points; the data being entered firstly in the final system XYZ, and then in the same order of points in the initial system xyz.

(iv) The normal equations are formed for solution of corrections $\partial\omega$, $\partial\phi$, $\partial\kappa$ to the current values of the rotations; the upper triangular and constant terms being:

$$\left[\bar{y}_i^2+\bar{z}_i^2\right]\partial\omega - \left[\bar{x}_i\bar{y}_i\right]\partial\phi - \left[\bar{x}_i\bar{z}_i\right]\partial\kappa - \lambda^{-1}.\left[\bar{z}_i(Y_i-Y_i')-\bar{y}_i(Z_i-Z_i')\right]$$

$$\left[\bar{x}_i^2+\bar{z}_i^2\right]\partial\phi - \left[\bar{y}_i\bar{z}_i\right]\partial\kappa - \lambda^{-1}.\left[\bar{x}_i(Z_i-Z_i')-\bar{z}_i(X_i-X_i')\right]$$

$$\left[\bar{x}_i^2+\bar{y}_i^2\right]\partial\kappa - \lambda^{-1}.\left[\bar{y}_i(X_i-X_i')-\bar{x}_i(Y_i-Y_i')\right]$$

(v) Updated values of the rotations are formed:

$$\omega^{n+1} = \omega^n+\partial\omega; \quad \phi^{n+1} = \phi^n+\partial\phi; \quad \kappa^{n+1} = \kappa^n+\partial\kappa$$

(vi) The program returns to (iii) above.

6.3 The iterations terminate when each of the corrections to rotations is smaller than 10^{-5} radians. In the event that the solution does not converge by 10 iterations, a "check data" message is printed and program execution stops. When the program terminates normally, the transformation parameters and the residual of the transformed coordinates are printed out. A radius vector standard error is also computed, and printed first in units of the final coordinates, secondly in units of the initial coordinates, the form of the error being:

$$\sigma = \sqrt{\frac{V_X V_X + V_Y V_Y + V_Z V_Z}{3n - 7}}$$

(i) Centre of gravity coordinates are calculated for both systems, the centre of gravity of the final system giving the three shift unknowns:

$$X_s = \frac{[X_i]}{n} \; ; \; x_s = \frac{[x_i]}{n}$$; and similarly for

Y_s, Z_s, y_s, z_s.

Following this the sets are reduced to the centres of gravity:

$\overline{X}_i = X_i - X_s$; $\overline{x}_i = x_i - x_s$; similarly for $\overline{Y}_i$, $\overline{Z}_i$, $\overline{y}_i$, $\overline{z}_i$.

(ii) The scalar λ is computed:

$$\lambda = \frac{\left[\sqrt{\overline{X}_i^2 + \overline{Y}_i^2 + \overline{Z}_i^2}\right]}{\left[\sqrt{\overline{x}_i^2 + \overline{y}_i^2 + \overline{z}_i^2}\right]}$$

(iii) Transformed coordinates X_i' Y_i' Z_i' are calculated from the orthogonal transformation in matrix form:

$$\begin{pmatrix} X_i' \\ Y_i' \\ Z_i' \end{pmatrix} = \lambda \, . \, R \begin{pmatrix} \overline{x}_i \\ \overline{y}_i \\ \overline{z}_i \end{pmatrix} + \begin{pmatrix} X_s \\ Y_s \\ Z_s \end{pmatrix}$$

in which R is a 3 x 3 rotation matrix of which the nine elements are the well known functions of three rotations ω, ϕ, κ. In the first iteration the matrix is a unit matrix unless predetermined values of the rotations have been stored.

At this stage, as many other points as may be desired may now be transformed.

Two versions of the program exist, one which compute from a maximum of 4 corresponding sets of coordinates in which only 51 storage registers are used, and one from a maximum of 12 sets in which 98 registers are used. The programs consists of 2035 instructions. A specimen input/output is shown in Table A.III.

7. INDEMODFORM

The core of this program is the previous ABSOR program, incorporated as a subroutine. The program has been compiled for a standard pattern of model joins consisting of a perspective center and three pass points corresponding to one-another in the two models to be joined.

Three types of data entry control stages of the program. Data entry type 1 consists of points in the first fixed model which are not join points. Data entry type 2 consists of the perspective centre and three model pass points of the fixed model at the first join, followed immediately by the corresponding points in the new model. At this stage absolute orientation is iterated, terminating when the test limit is reached. The mean strip coordinates of the model joins are printed, each followed by the half discrepancies. The number of iterations is printed. Data entry type 3 consists

ABSOLUTE
ORIENTATION

TOPOCART 18.8.73
....
G.J.F.HOLDEN
U.N.S.W. JAN 73

ENTER (N) NUMBER
OF COMMON POINTS
KNOWN IN BOTH
SYSTEMS (3 TO 12
IN THIS VERSION)
6.*

ENTER N SETS XYZ
OR ENH COORDS IN
FINAL SYSTEM

09A
910176.*
910483.*
5412.*

10A
1076853.*
909116.*
5196.*

10C
1073798.*
716565.*
5531.*

10B
1070298.*
526882.*
5824.*

09B
907972.*
528121.*
5982.*

09C
908542.*
719405.*
5778.*

ENTER N SETS XYZ
IN MODEL SYSTEM

395690.*
592170.*
5325.*

562200.*
595815.*
5115.*

565000.*
403341.*
5375.*

567200.*
213545.*
5625.*

404910.*
209975.*
5821.*

399775.*
401180.*
5675.00000*

ITERATIONS
2.00000

OMEGA
0.00025

PHI
0.00018

KAPPA
0.03004

(RADIANS)

X SHIFT
9.912731667 05

Y SHIFT
7.184286667 05

Z SHIFT
5620.50000

SCALAR
1.00014

RESIDUALS

44.
-8.
-18.

-65.
1.
16.

7.
54.
-10.

5.
-66.
-6.

-16.
1.
4.

25.
17.
14.

STANDARD ERROR
(VECTOR)
38.
38.

OTHER POINTS
ENTER XYZ
10E
557224.*
501668.*
5436.*
1068985.
815149.
5556.

DOMEGA 1.6 C
DPHI 1.1 C
SCALE 1/24997
ERROR -0.01%

TABLE A.III

of points in the new model which do not join to a succeeding model, and these are transformed by the stored orthogonal transformation into strip coordinates and printed. Data entry type 2 follows for the next join section. The first four points are transformed to strip coordinates and stored, and entry to absolute orientation started again.

If sufficient ground control exists in any model, the strip may be formed up in ground coordinates by starting the formation at this model, and treating the ground and model coordinates as a spurious model join. The remainder of the strip may then be formed first in one direction and then in the other.

As only 4 points are used in the computation of the absolute orientation, it was possible to use only 51 registers. The program consists of 1946 instructions, and a specimen input/output showing the beginning of a strip is given in Table A.IV.

INDEPENDENT
MODEL
TRIANGULATION

GJF HOLDEN UNSW
JAN 1973

DATA ENTRY TYPE1

STRIP 1348/1
51044
160336.
199593.*
63650.*

DATA ENTRY TYPE2

51040
240023.*
200203.*
200009.*

51041
238770.*
294271.*
64542.*

51042
240727.*
104595.*
65455.*

51043
240006.*
199177.*
64420.*

160046.*
200148.*
199994.*

159657.*
295195.*
64142.*

160473.*
104429.*
64327.*

160336.*
199593.*
63650.*

ITERATIONS
2.

MEAN MODEL JOINS

240023.
0.
200219.
16.
200005.
-4.

238768.
-2.
294263.
-8.
64555.
13.

240725.
-2.
104580.
-15.
65446.
-9.

240010.
4.
199184.
7.
64421.
1.

DATA ENTRY TYPE3

51045
193550.
117142.*
64422.*
273538.
117406.
65412.

DATA ENTRY TYPE2

51050
240023.*
200203.*
200009.*

TABLE A.IV

B I O G R A P H Y

JOE HOLDEN is a Lecturer in the School of Surveying, and was formerly a Career Officer in the Survey Branch of the Corps of Royal Engineers, where he also served on the Geographical Section General Staff. His interests are Cartographic and Terrestial Photogrammetry and Accuracy of Orthophoto Processes.

Publications from

THE SCHOOL OF SURVEYING, THE UNIVERSITY OF NEW SOUTH WALES

P.O. Box 1, Kensington, New South Wales, 2033

A U S T R A L I A

Reports

1.* The discrimination of radio time signals in Australia
G.G. Bennett — UNICIV Rep. D-1 (G1)

2.* A comparator for the accurate measurement of differential barometric pressure
J.S. Allman — 9pp — UNICIV Rep. D-3 (G2)

3. The establishment of geodetic gravity networks in South Australia
R.S. Mather — 26pp — UNICIV Rep. R-17 (G3)

4. The extension of the gravity field in South Australia
R.S. Mather — 26pp — UNICIV Rep. R-19 (G4)

5.* An analysis of the reliability of barometric elevations
J.S. Allman — 335pp — UNISURV Rep. 5 (S1)

6.* The free air geoid for South Australia and its relation to the equipotential surfaces of the earth's gravitational field
R.S. Mather — 491pp — UNISURV Rep. 6 (S2)

7.* Control for mapping (Proceedings of Conference, May 1967)
P.V. Angus-Leppan (Editor) — 329pp — UNISURV Rep. 7 (G5)

8.* The teaching of field astronomy
G.G. Bennett & J.G. Freislich — 30pp — UNISURV Rep. 8 (G6)

9.* Photogrammetric pointing accuracy as a function of properties of the visual image
J.C. Trinder — 64pp — UNISURV Rep. 9 (G7)

10.* An experimental determination of refraction over an icefield
P.V. Angus-Leppan — 23pp — UNISURV Rep. 10 (G8)

11.* The non-regularised geoid and its relation to the telluroid and regularised geoids
R.S. Mather — 49pp — UNISURV Rep. 11 (G9)

12.* The least squares adjustment of gyro-theodolite observations
G.G. Bennett — 53pp — UNISURV Rep. 12 (G10)

13. The free air geoid for Australia from gravity data available in 1968
R.S. Mather — 38pp — UNISURV Rep. 13 (G11)

14. Verification of geoidal solutions by the adjustment of control networks using geocentric Cartesian co-ordinate systems
R.S. Mather — 42pp — UNISURV Rep. 14 (G12)

15.* New methods of observation with the Wild GAKI gyro-theodolite
G.G. Bennett — 68pp — UNISURV Rep. 15 (G13)

* Out of Print

G General Series — Price: $ 4

S Special Series (Limited printing) — Price: $20

Reports (contd.)

16* Theoretical and practical study of a gyroscopic attachment for a theodolite
G.G. Bennett 343pp UNISURV Rep. 16 (S3)

17* Accuracy of monocular pointing to blurred photogrammetric signals
J.C. Trinder 231pp UNISURV Rep. 17 (S4)

18. The computation of three dimensional Cartesian co-ordinates of terrestrial networks by the use of local astronomic vector systems
A. Stolz 47pp UNISURV Rep. 18 (G14)

19. The Australian geodetic datum in earth space
R.S. Mather 130pp UNISURV Rep. 19 (G15)

20. The effect of the geoid on the Australian geodetic network
J.G. Fryer 221pp UNISURV Rep. 20 (S5)

21. The registration and cadastral survey of native-held rural land in the Territory of Papua and New Guinea
G.F. Toft 441pp UNISURV Rep. 21 (S6)

22. Communications from Australia to Section V, International Association of Geodesy, XV General Assembly, International Union of Geodesy & Geophysics, Moscow 1971
R.S. Mather et al 72pp UNISURV Rep. 22 (G16)

23. The dynamics of temperature in surveying steel and invar measuring bands
A.H. Campbell 195pp UNISURV Rep. S7

24. Three-D Cartesian co-ordinates of part of the Australian geodetic network by the use of local astronomic vector systems
A. Stolz UNISURV Rep. S8

25. Papers on Four-dimensional Geodesy, Network Adjustments and Sea Surface Topography
R.S. Mather, H.L. Mitchell, A. Stolz 73 pp UNISURV Rep. G 17

26. Papers on photogrammetry, co-ordinate systems for survey integration, geopotential networks and linear measurement
L. Berlin, G.J.F. Holden, P.V. Angus-Leppan, H.L. Mitchell and A. Campbell 80 pp UNISURV Rep. G 18

27. Aspects of Four-dimensional Geodesy
R.S. Mather, P.V. Angus-Leppan, A. Stolz and I. Lloyd 100 pp UNISURV Rep. G 19

28. Relations between MSL & Geodetic Levelling in Australia
H.L. Mitchell 264 pp UNISURV Rep. S 9

29. Study of Zero Error & Ground Swing of the Model MRA101 Tellurometer
A.J. Robinson 200 pp UNISURV Rep. S10

30. Papers on Network Adjustments, Photogrammetry and 4-Dimensional Geodesy.
J.S. Allman, R.D. Lister, J.C. Trinder and R.S. Mather 133 pp UNISURV Rep. G 20

Reports (contd)

31. An Evaluation of Orthophotography in an Integrated Mapping System
G.J.F. Holden 232 pp UNISURV REP. S12

32. The Analysis Precision and Optimization of Control Surveys
G.J. Hoar 200 pp UNISURV REP. S13

33. Papers on Refraction, Mathematical Geodesy and Coastal Geodesy
P.V. Angus-Leppan, E. Grafarend and R.S. Mather
66 pp UNISURV REP. G21

* Out of print

G General Series Price: $ 4.50**

S Special Series (Limited Printing) Price: $11.50**

Proceedings

Proceedings of conferences on refraction effects in geodesy & electronic distance measurement
P.V. Angus-Leppan (Editor) 264 pp Price: $10.00**

Australian Academy of Science/International Association of Geodesy Symposium on Earth's Gravitational Field & Secular Variations in Position UNISURV REP. S11
R.S. Mather & P.V. Angus-Leppan (eds)
764 pp Price: $25.00+

Monographs

1. The theory and geodetic use of some common projections (2nd edition)
R.S. Mather 125 pp Price: $ 4.50**

2. The analysis of the earth's gravity field
R.S. Mather 172 pp Price: $4.50**

3. Tables for Prediction of Daylight Stars
G.G. Bennett 24 pp Price: $ 2.00**

4. Star Prediction Tables for the fixing of position
G.G. Bennett; J.G. Freislich & M. Maughan
200 pp Price: $ 7.50**

5. Survey Computations
M. Maughan 98 pp Price: $ 3.00